



Landbird Population Trends in Mountain and Historical Parks of the North Coast and Cascades Network

2005–2016 synthesis

Natural Resource Report NPS/NCCN/NRR—2018/1673



ON THE COVER

Northern Flicker, one of the few species estimated to have declined in density during 2005-2016 within a portion of the North Coast and Cascades Inventory and Monitoring Network.

Photo by Rob McCay

Landbird Population Trends in Mountain and Historical Parks of the North Coast and Cascades Network

2005–2016 synthesis

Natural Resource Report NPS/NCCN/NRR—2018/1673

Chris Ray,¹ James F. Saracco,¹ Mandy L. Holmgren,¹ Robert L. Wilkerson,¹ Rodney B. Siegel,¹ Kurt J. Jenkins,² Jason I. Ransom,³ Patricia J. Happe,⁴ John R. Boetsch,⁴ and Mark H. Huff⁵

¹The Institute for Bird Populations
P.O. Box 1346
Point Reyes Station, CA 94956–1346

²U.S. Geological Survey
Forest and Rangeland Ecosystem Science Center
Olympic Field Station
Port Angeles, WA 98362

³North Cascades National Park Service Complex
810 State Route 20
Sedro-Woolley, WA 98284

⁴Olympic National Park
600 E Park Ave
Port Angeles, WA 98362

⁵Mount Rainier National Park
55210 238th Ave E
Ashford, WA 98304

July 2018

U.S. Department of the Interior
National Park Service
Natural Resource Stewardship and Science
Fort Collins, Colorado

The National Park Service, Natural Resource Stewardship and Science office in Fort Collins, Colorado, publishes a range of reports that address natural resource topics. These reports are of interest and applicability to a broad audience in the National Park Service and others in natural resource management, including scientists, conservation and environmental constituencies, and the public.

The Natural Resource Report Series is used to disseminate comprehensive information and analysis about natural resources and related topics concerning lands managed by the National Park Service. The series supports the advancement of science, informed decision-making, and the achievement of the National Park Service mission. The series also provides a forum for presenting more lengthy results that may not be accepted by publications with page limitations.

All manuscripts in the series receive the appropriate level of peer review to ensure that the information is scientifically credible, technically accurate, appropriately written for the intended audience, and designed and published in a professional manner.

Data in this report were collected and analyzed using methods based on established, peer-reviewed protocols and were analyzed and interpreted within the guidelines of the protocols. This report also received formal peer review by subject-matter experts who were not directly involved in the collection, analysis, or reporting of the data, and whose background and expertise put them on par technically and scientifically with the authors of the information.

Views, statements, findings, conclusions, recommendations, and data in this report do not necessarily reflect views and policies of the National Park Service, U.S. Department of the Interior. Mention of trade names or commercial products does not constitute endorsement or recommendation for use by the U.S. Government.

This report is available in digital format from the [North Coast and Cascades Network Inventory and Monitoring website](#) and the [Natural Resource Publications Management website](#). If you have difficulty accessing information in this publication, particularly if using assistive technology, please email irma@nps.gov.

Please cite this publication as:

Ray, C., J. F. Saracco, M. L. Holmgren, R. L. Wilkerson, R. B. Siegel, K. J. Jenkins, J. I. Ransom, P. J. Happe, J. R. Boetsch, and M. H. Huff. 2018. Landbird population trends in mountain and historical parks of the North Coast and Cascades Network: 2005–2016 synthesis. Natural Resource Report NPS/NCCN/NRR—2018/1673. National Park Service, Fort Collins, Colorado.

Contents

	Page
Figures.....	iv
Tables.....	vi
Executive Summary.....	vii
Acknowledgments.....	vii
Introduction.....	1
Methods.....	2
Sampling frame.....	2
Survey and habitat covariates.....	4
Analyses.....	4
Results and Discussion.....	9
Climatic variation during the monitoring period.....	18
Fitted models.....	22
Effective survey area.....	28
Parameter estimates by park, stratum and region.....	30
San Juan Island National Historical Park.....	30
Lewis and Clark National Historical Park.....	37
Effects of climate in the historical parks.....	43
Mountain parks overview.....	44
Effects of elevation in the mountain parks.....	55
Effects of climate in the mountain parks.....	61
Regional stability in locally declining species.....	65
Conclusions.....	68
Literature cited.....	69
Appendix 1. Procedures for synthesis of NCCN landbird trends.....	74
Appendix 2. Fitted model results.....	79

Figures

	Page
Figure 1. Precipitation-as-snow anomaly for data from August 1 st of year $t-1$ to July 31 st of year t , expressed as yearly anomalies for each point-count station in the North Coast and Cascades Network or as anomalies averaged over 12 years for each station.....	19
Figure 2. Mean spring temperature anomaly for data from March 1 st to May 31 st of year t , expressed as yearly anomalies for each point-count station in the North Coast and Cascades Network or as anomalies averaged over 12 years for each station.	20
Figure 3. Anomalies in precipitation-as-snow and mean spring temperature for each park monitored.	21
Figure 4. Effective area surveyed at each point-count station, differentiated by park, presented on a log ₁₀ scale for each species analyzed.	29
Figure 5. Population trends for species in San Juan Island National Historical Park.	31
Figure 6. Effort-adjusted counts for several of the flocking or less common species at San Juan Island National Historical Park.....	33
Figure 7. Yearly estimates of population density for 41 species commonly detected in San Juan Island National Historical Park.....	34
Figure 8. Effort-adjusted counts for 41 species commonly detected in San Juan Island National Historical Park.....	36
Figure 9. Population trends for species in Lewis and Clark National Historical Park.....	38
Figure 10. Effort-adjusted counts for several of the less common species at Lewis and Clark National Historical Park.....	39
Figure 11. Yearly estimates of population density for 39 species commonly detected in Lewis and Clark National Historical Park.	41
Figure 12. Effort-adjusted counts for 39 species commonly detected in Lewis and Clark National Historical Park.....	42
Figure 13. Linear effects of climate in one year on breeding landbird density estimates for the following year in San Juan Island National Historical Park and Lewis and Clark National Historical Park.....	43
Figure 14. Population trends for species in Mount Rainier National Park	45
Figure 15. Population trends for species in North Cascades National Park Complex.....	46
Figure 16. Population trends for species in Olympic National Park Complex	47

Figures (continued)

	Page
Figure 17. Yearly estimates of population density for 35 species commonly detected in Mount Rainier National Park.....	49
Figure 18. Effort-adjusted counts for 35 species commonly detected in Mount Rainier National Park.	50
Figure 19. Yearly estimates of population density for 41 species commonly detected in North Cascades National Park Complex.....	51
Figure 20. Effort-adjusted counts for 41 species commonly detected in North Cascades National Park Complex.....	52
Figure 21. Yearly estimates of population density for 33 species commonly detected in Olympic National Park	53
Figure 22. Effort-adjusted counts for 33 species commonly detected in Olympic National Park	54
Figure 23. Effects of elevation on breeding landbird densities for 42 species commonly detected in mountain parks of the North Coast and Cascades Network.	56
Figure 24. Yearly estimates of mean population density, differentiated by elevational stratum, for 33 of 35 landbird species common to Mount Rainier National Park	58
Figure 25. Yearly estimates of mean population density, differentiated by elevational stratum, for 36 of 41 landbird species common to North Cascades National Park Complex.....	59
Figure 26. Yearly estimates of mean population density, differentiated by elevational stratum, for 31 of 33 landbird species common to Olympic National Park.....	60
Figure 27. Mean annual effects of local precipitation-as-snow in one year on breeding landbird densities in the following year for 42 species commonly detected in mountain parks of the North Coast and Cascades Network.....	62
Figure 28. Residual effects of mean spring temperature (MST), after accounting for covariance between MST and PAS.....	64
Figure 29. Similarity in trend estimates between basic and climate models for 175 populations differentiated by park.	65
Figure 30. Regional trends in abundance for species exhibiting local decline.	67

Tables

	Page
Table 1. Area of each park unit and elevational stratum surveyed, excluding the largely glaciated areas above 2500 m in MORA and 2029 m in OLYM.....	3
Table 2. Models used to estimate components of detection probability and abundance of landbird populations in the NCCN during 2005-2016.....	6
Table 3. Survey effort by year and park.....	9
Table 4. Unique point-count stations grouped by number of surveys completed during 2005–2016.....	10
Table 5. Size and number of species-specific groups detected during 2005–2016.....	10
Table 6. Total and park-specific counts for 116 bird species detected 10 or more times during 2005–2016 point-count surveys across five parks of the North Coast and Cascades Inventory and Monitoring Network.....	12
Table 7. Summary of models fitted to species commonly detected in San Juan Island National Historical Park and Lewis and Clark National Historical Park.....	22
Table 8. Summary of models fitted to species commonly detected in the mountain parks.	25

Executive Summary

Long-term monitoring of landbird populations within the National Park Service (NPS) North Coast and Cascades Inventory and Monitoring Network (NCCN) began in 2005, with the goal of detecting trends to inform the conservation and management of landbirds and their habitats. Here we use 2005–2016 data from over 3500 point-count stations to report landbird occurrence and trends in each of five NCCN parks, including three national parks in mountain wilderness areas (Mount Rainier National Park, North Cascades National Park Complex and Olympic National Park) and two historical parks (Lewis and Clark National Historical Park and San Juan Island National Historical Park). Recent advances in point-count modeling were applied to characterize population trends for 68 landbird species, including up to 41 species in each park. Fitted models suggest that almost all species exhibited stable or increasing trends over the study period. Notable exceptions were a decline in the Olive-sided Flycatcher in two parks and single-park declines in the Norther Flicker, Hutton’s Vireo, Clark’s Nutcracker, Mountain Chickadee, Wilson’s Warbler and Dark-eyed Junco. Negative effects of precipitation-as-snow were supported in over one-third of our population models. Lower precipitation-as-snow in the mountain parks might have contributed to rising landbird densities during the study period. Population density also varied with elevation in mountain parks, but temporal trends were similar among elevational strata for each species analyzed, suggesting no evidence of elevational range-shifts during this study. These results reinforce recent analyses of the first 10 years of point-count data from the three mountain parks (Ray et al. 2017 a). In the current analysis, models were extended to explore effects of covariates on species detection probability. Negative effects of ambient noise level on detection were supported in several cases, but adding covariates of detection generally did not lead to substantial improvements in model fit. In some cases, model fit was improved by reducing the scope of inference to a portion of the focal region, suggesting important effects of habitat heterogeneity.

Acknowledgments

This analysis was funded by the National Park Service (NPS) under Agreement P15AC00468, with additional in-kind support from the NPS North Coast and Cascades Inventory and Monitoring Network (NCCN), NPS Olympic and North Cascades National Parks, The Institute for Bird Populations (IBP), San Juan Island National Historical Park, Lewis and Clark National Historical Park, Mount Rainier National Park, North Cascades National Park Complex, Olympic National Park, and the U. S. Geological Survey Forest and Rangeland Ecosystem Science Center. Data for the analyses were collected and managed by the NCCN under the auspices of its Landbird Monitoring Project and Cooperative Agreement with IBP. We thank Katherine Beirne for providing logistical and data management support that made this analysis possible, as well as dozens of highly trained volunteer field technicians who have helped to collect data. Thanks to Taza Schaming and Ryan Monello for providing external peer review comments on this manuscript. Any use of trade, firm, or product names is for descriptive purposes only and does not imply endorsement by the U.S. Government.

This report is Contribution Number 579 of The Institute for Bird Populations.

Introduction

In 2005, the National Park Service (NPS) North Coast and Cascades Inventory and Monitoring Network (NCCN) began monitoring landbird populations in five National Parks, under a peer-reviewed protocol (Siegel et al. 2007) that has served as a model for other resource monitoring efforts within the NCCN and in other networks. Landbird monitoring is part of a suite of monitoring activities designed to track “vital signs” related to NPS resources (Fancy et al. 2009, Weber et al. 2009). Landbird populations were identified as vital signs by the NPS because several aspects of terrestrial ecosystem change can be inferred efficiently by monitoring trends in these species, which occupy relatively high trophic positions and provide important ecological functions such as seed dispersal and insect control. Within the National Parks, landbird populations should be less impacted by many of the anthropogenic processes local to non-park landscapes, while still being impacted by global processes such as climate change. Thus, monitoring trends in National Parks should help infer responses to climate and other stressors related to global change. Vital signs monitoring is especially urgent in mountain parks, because montane habitats are among those most immediately susceptible to effects of climate change (IPCC 2013, 2014).

The seven park units in the NCCN include three large, predominantly montane natural areas and four smaller parks established to preserve historical resources. Landbird monitoring occurs in two of the four “historical” parks and in all three of the “mountain” parks: San Juan Island National Historical Park (SAJH), Lewis and Clark National Historical Park (LEWI), Mount Rainier National Park (MORA), North Cascades National Park Service Complex (NOCA) and Olympic National Park (OLYM). Together, these parks provide refuge for landbirds dependent on a variety of habitats and also serve as reference sites for assessing the effects of land-use and land-cover change on bird populations throughout the Pacific Northwest (Silsbee and Peterson 1991, Simons et al. 1999, Siegel et al. 2012).

A synthesis of landbird monitoring results from five parks over 12 years should provide substantial insight into trends relevant to terrestrial ecosystems in the Pacific Northwest. Here, we apply recent developments in point-count analysis to estimate trends in population density for 68 species. We explore lagged effects of precipitation and temperature on the annual density of each species in every park, and effects of survey conditions on species detection. Applying a unified framework for trend analysis at local and regional scales, this synthesis extends landbird monitoring results summarized in several peer-reviewed publications (Siegel and Kuntz 2009, Siegel et al. 2012, Saracco et al. 2014, Ray et al. 2017 a, b) and in annual reports to the NCCN (Siegel et al. 2006, 2008, 2009; Wilkerson et al. 2007, 2009, 2010; Holmgren et al. 2011, 2012, 2013, 2014, 2015, 2016, 2017).

Methods

With the goal of monitoring population trends in multiple species, breeding-season point-counts are conducted annually at over one-hundred points in each mountain park and every two years at dozens of points in each historical park (Siegel et al. 2007, Saracco et al. 2014). To minimize annual variability related to the observation process, The Institute for Bird Populations (IBP) recruits qualified observers who must attend a three-week training session and pass an examination demonstrating proficiency in bird identification skills prior to conducting surveys. To minimize variability due to seasonal processes, surveys are timed to coincide with the peak in breeding activities—especially singing—for most species. In each year during 2005–2016, all surveys were conducted between May 20 and July 31, and points at lower elevations were targeted for survey earlier in the season than points at higher elevations, to better track peak breeding season by elevation. The survey design for each park is detailed in Siegel et al. (2007), Saracco et al. (2014) and Ray et al. (2017 a, b), and the design geodatabase is published within the NPS Data Store Integrated Resource Management Applications at <https://irma.nps.gov/DataStore/Reference/Profile/2208863>.

Sampling frame

Each historical park is surveyed in odd-numbered (SAJH) or even-numbered (LEWI) years at point-count stations distributed in a grid. The sampling frame for SAJH includes two park sub-units: American Camp on the southwest shore of San Juan Island, and the central portion of British Camp on the northwest shore. The sampling frame for LEWI includes Fort Clatsop and most of Cape Disappointment as well as Sunset Beach and the Yeon Property (Table 1). Although the Yeon Property was added to the park several years after monitoring began, we can estimate annual abundance at the stations in that sub-unit for every year of the monitoring effort because our modeling framework effectively allows for retroactive adjustments of the sampling frame. Annual population density can be estimated around every point-count station within the frame, regardless of missing data. This feature allowed seamless estimation of trends throughout the monitoring period despite a major reduction in the number of point-count stations after the first year of surveys in each historical park.

Table 1. Area (in hectares) of each park unit and elevational stratum surveyed, excluding the largely glaciated areas above 2500 m in MORA and 2029 m in OLYM. Boundaries defining high-, mid- and low-elevation strata were set at 1350 and 640 m above sea level in NOCA and OLYM, and at 1350 and 800 m in MORA.

Park / Total Area (ha)	Subunit/Stratum	Area (ha)
SAJH / 710	American Camp	505
	British Camp	205
LEWI / 1,216	Fort Clatsop	522
	Cape Disappointment	564
	Sunset Beach	90
	Yeon Property	39
MORA / 89,097	High-elevation	55,684
	Mid-elevation	29,602
	Low-elevation	3,811
NOCA / 275,448	High-elevation	142,376
	Mid-elevation	102,908
	Low-elevation	30,164
OLYM / 368,216	High-elevation	81,341
	Mid-elevation	175,751
	Low-elevation	111,124

Mountain parks are surveyed annually along point-count transects that originate on maintained travel routes (trails and some roads) and extend 1–2 km into off-trail habitats. The sampling frame in each mountain park consists of all potential transects with origins spaced every 50 m along maintained routes, excepting busy, steep or waterfront areas where off-trail sampling would not be possible. To ensure adequate sampling across elevations, origins were drawn from three elevational strata (Table 1), defined as low-elevation (<650 m above sea level), mid-elevation (650–1350 m) or high-elevation (>1350 m), with one exception: in MORA, where lower elevation habitat is more limited, the boundary between lower and middle elevations was set at 800 m. After excluding glaciated and barren areas unsuitable for breeding (above 2500 m in MORA and 2029 m in OLYM; no exclusions applied in NOCA), a set of spatially dispersed transect origins was selected for each mountain park using the Generalized Random-Tessellation Stratified (GRTS) sampling method (Stevens and Olsen 2004). Selected transects were grouped at random into six panels, one “annual” and five “alternating”; the annual and one alternating panel are surveyed each year. In NOCA and OLYM, each panel includes four transects from each elevational stratum, for 12 transects per panel and 72 transects per park. In MORA, each panel includes two fewer transects from the low stratum, for 10 transects per panel and 60 per park (Table 1 of Ray et al. 2017 a). Each transect links a set of point-count stations spaced at 200-m intervals, and each half-transect extends away from the trail at right angles or continues along the trail until a right-angle departure is feasible. Even though the areas sampled could not perfectly represent the mix of habitats and environmental conditions across the

entire landscapes of the parks, in all cases they included a broad diversity of habitats such that any bias introduced by this sampling design was deemed acceptably small relative to the safety and logistic benefits (Siegel et al. 2007, Saracco et al. 2014)

Survey and habitat covariates

At all parks, all bird species heard or seen during a seven-minute survey are recorded, along with the time-to-detection and distance-to-detection of each bird or of each group of birds acting as a flock, enabling analyses that account for birds present but undetected during each survey (Royle et al. 2004, Alldredge et al. 2007, Amundson et al. 2014). Surveys were lengthened from five to seven minutes, beginning in 2011, to expand options for modeling detection probability. Potential covariates of detection and abundance recorded during surveys include point coordinates, group size (number of birds acting as a unit—usually one bird), observer, date, start time, ambient noise level, vegetation type, presence of forest cover, and cover density. Potential covariates calculated from a digital elevation model using annual field records of point coordinates include elevation, aspect and slope.

We hypothesized that years of heavy snow and cooler spring temperatures could delay initiation of breeding and result in food scarcity early in the nesting season (Hahn et al. 2004, Pereyra 2011, Mathewson et al. 2012), leading to lower recruitment and lagged effects of lower breeding bird abundance in the subsequent year (DeSante 1990). To test this hypothesis, we used ClimateWNA as a source of downscaled climate data for Western North America because it uses bilinear interpolation and local elevation adjustment to downscale monthly, gridded, climate data as scale-free point data (Wang et al. 2016), providing climate metrics directly estimated for each point along our transects. Records from park SNOTEL sites and other local weather data are represented as inputs to the gridded climate product. Using the protocol and code in Appendix 3 of Ray et al. (2017 b), annual data and 1971–2000 normals were accessed from <http://www.climatewna.com>. As covariates of density, we considered metrics of precipitation and temperature hypothesized to affect breeding success. To characterize spring conditions, we selected mean spring temperature (MST, the average daily temperature from March 1 through May 31) and annual precipitation-as-snow (PAS, millimeters of snow falling between August 1 and July 31). Specifically, we calculated MST and PAS as anomalies, relative to 1971–2000 normals, under the expectation that breeding and recruitment would be inversely related to snowfall and directly related to temperature. For surveys in year t , lag-1 MST was the mean temperature anomaly from March 1 to May 31 of year $t-1$, and lag-1 PAS was the snowfall anomaly from Aug 1 of year $t-2$ to July 31 of year $t-1$. Following Graham (2003), we considered simultaneous effects of these correlated predictors by replacing MST with residual MST (rMST), the residuals of a linear regression of MST on PAS.

Analyses

In this synthesis of results from the first 12 years of monitoring, we focused on effects of park, elevation and climate on population density for species detected frequently enough to support estimates of detection probability and trend. Temporal trends in population density and effects of covariates on species detection and density were estimated for each park using a Bayesian hierarchical modeling framework outlined briefly here and detailed in Ray et al. (2017 a, b). Code and procedures used for generating this report are detailed in Appendix 1.

Hierarchical models involve the decomposition of a complex relationship into a series of interdependent sub-models to facilitate understanding and computation as well as to clarify each level of uncertainty in the relationship. A simple example would involve a count of y individuals from a population of size N and an individual detection probability of p . The hierarchy in this example involves one level at which y is a function of N and p , and another level at which p is a function of potential covariates like observer identity and day of year. Bayesian models allow estimation of the “posterior” probability density of each parameter value, provided that a “prior” probability density is supplied that summarizes any prior information about the distribution of values the parameter might take. Bayesian methods require estimation of the joint probability density of all model parameters, a computationally intensive process facilitated by simulation methods such as Markov chain Monte Carlo (MCMC). MCMC can be used to sample from the joint posterior distribution of model parameters by jumping around (almost) randomly in parameter space to test for parameter values that maximize the probability of obtaining the observed data given the proposed model. If we require that the joint probability of obtaining the observed data generally increases as we jump around, then a long series (MCMC chain) of jumps (samples) will eventually converge in the vicinity of the best estimates for each parameter, and plotting a histogram of samples from this vicinity will reveal the shape of each parameter’s posterior distribution. We used the JAGS programmable platform (Plummer 2003) to perform MCMC simulation and to provide summaries of the resulting samples, such as a credible interval (CRI) for each parameter estimate. In this report, a 95% CRI refers to a Bayesian credible interval which contains the value of the focal parameter with a subjective probability of 0.95.

Our three-level hierarchical model allowed estimation of 1) components of individual detection, including effects of covariates on probabilities of individual “availability” and “perceptibility”, where availability is the probability that a bird will perform a detectable action, like singing, while perceptibility is the probability that observers will perceive that action; 2) the relationship between bird abundance and yearly point-counts, as a function of availability and perceptibility; and 3) spatiotemporal trends in abundance, including effects of climate. Data from multiple count intervals were used to generate individual detection histories modeled within a closed-population framework to characterize availability (Alldredge et al. 2007). We followed Farnsworth et al. (2002) in modeling availability from time-removal data, in which each detection of a unique individual was assigned to one of three count intervals (minutes 0–3, 3–5 or 5–7), and subsequent detections of the same individual were ignored. We modeled availability as a function of q , the per-minute probability of a bird’s failure to sing or otherwise be available for detection. The probability that a bird was present and not available during all three count intervals (totaling seven minutes) was q^7 , and availability was $1-q^7$. We modeled availability as a function of point- and/or year-specific covariates, x_{kt} , as $\text{logit}(q_{kt}) = \alpha_0 + \sum_x \alpha_x x_{kt}$, where subscripts k and t indicate point and year. To characterize effects of distance on perceptibility, we first dropped about 10% of the farthest (least accurate) detections of each species to obtain the maximum effective detection distance (per Kéry and Royle 2016) and then sorted the remaining detection distances into variable-width bins, equalizing the number of detections in each bin (Amundson et al. 2014). We followed Buckland et al. (2001) in modeling the probability of detecting a bird in distance bin b using the half-normal distribution, which is controlled by shape

parameter σ , the decay rate of detections with distance. We then modeled perceptibility as a function of point- and year-specific covariates as $\log(\sigma_{kt}) = \log(\sigma_0) + \sum_x \alpha_x X_{kt}$.

We combined these models of q and σ (components of p) with a model of N in an “ N -mixture” or binomial mixture model. N -mixture models typically pair a Poisson model of N (abundance) with a binomial model of y (count). N -mixture models provide a hierarchical extension of generalized linear models (GLMs), linking multiple GLMs to allow for structure in parameters at each hierarchical level (Royle 2004). In this report, a Poisson model of λ (expected N) as a function of environmental covariates is linked with two binomial models expressing detection as functions of survey conditions. Table 2 summarizes the models considered here.

Table 2. Models used to estimate components of detection probability and abundance of landbird populations in the NCCN during 2005-2016. Metrics of availability (q), perceptibility (σ) and abundance (λ = expected N) of each population were estimated using generalized linear models linked to form an N -mixture model. Covariates of q and σ explored in basic and climate models of type B included *day*, *hour*, *observer*, *forest presence* and *noise*. Subscripts k and t indicate point-count station and year, respectively.

Model	Linear predictors
Basic A	$\text{logit}(q_{kt}) = \alpha_0$
	$\log(\sigma_{kt}) = \log(\sigma_0)$
	$\log(\lambda_{kt}) = \beta_0 + \beta_1 \text{year}_t$
Basic B	$\text{logit}(q_{kt}) = \alpha_0 + \sum_x \alpha_x X_{kt}$
	$\log(\sigma_{kt}) = \log(\sigma_0) + \sum_x \alpha_x X_{kt}$
	$\log(\lambda_{kt}) = \beta_{0,\text{park}[k]} + \beta_{1,\text{park}[k]} \text{year}_t + \beta_2 \text{elevation}_k + \beta_3 \text{elevation}_k^2 + \text{year}_t^* + \text{transect}_k^*$
Climate A	$\text{logit}(q_{kt}) = \alpha_0$
	$\log(\sigma_{kt}) = \log(\sigma_0)$
	$\log(\lambda_{kt}) = \beta_0 + \beta_1 \text{year}_t + \beta_2 \text{PAS}_{kt} + \beta_3 \text{rMST}_{kt}$
Climate B	$\text{logit}(q_{kt}) = \alpha_0 + \sum_x \alpha_x X_{kt}$
	$\log(\sigma_{kt}) = \log(\sigma_0) + \sum_x \alpha_x X_{kt}$
	$\log(\lambda_{kt}) = \beta_{0,\text{park}[k]} + \beta_{1,\text{park}[k]} \text{year}_t + \beta_2 \text{PAS}_{kt} + \beta_3 \text{PAS}_{kt}^2 + \beta_4 \text{rMST}_{kt} + \text{year}_t^* + \text{transect}_k^*$

*Random effects

Basic models (Table 2) featured a log-linear trend in expected N (λ_{kt}) and either (A) no covariates or (B) covariates of detection and abundance including fixed effects of park and elevation (linear and quadratic) as well as random effects of year and transect. Climate models featured either (A) a log-linear trend in abundance and fixed effects of PAS and rMST or (B) features in A plus fixed effects of PAS^2 , random effects of year and transect, and covariates of detection. In general, basic and climate models of type A were applied to data from historical parks, which were not suited to models with year and transect effects; these parks lacked transects and were never surveyed in the same year, so random effects of park and year would be confounded in any combined dataset. For this reason, we estimated trends in each historical park separately. In contrast, data from the three mountain parks were usually combined to fit basic or climate models of type B, which included park-specific trends

in abundance. By fitting a single model to data from multiple parks, we were able to borrow power from parks with higher counts to estimate parameters for parks with lower counts. The higher counts and larger datasets offered by the mountain parks also supported the estimation of more parameters in each model, allowing us to quantify nonlinear effects of elevation and PAS as well as covariates of detection.

In addition to fitting the coefficients in Table 2, we estimated annual population density (N per hectare) averaged over all point-count stations within a unit (park, elevational stratum or, for certain habitat specialists, park sub-unit) by dividing the sum of N across all stations in the unit by the number of stations in the unit and the effective area surveyed at each station. Effective area surveyed varied with detection distance for the species. For each species potentially in decline across the Pacific Northwest, we also estimated the 12-year time series of regional N averaged over all stations in all parks where the species was common enough to support parameter estimation. Model fit was characterized using Bayesian P -values, and convergence of parameter estimates was assessed using the Gelman-Rubin potential scale reduction parameter, R -hat, and visual inspection of MCMC samples as detailed in Ray et al. (2017 a).

For comparison with estimates of annual population density, we also present raw annual counts corrected for survey effort and rescaled for presentation. Effort was calculated as the total number of point-minutes surveyed in each year, which varied with the number of points accessed each year (by chance and due to the reduction in point-count station density after the first year of surveys) and with the number of count intervals per survey (increased from 2 to 3 intervals—from 5 to 7 minutes—in 2011). Raw counts from each year were divided by the year's effort and rescaled for ease of comparison on a log10 scale by setting the lowest non-zero, effort-adjusted count to 1. Specifically, the raw count for species x in year t , $Ct_{x,t}^{\text{raw}}$, was corrected for effort as $Ct_{x,t}^{\text{c}} = Ct_{x,t}^{\text{raw}}/P_t/M_t$, where P_t was the number of points surveyed and M_t was the number of minutes surveyed per point in year t . Counts corrected for survey effort were then rescaled as $Ct_{x,t} = Ct_{x,t}^{\text{c}}/\text{min}_{\text{nz}}(Ct_{x,t}^{\text{c}})$, where $\text{min}_{\text{nz}}(Ct_{x,t}^{\text{c}})$ was the smallest non-zero value of $Ct_{x,t}^{\text{c}}$. Zero values of $Ct_{x,t}$ appear as missing data, in order to emphasize years with zero detection of the focal species.

Estimates of N were obtained for all point-count stations, even in years without counts, because the modeling framework adopted here is robust to missing data (Kéry and Royle 2016). We exploited this feature to model data from every point-count station that was surveyed at least once during the study period, with one exception. This exception involved 10 stations retired from LEWI in 2006 that fell outside the final sampling frame, including eight stations in the northern portion of the Cape Disappointment peninsula (points 38–45) and two points in Dismal Nitch (87 and 89). Estimates of annual population density and effort-adjusted counts reported here were calculated after omitting these 10 stations, so that the scope of inference for LEWI does not include Dismal Nitch or the narrow, northern reach of Cape Disappointment.

The analytical approach adopted here is suited to situations in which only a single visit to each point-count station is possible within the breeding season (Amundson et al. 2014). We adopted this approach because the scale and topography of our sampling frame combined to preclude multiple visits within the short breeding season, given the monitoring resources available. However, single-

visit studies cannot estimate variation in detection probability throughout the breeding season (Schmidt et al. 2013, Mizel et al. 2017). Our models assume constant detection probability, which might limit our ability to isolate trends in abundance. For example, if we estimated N during a period of low detection probability in one year and during a period of high detection probability in the next year, we would be more likely to infer a decline in population size than if detection probability were truly constant. To minimize variation in detection probability, surveys are timed to coincide with the local peak in territorial breeding behavior, with the understanding that shifting phenology could advance or retard this peak over time, potentially confounding trends in abundance with trends in detection.

Results and Discussion

From 2005 to 2016, we completed 11,457 point-count surveys (Table 3) at 3,539 unique point-count stations distributed throughout the five monitored parks (163 at SAJH, 86 at LEWI, 1,012 at MORA, 1,181 at NOCA, and 1,097 at OLYM). Each station was surveyed 1–12 times (Table 4), depending on its park and panel membership; e.g., 810 stations were surveyed once and 251 were surveyed 12 times. Stations surveyed 12 times were on the annual panel of transects in a mountain park, while those surveyed once included points retired early in the monitoring period or those accessed infrequently because they were located at the distal end of a mountain park transect. The number of stations surveyed along each mountain transect during 2005–2016 was 15.15 ± 0.20 (mean \pm SE), with a range of 4–25.

Table 3. Survey effort by year and park. Number of point-count surveys completed and number of unique points surveyed during 2005–2016 at each park in the North Coast and Cascades Network landbird monitoring project.

Year	Number of point-count surveys completed					Survey minutes	
	SAJH	LEWI	MORA	NOCA	OLYM	Per point	Total
2005	109	–	135	167	125	5	2680
2006	–	81 [†]	140	181	123	5	2625
2007	54	–	268	316	300	5	4690
2008	–	68	287	316	303	5	4870
2009	54	–	289	361	310	5	5070
2010	–	71	251	275	318	5	4575
2011	54	–	140	298	331	7	5761
2012	–	71	287	396	346	7	7700
2013	54	–	306	409	349	7	7826
2014	–	74	330	429	355	7	8316
2015	54	–	355	374	374	7	8099
2016	–	73	353	382	361	7	8183
Total	379	438	3141	3904	3595	–	70395

[†]Of these 81 points, 10 (eight in Cape Disappointment State Park and two in Dismal Nitch) were retired after 2006 and data from all 10 were omitted from all LEWI analyses, including survey-effort adjustments.

Table 4. Unique point-count stations grouped by number of surveys completed during 2005–2016.

Number of surveys	Number of stations
1	810 [†]
2	2034
3	11
4	11
5	72
6	81
7	20
8	20
9	53
10	69
11	107
12	251

[†]Including 10 points in Lewis and Clark National Historical Park that were retired after 2006 and were omitted from all analyses reported here.

The point-counts resulted in 98,539 species-specific detections of individual birds or groups behaving as flocks. Individual birds accounted for 97.25% (95,828) of all detections (Table 5), while larger groups or flocks accounted for 2.59% (2,553). Counts of zero, where no species were detected, occurred in just 0.16% (158) of all point-count surveys. Most group sizes ranged up through five birds. Outliers in group size were set to seven to improve detection model fit.

Table 5. Size and number of species-specific groups detected during 2005–2016.

Group size	Number of groups
0	158
1	95828
2	920
3	608
4	267
5	251
6	106
7	59
8	65
9	18
10	54
11	8
12	33
13	9

Table 5 (continued). Size and number of species-specific groups detected during 2005–2016.

Group size	Number of groups
14	5
15	29
16	6
17	5
18	5
19	5
20	17
21	1
22	3
23	3
24	3
25	8
26	1
27	1
29	1
30	10
32	2
33	2
35	3
37	1
40	3
44	1
45	1
47	1
50	7
54	1
55	1
73	1
75	2
81	1
97	1
100	8
150	1
200	15

We detected at least 156 bird species in these five parks during 2005–2016, including 116 species detected at least 10 times (Table 6). Most of the species detected were landbirds, although seabirds were also common. Rarer species, detected less than 10 times across all parks, included American

Redstart, Black-backed Woodpecker, Common Murre, Double-crested Cormorant, Turkey Vulture, American Kestrel, Great Blue Heron, Ring-necked Pheasant, Canyon Wren, Lincoln's Sparrow, Northern Goshawk, Say's Phoebe, White-breasted Nuthatch, Black Oystercatcher, Cliff Swallow, Merlin, Red-naped Sapsucker, Rock Wren, White-tailed Ptarmigan, Barrow's Goldeneye, Cooper's Hawk, Pied-billed Grebe, Sharp-shinned Hawk, Virginia Rail, Western Bluebird, Blue-winged Teal, California Gull, Prairie Falcon, Western Screech-Owl, Whimbrel, American Golden-Plover, Brewer's Blackbird, Cackling Goose, Clay-colored Sparrow¹, Golden-crowned Sparrow, Greater Yellowlegs, Green-winged Teal, Williamson's Sapsucker, Wood Duck and hybrids of Hermit and Townsend's Warbler. Of these rarely detected species, Hermit-Townsend's Warbler hybrids were the most commonly recorded.

Table 6. Total and park-specific counts for 116 bird species detected 10 or more times during 2005–2016 point-count surveys across five parks of the North Coast and Cascades Inventory and Monitoring Network (NCCN): San Juan Island National Historical Park (SAJH), Lewis and Clark National Historical Park (LEWI), Mount Rainier National Park (MORA), North Cascades National Park Complex (NOCA) and Olympic National Park (OLYM). SAJH and LEWI were surveyed in even and odd years, respectively, while MORA, NOCA and OLYM were surveyed every year.

Code	Species	NCCN	SAJH	LEWI	MORA	NOCA	OLYM
DEJU	Dark-eyed Junco, <i>Junco hyemalis</i>	7909	107	154	2133	2183	3332
PISI	Pine Siskin, <i>Spinus pinus</i>	7083	107	3	1840	3166	1967
PAWR	Pacific Wren, <i>Troglodytes pacificus</i>	6798	75	481	2058	1616	2568
VATH	Varied Thrush, <i>Ixoreus naevius</i>	6646	26	11	2656	1852	2101
CBCH	Chestnut-backed Chickadee, <i>Poecile rufescens</i>	5186	186	213	1461	1568	1758
SWTH	Swainson's Thrush, <i>Catharus ustulatus</i>	4193	259	742	173	2639	380
PSFL	Pacific-slope Flycatcher, <i>Empidonax difficilis</i>	4171	300	423	782	304	2362
GCKI	Golden-crowned Kinglet, <i>Regulus satrapa</i>	4148	67	215	1236	1067	1563
TOWA	Townsend's Warbler, <i>Setophaga townsendi</i>	3953	99	27	871	2108	848
AMRO	American Robin, <i>Turdus migratorius</i>	3950	606	368	425	1334	1217
RBNU	Red-breasted Nuthatch, <i>Sitta Canadensis</i>	3344	162	33	970	1240	939
HETH	Hermit Thrush, <i>Catharus guttatus</i>	3338	0	0	1077	1364	897

¹ Vagrant, far outside of its expected breeding or migrating range

Table 6 (continued). Total and park-specific counts for 116 bird species detected 10 or more times during 2005–2016 point-count surveys across five parks of the North Coast and Cascades Inventory and Monitoring Network (NCCN): San Juan Island National Historical Park (SAJH), Lewis and Clark National Historical Park (LEWI), Mount Rainier National Park (MORA), North Cascades National Park Complex (NOCA) and Olympic National Park (OLYM). SAJH and LEWI were surveyed in even and odd years, respectively, while MORA, NOCA and OLYM were surveyed every year.

Code	Species	NCCN	SAJH	LEWI	MORA	NOCA	OLYM
RECR	Red Crossbill, <i>Loxia curvirostra</i>	2608	231	52	798	618	909
WETA	Western Tanager, <i>Piranga ludoviciana</i>	2489	61	113	130	1893	292
YRWA	Yellow-rumped Warbler, <i>Setophaga coronate</i>	2440	45	19	226	1964	186
HAFL	Hammond's Flycatcher, <i>Empidonax hammondi</i>	2383	2	1	260	1500	620
EVGR	Evening Grosbeak, <i>Coccothraustes vespertinus</i>	1878	1	18	492	1010	357
WAVI	Warbling Vireo, <i>Vireo gilvus</i>	1598	83	59	75	992	389
BRCR	Brown Creeper, <i>Certhia americana</i>	1560	69	55	577	392	467
YEWA	Yellow Warbler, <i>Setophaga petechia</i>	1148	20	70	16	950	92
WIWA	Wilson's Warbler, <i>Cardellina pusilla</i>	1101	96	373	45	154	433
GRAJ	Gray Jay, <i>Perisoreus canadensis</i>	1042	0	0	440	184	418
RUHU	Rufous Hummingbird, <i>Selasphorus rufus</i>	994	80	32	190	416	276
CHSP	Chipping Sparrow, <i>Spizella passerina</i>	958	21	0	84	839	14
MGWA	MacGillivray's Warbler, <i>Geothlypis tolmiei</i>	923	1	5	23	824	70
OSFL	Olive-sided Flycatcher, <i>Contopus cooperi</i>	896	61	67	96	360	312
GWGU	Glaucous-winged Gull, <i>Larus glaucescens</i>	867	726	141	0	0	0
SOSP	Song Sparrow, <i>Melospiza melodia</i>	744	161	273	25	180	105
SOGR	Sooty Grouse, <i>Dendragapus fuliginosus</i>	741	0	0	58	304	379
STJA	Steller's Jay, <i>Cyanocitta stelleri</i>	704	1	75	193	183	252
NOFL	Northern Flicker, <i>Colaptes auratus</i>	687	33	29	114	180	331
BTYW	Black-throated Gray Warbler, <i>Setophaga nigrescens</i>	667	67	112	17	258	213

Table 6 (continued). Total and park-specific counts for 116 bird species detected 10 or more times during 2005–2016 point-count surveys across five parks of the North Coast and Cascades Inventory and Monitoring Network (NCCN): San Juan Island National Historical Park (SAJH), Lewis and Clark National Historical Park (LEWI), Mount Rainier National Park (MORA), North Cascades National Park Complex (NOCA) and Olympic National Park (OLYM). SAJH and LEWI were surveyed in even and odd years, respectively, while MORA, NOCA and OLYM were surveyed every year.

Code	Species	NCCN	SAJH	LEWI	MORA	NOCA	OLYM
HAWO	Hairy Woodpecker, <i>Picoides villosus</i>	625	13	20	110	226	256
BHGR	Black-headed Grosbeak, <i>Pheucticus melanocephalus</i>	606	39	150	18	358	41
WCSP	White-crowned Sparrow, <i>Zonotrichia leucophrys</i>	583	328	118	18	29	90
AMCR	American Crow, <i>Corvus brachyrhynchos</i>	578	199	312	2	4	61
VASW	Vaux's Swift, <i>Chaetura vauxi</i>	522	5	1	181	138	197
NAWA	Nashville Warbler, <i>Oreothlypis ruficapilla</i>	508	1	0	2	505	0
BHCO	Brown-headed Cowbird, <i>Molothrus ater</i>	497	277	114	0	104	2
MOCH	Mountain Chickadee, <i>Poecile gambeli</i>	491	0	0	120	371	0
OCWA	Orange-crowned Warbler, <i>Oreothlypis celata</i>	480	269	141	7	15	48
AMPI	American Pipit, <i>Anthus rubescens</i>	432	0	0	257	51	124
SAVS	Savannah Sparrow, <i>Passerculus sandwichensis</i>	412	368	21	13	10	0
WEWP	Western Wood-Pewee, <i>Contopus sordidulus</i>	400	3	11	6	366	14
AMGO	American Goldfinch, <i>Spinus tristis</i>	393	309	80	0	4	0
CEDW	Cedar Waxwing, <i>Bombycilla cedrorum</i>	378	44	68	10	237	19
CAVI	Cassin's Vireo, <i>Vireo cassinii</i>	373	35	2	1	334	1
SPTO	Spotted Towhee, <i>Pipilo maculatus</i>	370	269	36	1	59	5
CATE	Caspian Tern, <i>Hydroprogne caspia</i>	367	1	366	0	0	0
CORA	Common Raven, <i>Corvus corax</i>	366	70	67	86	54	89
CAFI	Cassin's Finch, <i>Haemorhous cassinii</i>	342	0	0	36	306	0
HOWR	House Wren, <i>Troglodytes aedon</i>	315	265	0	0	46	4

Table 6 (continued). Total and park-specific counts for 116 bird species detected 10 or more times during 2005–2016 point-count surveys across five parks of the North Coast and Cascades Inventory and Monitoring Network (NCCN): San Juan Island National Historical Park (SAJH), Lewis and Clark National Historical Park (LEWI), Mount Rainier National Park (MORA), North Cascades National Park Complex (NOCA) and Olympic National Park (OLYM). SAJH and LEWI were surveyed in even and odd years, respectively, while MORA, NOCA and OLYM were surveyed every year.

Code	Species	NCCN	SAJH	LEWI	MORA	NOCA	OLYM
RBSA	Red-breasted Sapsucker, <i>Sphyrapicus ruber</i>	293	1	0	22	246	24
CLNU	Clark's Nutcracker, <i>Nucifraga columbiana</i>	288	0	0	82	200	6
PUFI	Purple Finch, <i>Haemorhous purpureus</i>	285	90	159	3	32	1
FOSP	Fox Sparrow, <i>Passerella iliaca</i>	272	0	0	105	167	0
TOSO	Townsend's Solitaire, <i>Myadestes townsendi</i>	248	0	0	34	101	113
RWBL	Red-winged Blackbird, <i>Agelaius phoeniceus</i>	244	126	112	2	3	1
CANG	Canada Goose, <i>Branta canadensis</i>	240	137	74	0	27	2
BTPI	Band-tailed Pigeon, <i>Patagioenas fasciata</i>	228	11	35	24	14	144
HEWA	Hermit Warbler, <i>Setophaga occidentalis</i>	208	0	145	48	0	15
BRPE	Brown Pelican, <i>Pelecanus occidentalis</i>	184	0	184	0	0	0
PIWO	Pileated Woodpecker, <i>Dryocopus pileatus</i>	181	24	7	35	56	59
COYE	Common Yellowthroat, <i>Geothlypis trichas</i>	175	44	116	1	12	2
BARS	Barn Swallow, <i>Hirundo rustica</i>	171	70	70	30	1	0
PIGR	Pine Grosbeak, <i>Pinicola enucleator</i>	169	0	0	30	43	96
RCKI	Ruby-crowned Kinglet, <i>Regulus calendula</i>	167	0	0	3	100	64
VGSW	Violet-green Swallow, <i>Tachycineta thalassina</i>	148	9	56	13	56	14
MAWR	Marsh Wren, <i>Cistothorus palustris</i>	130	0	130	0	0	0
GCRF	Gray-crowned Rosy-Finch, <i>Leucosticte tephrocotis</i>	129	0	0	86	22	21
BAEA	Bald Eagle, <i>Haliaeetus leucocephalus</i>	121	71	35	0	5	10
DUFL	Dusky Flycatcher, <i>Empidonax oberholseri</i>	118	1	0	1	115	1

Table 6 (continued). Total and park-specific counts for 116 bird species detected 10 or more times during 2005–2016 point-count surveys across five parks of the North Coast and Cascades Inventory and Monitoring Network (NCCN): San Juan Island National Historical Park (SAJH), Lewis and Clark National Historical Park (LEWI), Mount Rainier National Park (MORA), North Cascades National Park Complex (NOCA) and Olympic National Park (OLYM). SAJH and LEWI were surveyed in even and odd years, respectively, while MORA, NOCA and OLYM were surveyed every year.

Code	Species	NCCN	SAJH	LEWI	MORA	NOCA	OLYM
BLSW	Black Swift, <i>Cypseloides niger</i>	115	0	0	10	104	1
HOFI	House Finch, <i>Haemorhous mexicanus</i>	110	108	2	0	0	0
REVI	Red-eyed Vireo, <i>Vireo olivaceus</i>	110	0	0	0	110	0
EUST	European Starling, <i>Sturnus vulgaris</i>	104	70	29	0	0	5
SPSA	Spotted Sandpiper, <i>Actitis macularius</i>	104	0	0	26	31	47
PECO	Pelagic Cormorant, <i>Phalacrocorax pelagicus</i>	99	14	85	0	0	0
BEWR	Bewick's Wren, <i>Thryomanes bewickii</i>	84	35	48	1	0	0
HUVI	Hutton's Vireo, <i>Vireo huttoni</i>	75	9	50	2	0	14
AMDI	American Dipper, <i>Cinclus mexicanus</i>	73	0	0	19	20	34
BCCH	Black-capped Chickadee, <i>Poecile atricapillus</i>	72	1	59	4	6	2
MOBL	Mountain Bluebird, <i>Sialia currucoides</i>	67	0	0	42	25	0
CAHU	Calliope Hummingbird, <i>Selasphorus calliope</i>	59	0	0	5	54	0
SUSC	Surf Scoter, <i>Melanitta perspicillata</i>	55	55	0	0	0	0
RHAU	Rhinoceros Auklet, <i>Cerorhinca monocerata</i>	52	52	0	0	0	0
VEER	Veery, <i>Catharus fuscescens</i>	48	0	0	1	47	0
MAMU	Marbled Murrelet, <i>Brachyramphus marmoratus</i>	47	0	0	1	0	46
DOWO	Downy Woodpecker, <i>Picoides pubescens</i>	46	0	12	0	23	11
CAQU	California Quail, <i>Callipepla californica</i>	44	44	0	0	0	0
NRWS	Northern Rough-winged Swallow, <i>Stelgidopteryx serripennis</i>	43	16	8	0	4	15
LAZB	Lazuli Bunting, <i>Passerina amoena</i>	42	0	0	4	37	1

Table 6 (continued). Total and park-specific counts for 116 bird species detected 10 or more times during 2005–2016 point-count surveys across five parks of the North Coast and Cascades Inventory and Monitoring Network (NCCN): San Juan Island National Historical Park (SAJH), Lewis and Clark National Historical Park (LEWI), Mount Rainier National Park (MORA), North Cascades National Park Complex (NOCA) and Olympic National Park (OLYM). SAJH and LEWI were surveyed in even and odd years, respectively, while MORA, NOCA and OLYM were surveyed every year.

Code	Species	NCCN	SAJH	LEWI	MORA	NOCA	OLYM
WIFL	Willow Flycatcher, <i>Empidonax traillii</i>	40	1	0	1	31	7
MALL	Mallard, <i>Anas platyrhynchos</i>	39	13	22	0	1	3
HOLA	Horned Lark, <i>Eremophila alpestris</i>	38	0	0	13	2	23
OSPR	Osprey, <i>Pandion haliaetus</i>	37	1	7	10	13	6
PIGU	Pigeon Guillemot, <i>Cephus columba</i>	35	35	0	0	0	0
BEKI	Belted Kingfisher, <i>Megasceryle alcyon</i>	32	5	1	0	8	18
MODO	Mourning Dove, <i>Zenaida macroura</i>	31	29	0	0	0	2
WEGU	Western Gull, <i>Larus occidentalis</i>	31	0	31	0	0	0
BADO	Barred Owl, <i>Strix varia</i>	28	0	1	4	15	8
RUGR	Ruffed Grouse, <i>Bonasa umbellus</i>	25	0	0	9	6	10
ATTW	American Three-toed Woodpecker, <i>Picoides dorsalis</i>	22	0	0	4	14	4
TRES	Tree Swallow, <i>Tachycineta bicolor</i>	22	1	10	0	2	9
EUCD	Eurasian Collared-Dove, <i>Streptopelia decaocto</i>	21	10	9	0	0	2
BUSH	Bushtit, <i>Psaltriparus minimus</i>	19	14	4	0	0	1
NOPO	Northern Pygmy-Owl, <i>Glaucidium gnoma</i>	19	0	1	4	4	10
RTHA	Red-tailed Hawk, <i>Buteo jamaicensis</i>	18	7	3	2	1	5
CONI	Common Nighthawk, <i>Chordeiles minor</i>	15	0	0	3	7	5
ANHU	Anna's Hummingbird, <i>Calypte anna</i>	13	1	12	0	0	0
COLO	Common Loon, <i>Gavia immer</i>	13	4	1	0	8	0
PALO	Pacific Loon, <i>Gavia pacifica</i>	13	11	2	0	0	0

Table 6 (continued). Total and park-specific counts for 116 bird species detected 10 or more times during 2005–2016 point-count surveys across five parks of the North Coast and Cascades Inventory and Monitoring Network (NCCN): San Juan Island National Historical Park (SAJH), Lewis and Clark National Historical Park (LEWI), Mount Rainier National Park (MORA), North Cascades National Park Complex (NOCA) and Olympic National Park (OLYM). SAJH and LEWI were surveyed in even and odd years, respectively, while MORA, NOCA and OLYM were surveyed every year.

Code	Species	NCCN	SAJH	LEWI	MORA	NOCA	OLYM
COME	Common Merganser, <i>Mergus merganser</i>	12	0	0	1	9	2
PEFA	Peregrine Falcon, <i>Falco peregrinus</i>	11	0	8	2	1	0
VESP	Vesper Sparrow, <i>Pooecetes gramineus</i>	11	10	0	1	0	0
KILL	Killdeer, <i>Charadrius vociferus</i>	10	7	3	0	0	0

Climatic variation during the monitoring period

Our metrics of spring conditions, precipitation-as-snow (PAS) and mean spring temperature (MST), exhibited no clear trend during the monitoring period. Focusing on the covariates used in our analyses, lagged one year to allow for demographic response to breeding habitat conditions, the annual PAS anomaly generally increased during 2004–2011 and then declined (Figure 1), while the annual MST anomaly generally declined during 2004–2011 and then increased (Figure 2). The PAS anomaly during 2004–2015 was lower than 1971–2000 normals (Figure 1), while the MST anomaly was higher than 1971–2000 normals (Figure 2). Thus, snows were lighter and springs warmer during the monitoring period relative to the long-term average. Differentiating our metrics of spring conditions by park (Figure 3) suggests that only mountain parks experienced lighter snowpacks and warmer springs during the monitoring period. Among mountain parks, MORA and NOCA experienced the lightest snowpacks and warmest springs.

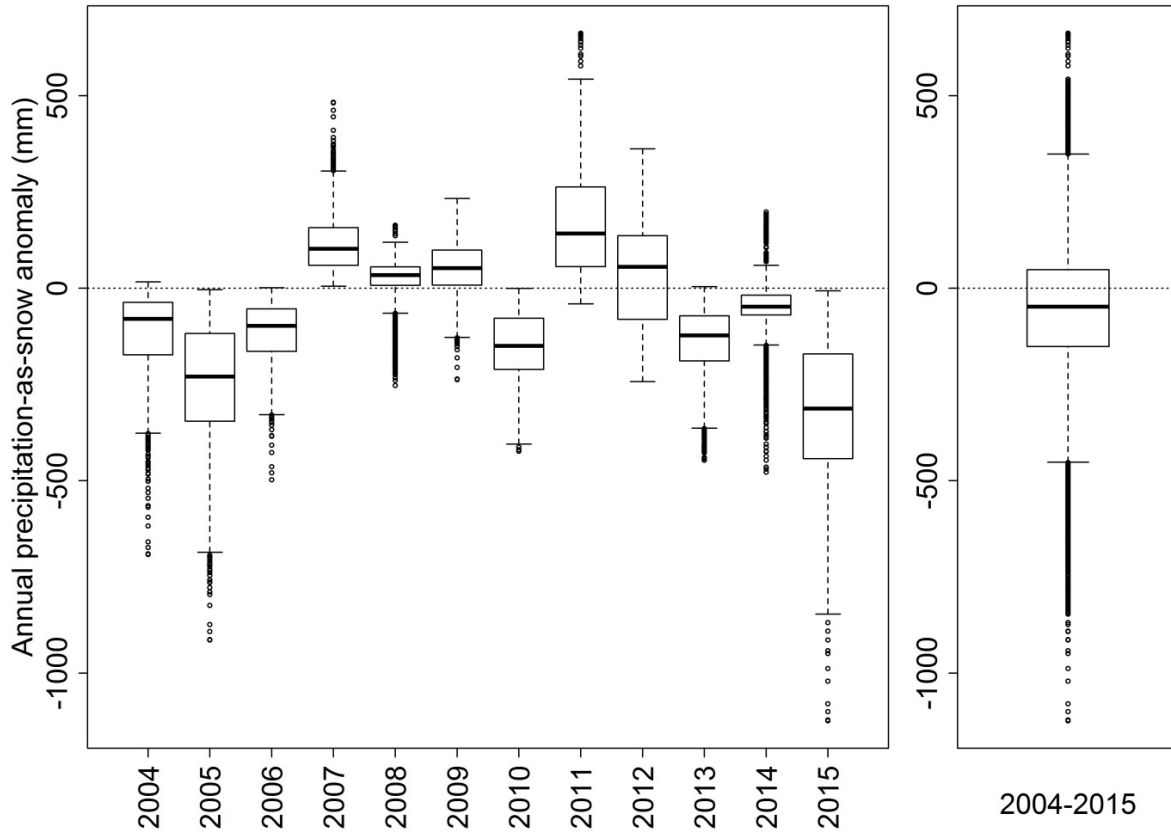


Figure 1. Precipitation-as-snow (PAS) anomaly (deviation from 1971–2000 normals) for data from August 1st of year $t-1$ to July 31st of year t , expressed as yearly anomalies for each point-count station in the North Coast and Cascades Network (left-hand panel) or as anomalies averaged over 12 years for each station (right-hand panel). As a covariate, this anomaly would be lagged one year; e.g., the 2015 anomaly is based on 08/01/2014–07/31/2015 PAS and serves as a potential covariate of breeding bird counts in 2016. Each boxplot indicates the median (thick horizontal line), interquartile range (box), and range of the data (whiskers), excepting outliers (dots) that occur outside the box by more than 1.5 times the interquartile range.

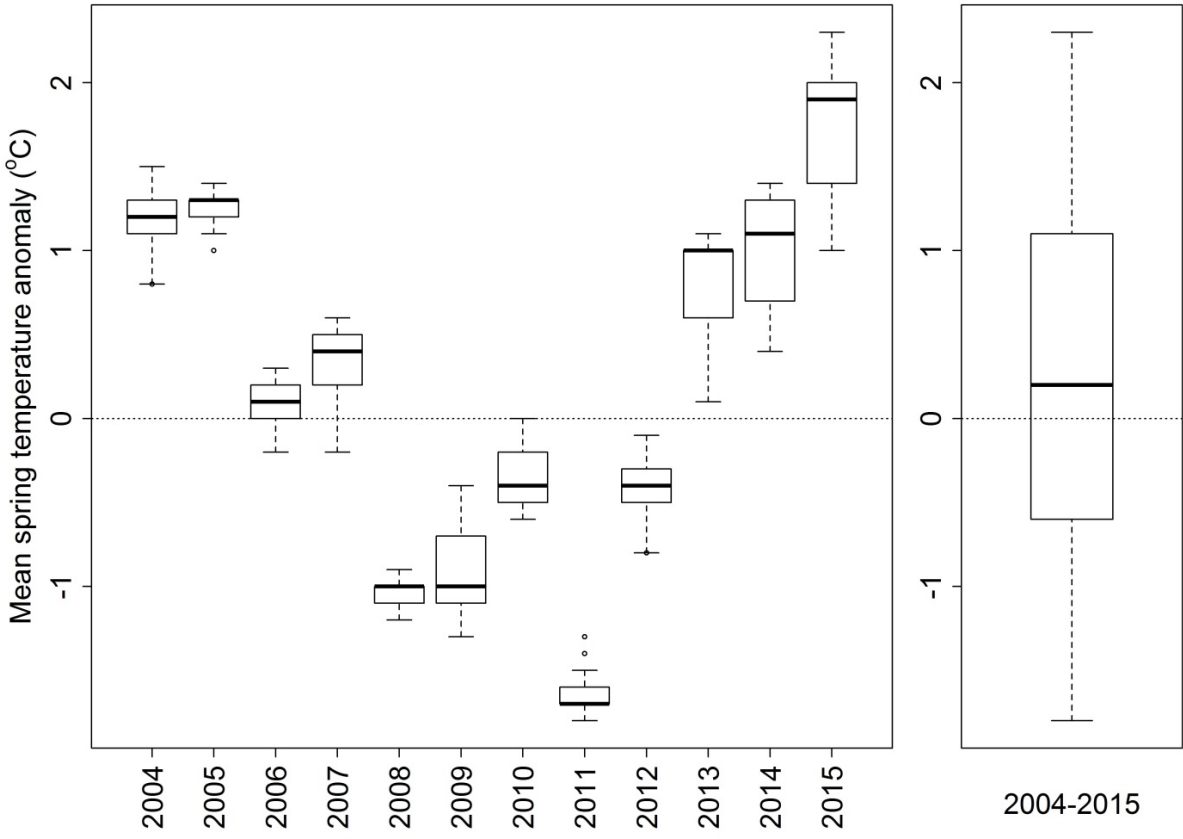


Figure 2. Mean spring temperature (MST) anomaly (deviation from 1971–2000 normals) for data from March 1st to May 31st of year t , expressed as yearly anomalies for each point-count station in the North Coast and Cascades Network (left-hand panel) or as anomalies averaged over 12 years for each station (right-hand panel). As a covariate, this anomaly would be lagged one year; e.g., the 2015 anomaly is based on 03/01/2015–05/31/2015 MST and serves as a potential covariate of breeding bird counts in 2016. Each boxplot indicates the median (thick horizontal line), interquartile range (box), and range of the data (whiskers), excepting outliers (dots) that occur outside the box by more than 1.5 times the interquartile range.

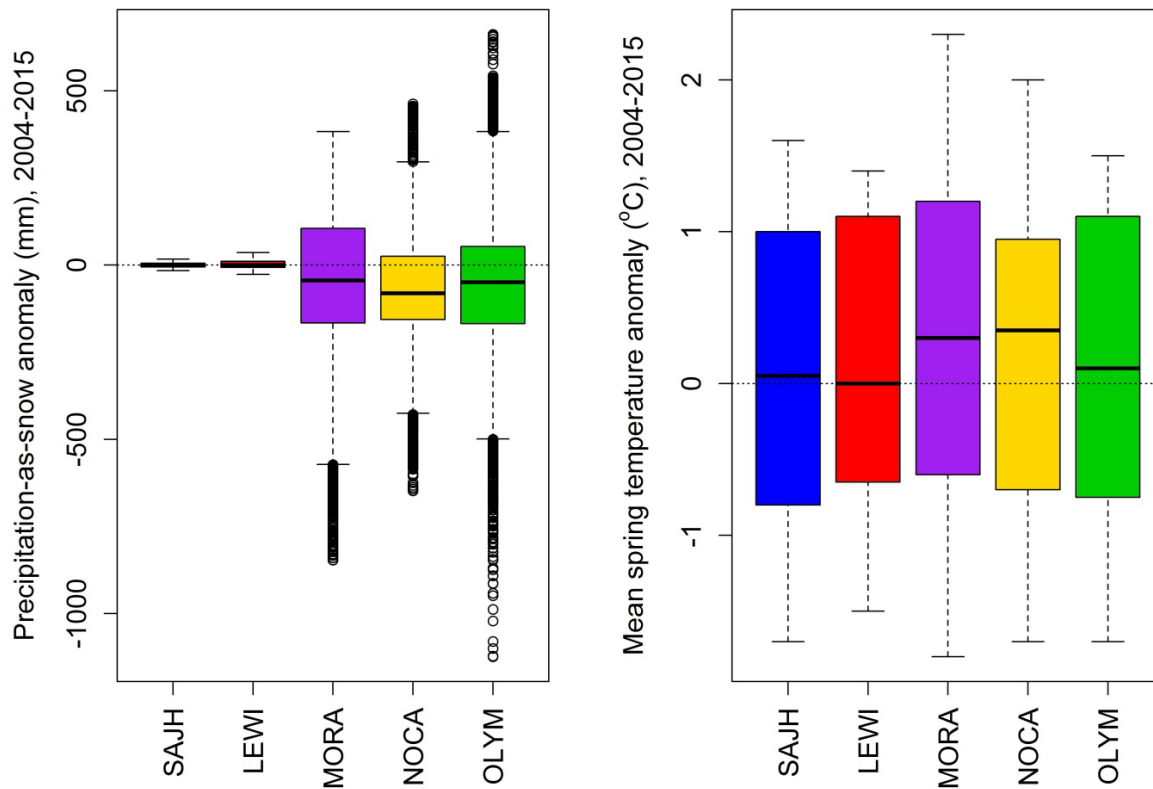


Figure 3. Anomalies in precipitation-as-snow (left-hand panel) and mean spring temperature (right-hand panel) for each park monitored. Each anomaly represents the deviation from 1971–2000 normals for a point-count station in the given park, averaged over the 12 years (2004–2015) expected to affect landbird counts during the focal monitoring period (2005–2016). Each boxplot indicates the median (thick horizontal line), interquartile range (box), and range of the data (whiskers), excepting outliers (dots) that occur outside the box by more than 1.5 times the interquartile range.

The historical parks, which are located at low elevations in coastal climates, experienced a range of anomalies in MST comparable to the mountain parks (Figure 3). However, historical parks experienced a much smaller range of anomalies in PAS relative the mountain parks, reflecting the smaller range of (lagged) PAS received annually during the monitoring period: 6–44 mm in SAJH and 13–83 mm in LEWI, compared to 47–2681 mm in MORA, 41–2143 mm in NOCA and 19–2992 mm in OLYM. The smaller range of anomalies in PAS experienced by historical parks might also reflect the smaller sampling areas and sample sizes for annual PAS in those parks, corresponding to a smaller number of point-count stations: $n = 1,956$ samples of annual PAS in SAJH and 912 in LEWI, compared with 12,144 in MORA, 14,172 in NOCA and 13,164 in OLYM. However, recalling that the range of anomalies in MST experienced by historical parks was comparable to that of mountain parks (Figure 3), and noting that the sample sizes for MST were the same as the sample sizes for PAS, it seems unlikely that sampling effects were an important factor in reducing the range of PAS. The narrow range of anomalies in PAS for historical parks was likely due to their small size and coastal locations.

Note that we include even- and odd-year samples in this summary: despite the biennial survey plan for historical parks, annual PAS data are needed to estimate annual population sizes based on climate model A.

Fitted models

Models were fitted successfully to data from 68 of the species detected in one or more of the five parks monitored, including 51 species in the historical parks (Table 7) and 42 species in the mountain parks (Table 8). The set of species analyzed in each park was largely overlapping, but only 17 species were detected regularly enough to support the estimation of model parameters in every park. Of the 51 species analyzed in historical parks, 29 (57%) were modeled in both parks, albeit in two separate models. Of the 42 species analyzed in mountain parks, 32 (76%) were modeled in all three parks, a higher percentage than in historical parks due in part to the potential for combining data from all mountain parks in the same model. Graphical summaries of model results are presented here, and numerical results are provided in Appendix 2 of this report, which features detection distances, population densities and trends for each species analyzed.

Table 7. Summary of models fitted to species commonly detected in San Juan Island National Historical Park (SAJH) and Lewis and Clark National Historical Park (LEWI). “Basic” models of type A included no covariates of species abundance or detection, and “Climate A” models included only linear effects of precipitation-as-snow and residual mean spring temperature (accounting for covariance between climate metrics), as described in text. Data from species detected only in certain park units (e.g., Barn Swallow in American Camp or “AMCA” and Hermit Warbler in Fort Clatsop or “FOCL”) were fitted to unit-specific models as indicated. Missing models (“NA”) indicate that the species was too rare in the given park to support convergence of model parameter estimates. Species codes are identified in Table 6.

Species code	Basic model SAJH	Basic model LEWI	Climate model SAJH	Climate model LEWI
CANG	Basic A	NA	Climate A	NA
BAEA	Basic A	Basic A	Climate A	Climate A
CAQU	Basic A	NA	NA	NA
BTPI	NA	Basic A	NA	Climate A
MODO	Basic A	NA	NA	NA
RUHU	Basic A	Basic A	Climate A	Climate A
HAWO	NA	Basic A	NA	NA
NOFL	NA	Basic A	NA	Climate A
OSFL	Basic A	Basic A	Climate A	Climate A
PSFL	Basic A	Basic A	Climate A	Climate A
CAVI	Basic A	NA	NA	NA

¹Species detected only in the American Camp (AMCA) sub-unit of SAJH; species data were used to develop a model specific to AMCA.

²Species was detected only in the Fort Clatsop (FOCL) sub-unit of LEWI; species data were used to develop a model specific to FOCL.

³Species was recorded only after 2007, and was recorded as Townsend’s Warbler prior to 2008; species data were used to develop a model specific to 2008–2016.

Table 7 (continued). Summary of models fitted to species commonly detected in San Juan Island National Historical Park (SAJH) and Lewis and Clark National Historical Park (LEWI). “Basic” models of type A included no covariates of species abundance or detection, and “Climate A” models included only linear effects of precipitation-as-snow and residual mean spring temperature (accounting for covariance between climate metrics), as described in text. Data from species detected only in certain park units (e.g., Barn Swallow in American Camp or “AMCA” and Hermit Warbler in Fort Clatsop or “FOCL”) were fitted to unit-specific models as indicated. Missing models (“NA”) indicate that the species was too rare in the given park to support convergence of model parameter estimates. Species codes are identified in Table 6.

Species code	Basic model SAJH	Basic model LEWI	Climate model SAJH	Climate model LEWI
HUVI	NA	Basic A	NA	Climate A
WAVI	Basic A	Basic A	Climate A	Climate A
STJA	NA	Basic A	NA	Climate A
AMCR	Basic A	Basic A	Climate A	Climate A
CORA	Basic A	Basic A	Climate A	NA
BARS	Basic A, AMCA ¹	NA	Climate A, AMCA ¹	NA
BCCH	NA	Basic A	NA	Climate A
CBCH	Basic A	Basic A	Climate A	Climate A
RBNU	Basic A	Basic A	Climate A	Climate A
BRCR	Basic A	Basic A	Climate A	Climate A
BEWR	NA	Basic A	NA	NA
HOWR	Basic A	NA	Climate A	NA
PAWR	Basic A	Basic A	Climate A	Climate A
MAWR	NA	Basic A	NA	Climate A
GCKI	Basic A	Basic A	Climate A	Climate A
SWTH	Basic A	Basic A	Climate A	Climate A
AMRO	Basic A	Basic A	Climate A	Climate A
EUST	Basic A, AMCA ¹	NA	NA	NA
CEDW	Basic A, AMCA ¹	NA	NA	NA
OCWA	Basic A	Basic A	Climate A	Climate A
YEWA	Basic A	Basic A	NA	Climate A
YRWA	Basic A	NA	NA	NA
BTYW	Basic A	Basic A	Climate A	Climate A
TOWA	Basic A	NA	Climate A	NA

¹Species detected only in the American Camp (AMCA) sub-unit of SAJH; species data were used to develop a model specific to AMCA.

²Species was detected only in the Fort Clatsop (FOCL) sub-unit of LEWI; species data were used to develop a model specific to FOCL.

³Species was recorded only after 2007, and was recorded as Townsend’s Warbler prior to 2008; species data were used to develop a model specific to 2008–2016.

Table 7 (continued). Summary of models fitted to species commonly detected in San Juan Island National Historical Park (SAJH) and Lewis and Clark National Historical Park (LEWI). “Basic” models of type A included no covariates of species abundance or detection, and “Climate A” models included only linear effects of precipitation-as-snow and residual mean spring temperature (accounting for covariance between climate metrics), as described in text. Data from species detected only in certain park units (e.g., Barn Swallow in American Camp or “AMCA” and Hermit Warbler in Fort Clatsop or “FOCL”) were fitted to unit-specific models as indicated. Missing models (“NA”) indicate that the species was too rare in the given park to support convergence of model parameter estimates. Species codes are identified in Table 6.

Species code	Basic model SAJH	Basic model LEWI	Climate model SAJH	Climate model LEWI
HEWA	NA	Basic A, FOCL, ² 2008+ ³	NA	Climate A
COYE	Basic A	Basic A	NA	Climate A
WIWA	Basic A	Basic A	Climate A	Climate A
WETA	Basic A	Basic A	Climate A	Climate A
SPTO	Basic A	Basic A	Climate A	NA
SAVS	Basic A	Basic A	Climate A	NA
SOSP	Basic A	Basic A	Climate A	Climate A
WCSP	Basic A	Basic A	Climate A	Climate A
DEJU	Basic A	Basic A	Climate A	Climate A
BHGR	NA	Basic A	NA	Climate A
RWBL	Basic A	Basic A	Climate A	Climate A
BHCO	Basic A	Basic A	Climate A	Climate A
PUFI	Basic A	Basic A	Climate A	Climate A
HOFI	Basic A	NA	Climate A	NA
PISI	Basic A	NA	Climate A	NA
AMGO	Basic A	Basic A	Climate A	Climate A

¹Species detected only in the American Camp (AMCA) sub-unit of SAJH; species data were used to develop a model specific to AMCA.

²Species was detected only in the Fort Clatsop (FOCL) sub-unit of LEWI; species data were used to develop a model specific to FOCL.

³Species was recorded only after 2007, and was recorded as Townsend’s Warbler prior to 2008; species data were used to develop a model specific to 2008–2016.

Table 8. Summary of models fitted to species commonly detected in the mountain parks. “Basic B” models included linear and nonlinear elevational covariates of species abundance, and “Climate B” models included linear and nonlinear effects of precipitation-as-snow as well as linear effects of residual mean spring temperature (accounting for covariance between climate metrics), as described in text. Data from species detected primarily in certain park units (e.g., Red-breasted Sapsucker in North Cascades National Park) were fitted to park-specific models as indicated. Covariates of detection were included in several models (e.g., effects of “Noise” and “Forest” on the scale parameter of the detection-distance function). “No Yr” indicates that the species was detected too infrequently to support the estimation of year effects on abundance. Missing models (“NA”) indicate that the species was too rare in the given park to support convergence of model parameter estimates. The list of climate models includes some cases in which a species model was successfully fitted to data from all three parks, even though Elevation models failed to converge for some parks. In these cases, fits from parks where Elevation models failed to converge were omitted from this report. Species codes are identified in Table 6.

Species code	Elevation models			Climate models
	MORA	NOCA	OLYM	
SOGR	Basic B	Basic B	Basic B	Climate B
RUHU	Basic B	Basic B	Basic B	Climate B
RBSA	NA	Basic B, NOCA	NA	Climate B
HAWO	Basic B	Basic B	Basic B	Climate B
NOFL	Basic B	Basic B	Basic B	Climate B
PIWO	Basic B	Basic B	Basic B	Climate B
OSFL	Basic B	Basic B	Basic B	Climate B
WEWP	NA	Basic B, NOCA	NA	Climate B
HAFL	Basic B	Basic B	Basic B	Climate B
PSFL	Basic B	Basic B	Basic B	Climate B
CAVI	NA	Basic B	NA	Climate B
WAVI	Basic B	Basic B	Basic B	Climate B
GRAJ	Basic B	Basic B	Basic B	Climate B, Noise
STJA	Basic B, Noise	Basic B, Noise	Basic B, Noise	Climate B
CLNU	Basic B, No Yr	Basic B, No Yr	NA	Climate B, MORA, NOCA, No Yr
CORA	Basic B	Basic B	Basic B	Climate B
MOCH	Basic B	Basic B	NA	Climate B, MORA, NOCA, No Yr
CBCH	Basic B	Basic B	Basic B	Climate B
RBNU	Basic B	Basic B	Basic B	Climate B
BRCR	Basic B	Basic B	Basic B	Climate B
PAWR	Basic B	Basic B	Basic B	Climate B
GCKI	Basic B	Basic B	Basic B	Climate B
TOSO	Basic B	Basic B	Basic B	Climate B
SWTH	Basic B	Basic B	Basic B	Climate B
HETH	Basic B	Basic B	Basic B	Climate B
AMRO	Basic B, Noise	Basic B, Noise	Basic B, Noise	Climate B, Noise

Table 8 (continued). Summary of models fitted to species commonly detected in the mountain parks. “Basic B” models included linear and nonlinear elevational covariates of species abundance, and “Climate B” models included linear and nonlinear effects of precipitation-as-snow as well as linear effects of residual mean spring temperature (accounting for covariance between climate metrics), as described in text. Data from species detected primarily in certain park units (e.g., Red-breasted Sapsucker in North Cascades National Park) were fitted to park-specific models as indicated. Covariates of detection were included in several models (e.g., effects of “Noise” and “Forest” on the scale parameter of the detection-distance function). “No Yr” indicates that the species was detected too infrequently to support the estimation of year effects on abundance. Missing models (“NA”) indicate that the species was too rare in the given park to support convergence of model parameter estimates. The list of climate models includes some cases in which a species model was successfully fitted to data from all three parks, even though Elevation models failed to converge for some parks. In these cases, fits from parks where Elevation models failed to converge were omitted from this report. Species codes are identified in Table 6.

Species code	Elevation models			Climate models
	MORA	NOCA	OLYM	
VATH	Basic B, Noise	Basic B, Noise	Basic B, Noise	Climate B, Noise
AMPI	Basic B, MORA	NA	Basic B, OLYM	Climate B, MORA, OLYM, No Yr
NAWA	NA	Basic B	NA	Climate B
YEWA	Basic B	Basic B	Basic B	Climate B, NOCA
YRWA	Basic B	Basic B	Basic B	Climate B
BTYW	NA	Basic B, NOCA	Basic B, OLYM	Climate B, NOCA, OLYM
TOWA	Basic B	Basic B	Basic B	Climate B
MGWA	NA	Basic B	Basic B	Climate B
WIWA	Basic B	Basic B	Basic B	Climate B
WETA	Basic B	Basic B	Basic B	Climate B
CHSP	Basic B, Noise	Basic B, Noise	Basic B, Noise	Climate B, Noise
FOSP	Basic B, MORA	Basic B, NOCA	NA	Climate B
SOSP	Basic B	Basic B	Basic B	Climate B
DEJU	Basic B, Forest	Basic B, Forest	Basic B, Forest	Climate B, Forest
BHGR	NA	Basic B, NOCA	NA	Climate B
CAFI	Basic B	Basic B	NA	Climate B

Spatial heterogeneity in species distributions within parks presented an additional challenge. SAJH and LEWI supported four species that were commonly detected in only one park sub-unit (Table 7). Model fit and the convergence of parameter estimates for these species (Barn Swallow, European Starling and Cedar Waxwing in American Camp, and Hermit Warbler in Fort Clatsop) was greatly improved by limiting the data to the sub-unit that was occupied; i.e., by not attempting to model the zeros in other parts of the park. The Hermit Warbler analysis was further limited to a shortened time series, because this species was only recorded in surveys from 2008 and later. Although missing data can be estimated using the modeling approach adopted here, data missing from either end of a trend is more likely to be estimated with bias (Kéry and Royle 2016). For this reason, trends in SAJH were estimated for the period 2005–2015, while trends in LEWI were estimated for the period 2006–2016:

each time series of population estimates was bracketed by the first and last survey years for the focal park.

Tables 7 and 8 show only the “best” models fitted to data for each species in each park. Especially in mountain parks, additional models were fitted to the data for many species in attempts to improve model fit and the convergence of parameter estimates. For example, several potential covariates of the detection model parameters q and σ were explored for many species, including fixed and random effects of day, fixed effects of hour, random effects of observer, a fixed effect of the most frequent observer (Mandy Holmgren), a fixed effect forest presence, a fixed effect of cover density and a fixed effect of noise class during the survey. In only a few cases did covariates improve detection model fit, and each case involved either effects of noise or forest presence (Table 8). Effects of day and hour were minimized through survey design, because surveys were timed to occur during peak days and hours of breeding behavior. Observer effects were difficult to implement because the observer covariate was missing for many of the station-years being modeled. A value for observer must be assigned for every station-year in which a count was not obtained. For stations in the alternating panels, missing data occur in four out of every five years. If a single value for the “observer” factor is assigned to all station-years with missing data, that value becomes the most common “observer” in the dataset, biasing results from a random-effects model. Fixed-effect models coding the predominant observer as 1 and all others (including missing observers) as 0 were occasionally better than models without an observer effect. However, this approach to coding observer effects broke down when the predominant observer and park were confounded, which was commonly the case because the predominant observer could only visit one park at a time.

Overall, fixed effects of forest presence and especially noise during the survey were the most commonly supported ways to improve model fit and the convergence of parameter estimates. However, modeling these effects resulted in only minor improvements in metrics of model fit. Much larger improvements were sometimes gained when whole parks or park sub-units could be dropped from the analysis due to infrequent detection of the focal species. Such “habitat specialists” were easy to accommodate in the historical parks, because both historical parks were comprised of discrete sub-units that could be dropped if necessary where the focal species was rare. In models for the mountain parks, whole parks were dropped if necessary, but opportunities still exist for more nuanced modeling of habitat specificity for some species.

Climate models were less likely to be supported for species in the more coastal climate of the historical parks (Table 7). The relatively sparse data from historical parks often could only support basic trend models lacking added covariates and random effects. Of 41 species fitted to the basic A model in SAJH, eight (20%) could not be fitted to the climate A model (parameter estimates failed to converge). Similarly, of 39 species fitted to the basic A model in LEWI, five (13%) could not be fitted to the climate A model. In contrast, climate models were always supported for species in the mountain parks (Table 8). In mountain parks, swapping basic (elevation) models of type B for climate models of type B allowed estimation of population density in additional parks for 8 species: Red-breasted Sapsucker, Western Wood-Pee-wee, Cassin’s Vireo, Nashville Warbler, MacGillivray’s Warbler, Fox Sparrow, Black-headed Grosbeak and Cassin’s Finch. Conversely, swapping climate

models for elevation models allowed estimation of population density in additional parks for only one species: Yellow Warbler. Climate and elevation effects were not included in the same model, due to their covariance.

Effective survey area

The estimate of population density for each species depends sensitively on its distribution of detection distances, and especially on the tail of that distribution. Characterizing the detection distance distribution requires data from a large number of detections. Few species were encountered frequently enough in a given year to generate a smooth histogram of detection distances for that year. Therefore, we estimated the maximum detection distance and σ , the decay rate of detection with distance, using data from all detections of a species across all years, after censoring the farthest 10% of detections according to common practice (Kéry and Royle 2016). Adopting this approach resulted in a constant value for the focal species maximum detection distance and its associated effective survey area. Holding effective survey area constant has implications for trend detection, much like holding detection probability constant (see Methods). If effective survey area actually varies over time, then trends in abundance and survey area could be confounded. However, the effective survey area for a species appeared to be fairly consistent among parks (Figure 4).

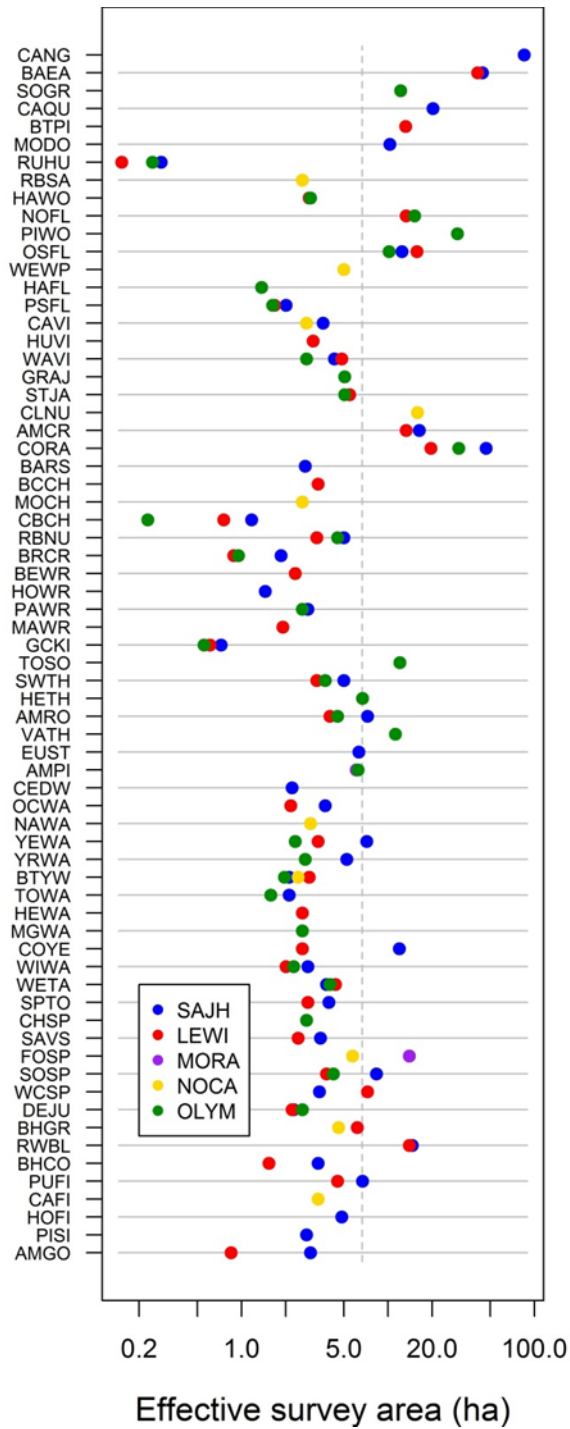


Figure 4. Effective area surveyed at each point-count station, differentiated by park, presented on a \log_{10} scale for each species analyzed. Up to four estimates of effective survey area were obtained for each species, and these independent estimates generally cluster along the x axis for a given species. Species codes are identified in Table 6.

Up to four separate estimates of effective survey area were obtained for each species: one for each historical park model, one for the combined mountain park model, and one more if the species was

modeled separately in two of the mountain parks. Based on the maximum detection distance of a species (d_{\max}), measured in meters, the effective area surveyed (A^{eff}), measured in hectares, was calculated as $A^{\text{eff}} = \pi(d_{\max})^2/10000$. In general, multiple estimates of effective survey area were relatively similar for a given species (Figure 4), suggesting similar effective survey areas across parks. Given a space-for-time substitution, consistency across parks might suggest consistency over time within parks. This assumption should be investigated as sufficient data accumulate to characterize the distribution of detection distances at different points in time.

Parameter estimates by park, stratum and region

Trends were estimated for 68 species across the NCCN, including up to 41 species per park. Estimates indicated that these species were either stable or increasing across the sampling frame in most parks during 2005–2016. Many populations were affected by our metrics of spring conditions (PAS and MST), especially by precipitation in mountain parks. For a few species, there was evidence of population decline in one park offset by increase in another. For ease of presentation, we report results from each historical park first, followed by results from the more complex models fitted to data from the mountain parks.

San Juan Island National Historical Park

Point-count surveys conducted in odd-numbered years from 2005 to 2015 in San Juan Island National Historical Park (SAJH) resulted in the detection of 82 landbird species along with several seabirds, shorebirds and waterfowl (Table 6). The Glaucous-winged Gull (count = 726) was the most common bird detected during point counts, followed by the American Robin (count = 606). Over one-third ($n = 34$) of the landbird species detected in SAJH were recorded fewer than 17 times each during 2005–2015, too infrequently to support our models of detectability and population trend. The Yellow Warbler, detected only 20 times in SAJH, was the most rarely detected species to support our models, but trends could not be estimated for several species with total counts higher than 20: Chipping Sparrow (count = 21), Pileated Woodpecker (24), Varied Thrush (26), Bewick's Wren (35), Northern Flicker (36), Black-headed Grosbeak (40) and Red Crossbill (231). In the latter species, flocking behavior likely introduced un-modeled heterogeneity in detection probability that precluded the convergence of parameter estimates or contributed to poor fit.

Mean annual trends in population density (Figure 5) were estimated as stable or increasing during the survey period (2005–2015) for each of 41 landbird species detected commonly in SAJH. Trends were clearly positive for almost half of these species, and no declines were supported. Estimates of average population density per hectare ranged from 0.012 for both the Mourning Dove and the California Quail, to 1.439 for the Chestnut-backed Chickadee and 3.187 for the Rufous Hummingbird. However, hummingbird density was likely overestimated due to their unusual attraction to observers, which results in low detection distances for this species.

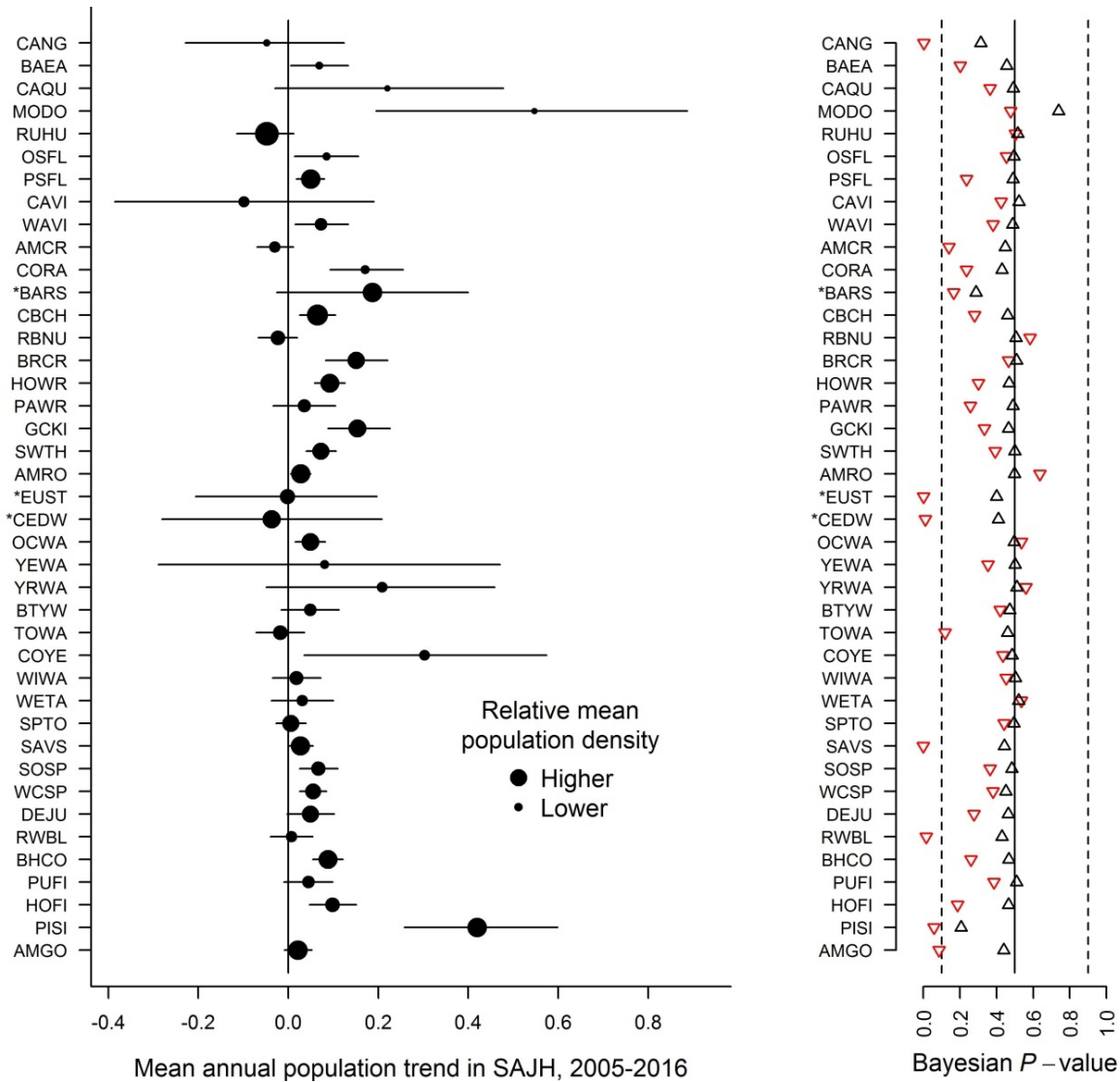


Figure 5. Population trends for species in San Juan Island National Historical Park (SAJH). Mean annual trends in population density (left-hand panel) were estimated to be stable or increasing during the survey period (2005–2015) for each of 41 landbird species detected commonly in this park. Species are listed top to bottom in taxonomic order (species codes are identified in Table 6). Mean trends (dots) and 95% credible intervals (horizontal lines) indicate strong support for increasing density in almost half of these species, and no declines were supported. Estimates of average population density per hectare (relative dot size) ranged from 0.012 for both the Mourning Dove (MODO) and the California Quail (CAQU), to 1.439 for the Chestnut-backed Chickadee (CBCH) and 3.187 for the Rufous Hummingbird (RUHU), although hummingbird behavior (attraction to observers) likely leads to overestimation of hummingbird density. Components of model fit were considered adequate if the Bayesian P -value was not extreme (right-hand panel). Fit to the sub-model of species availability (black triangles) was always adequate but fit to the sub-model of perceptibility (inverted red triangles) varied widely. For the Barn Swallow (BARS), European Starling (EUST) and Cedar Waxwing (CEDW), convergence of parameter estimates was achieved by restricting the scope of inference to the American Camp portion of SAJH, the only location where they were detected.

Our default detection model assumed constant availability and perceptibility of a species, corresponding to a constant probability of detection per minute (q) as well as a constant value for the shape parameter of the (half-normal) detection-distance function (σ). We evaluated fit for each component of detection using Bayesian P -values (Figure 5, right-hand panel), distinguishing fit to the model of availability (black triangles) from fit to the model of perceptibility (inverted red triangles). Results suggest that constant availability was an acceptable assumption for every species modeled (Bayesian P -values were close to 0.5) and the constant perceptibility model was adequate for the vast majority of species. However, extreme Bayesian P -values suggest that the default model of perceptibility was less than adequate for seven of the 41 species (Canada Goose, European Starling, Cedar Waxwing, Savannah Sparrow, Red-winged Blackbird, Pine Siskin and American Goldfinch). Flocking behavior likely contributed to poor model fit in most of these species.

Some bias in reporting on trends across species might be introduced by focusing on non-flocking species and species common enough to support parameter estimation. To explore this possibility, we plotted effort-adjusted counts per point for several species detected too often in flocks or detected too infrequently in SAJH to support model fitting (Figure 6). If declines were suggested more often among these species than among modeled species, we might suspect bias in our reporting. However, apparent declines are not especially evident in Figure 6.

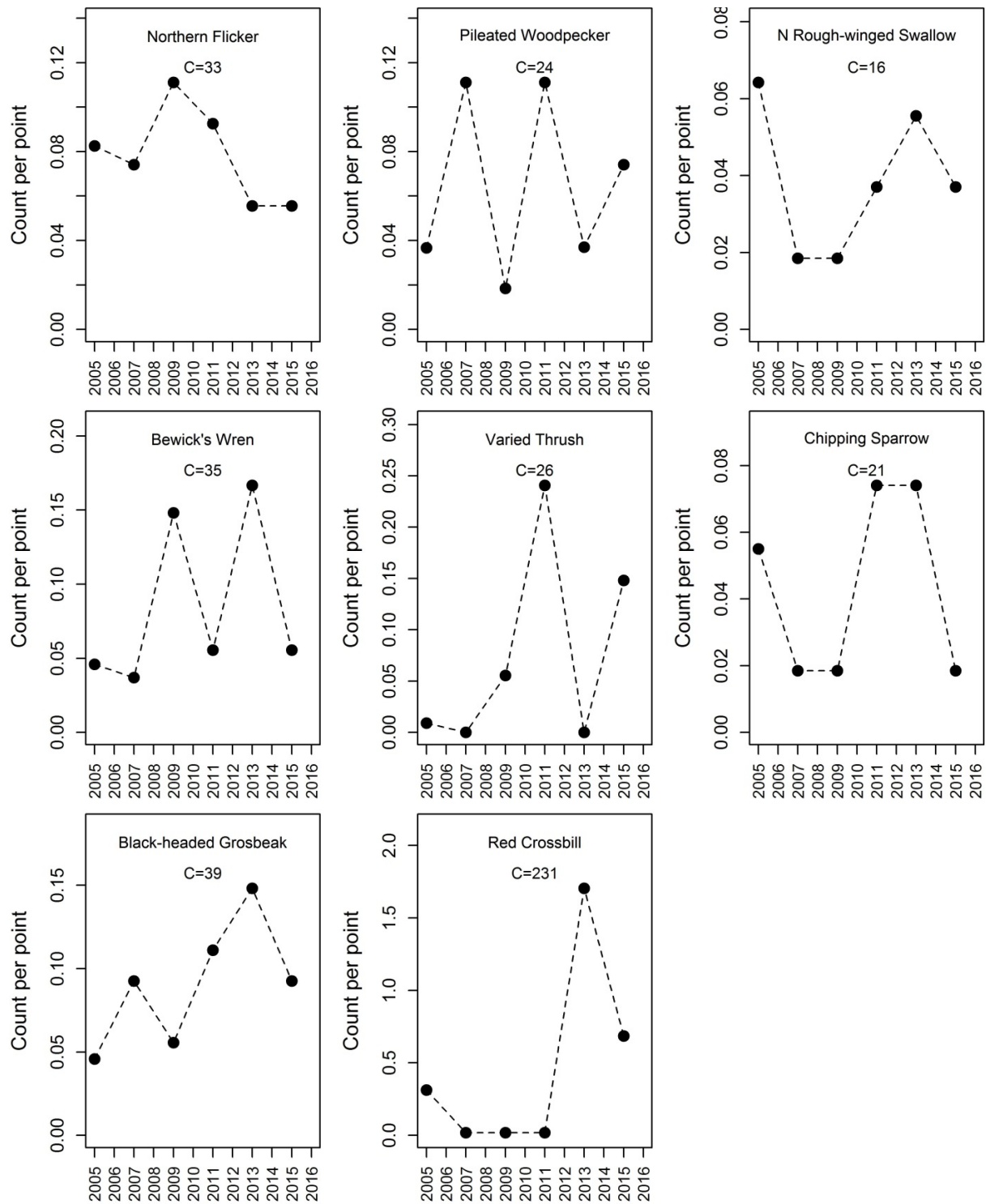


Figure 6. Effort-adjusted counts for several of the flocking or less common species at San Juan Island National Historical Park. Note variations in the vertical scale and in total count across years (C). Population trends were not estimated for these species because flocking behavior and/or low numbers caused poor model performance. Species are displayed in taxonomic order from upper left to lower right.

In addition to fitting a linear trend to the annual data for each focal species in SAJH (Figure 5), we also estimated mean annual population density as N_t per hectare using basic models of type A (Figure 7). The mean trajectory (solid line) for almost every species suggests stability or increase over the monitoring period, with the possible exception of Rufous Hummingbird, Cassin's Vireo, American Crow and Red-breasted Nuthatch. The 95% credible intervals on each time series of population density suggest at least the potential for stable dynamics in every species.

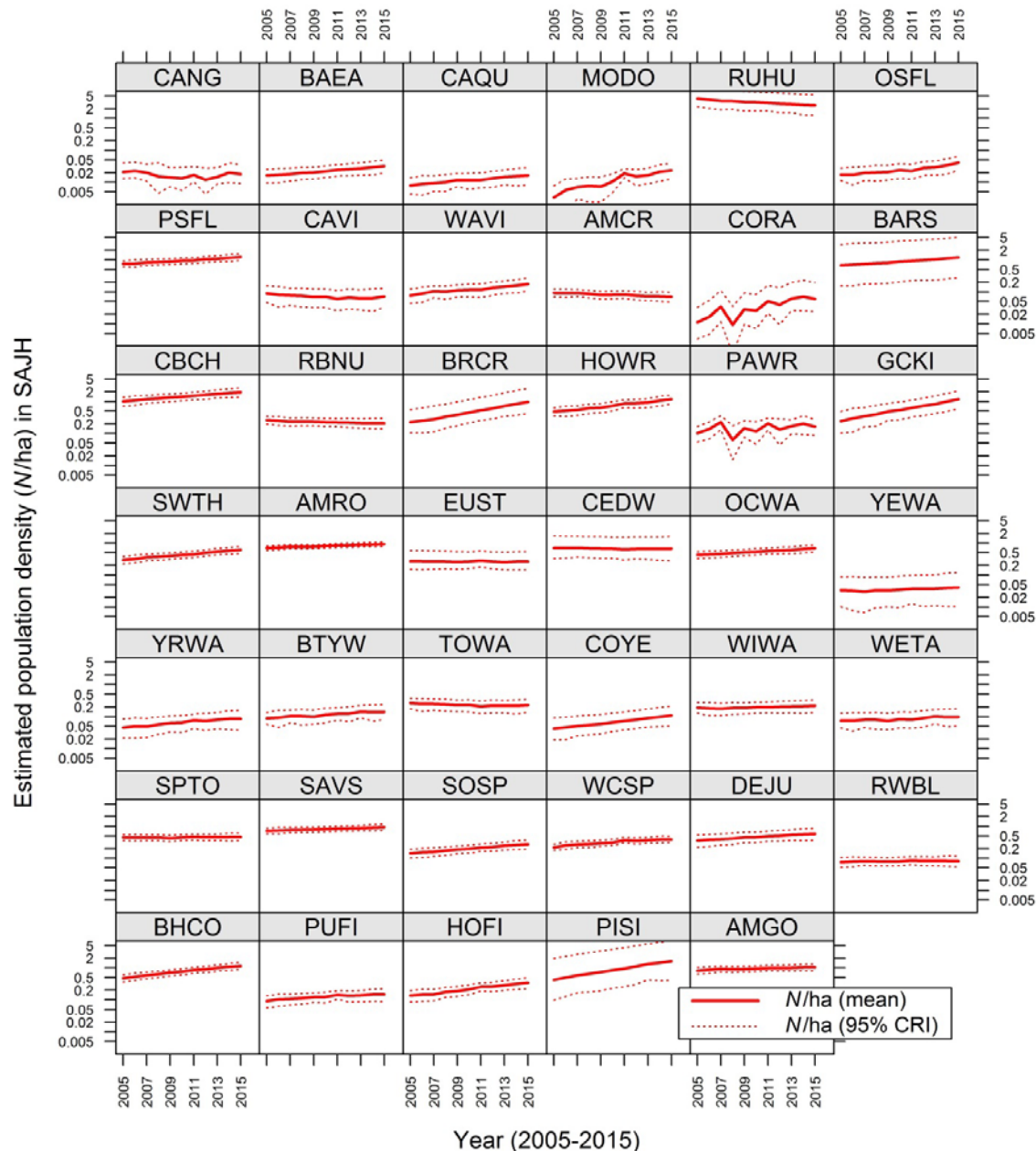


Figure 7. Yearly estimates of population density (N/ha) for 41 species commonly detected in San Juan Island National Historical Park (SAJH). Density estimates, summarized here on a \log_{10} scale by means (solid lines) and 95% credible intervals (dotted lines), were based on the basic models of type A listed in Table 2. Species codes are identified in Table 6.

We have also plotted effort-adjusted counts for each focal species in SAJH (Figure 8), for comparison with modeled estimates of trend and population density. Counts are missing in even-numbered years when surveys were not conducted in SAJH. Although counts are temporally sparse in the SAJH dataset, and counts do not reflect effects of detection probability and covariates, we see at least general congruence when comparing modeled estimates of annual population density (Figure 7) with effort-adjusted counts (Figure 8). Species with rising estimates of density over the monitoring period tend to have rising counts. Species with more variable counts generally exhibit more variable mean estimates of density associated with wider 95% credible intervals.

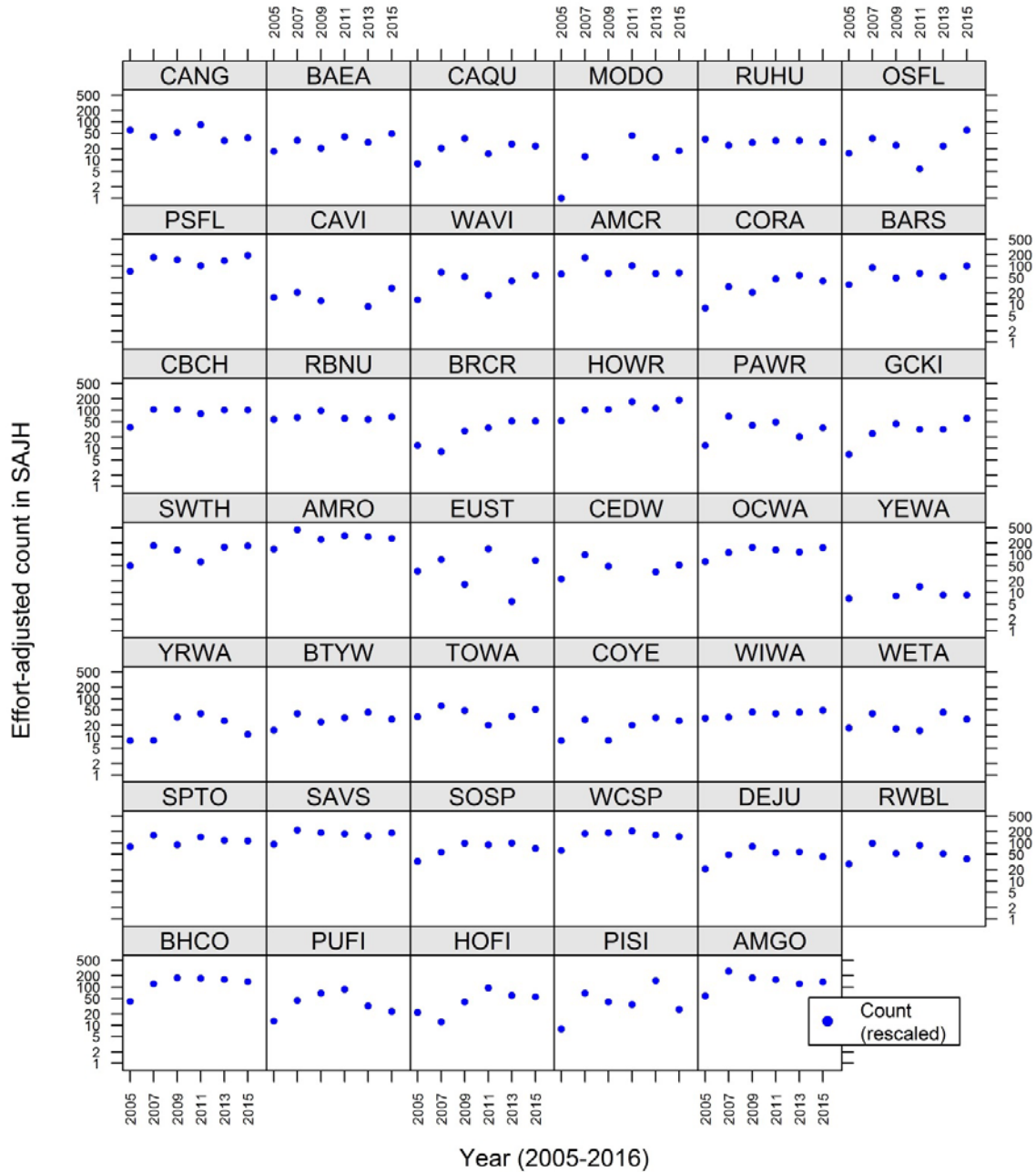


Figure 8. Effort-adjusted counts for 41 species commonly detected in San Juan Island National Historical Park (SAJH). Surveys in SAJH were conducted in odd-numbered years. Counts per point and minute surveyed were rescaled for comparison on a log10 scale by setting the lowest non-zero count to 1. Counts are missing for even-numbered years when surveys were not conducted in this park, and counts of zero are not plotted. The number of birds counted (this figure) varies less among species than the estimated population size (Figure 7) due to variation among species in effective survey area. Species codes are identified in Table 6.

Climate models based on data from SAJH and LEWI are reported below, after trends in LEWI.

Lewis and Clark National Historical Park

Point-count surveys conducted in even-numbered years from 2006 to 2016 in Lewis and Clark National Historical Park resulted in the detection of 73 landbird species along with several seabirds, shorebirds and waterfowl (Table 6). Swainson's Thrush (count = 742) was the most common bird detected during point counts, followed by the Pacific Wren (count = 481). Over 1/3rd (n = 27) of the landbird species detected in LEWI were recorded fewer than 20 times each during 2006–2016, too infrequently to support our models of detectability and population trend. The Hairy Woodpecker, detected only 20 times in LEWI, was the most rarely detected species to support our models, but trends could not be estimated for several species with higher total counts: European Starling (N = 29), Red Crossbill (N = 52), Violet-green Swallow (N = 56), Barn Swallow (N = 70), Cedar Waxwing (N = 68) and Canada Goose (N = 74). Flocking behavior likely introduced un-modeled heterogeneity in detection probability that precluded the convergence of parameter estimates or contributed to poor fit.

Mean annual trends in population density (Figure 9) were estimated as stable or increasing during the survey period (2006–2016) for all but three of 39 landbird species detected commonly in LEWI. Trends were clearly positive for at least 20 of these species, but declines were supported for Northern Flicker (NOFL), Olive-sided Flycatcher (OSFL) and Hutton's Vireo (HUVI). Estimates of mean population density per hectare ranged from 0.023 for the Common Raven to 2.230 for the Chestnut-backed Chickadee and 2.884 for the Rufous Hummingbird. Constant availability was an acceptable assumption for every species modeled (Figure 9), but the constant perceptibility model was less than adequate for six of the 39 species (Bald Eagle, Marsh Wren, Common Yellowthroat, White-crowned Sparrow, Dark-eyed Junco and Red-winged Blackbird). Effort-adjusted counts for several species that could not be fit to models (Figure 10) do not suggest that trends were more common in these species than in those modeled successfully.

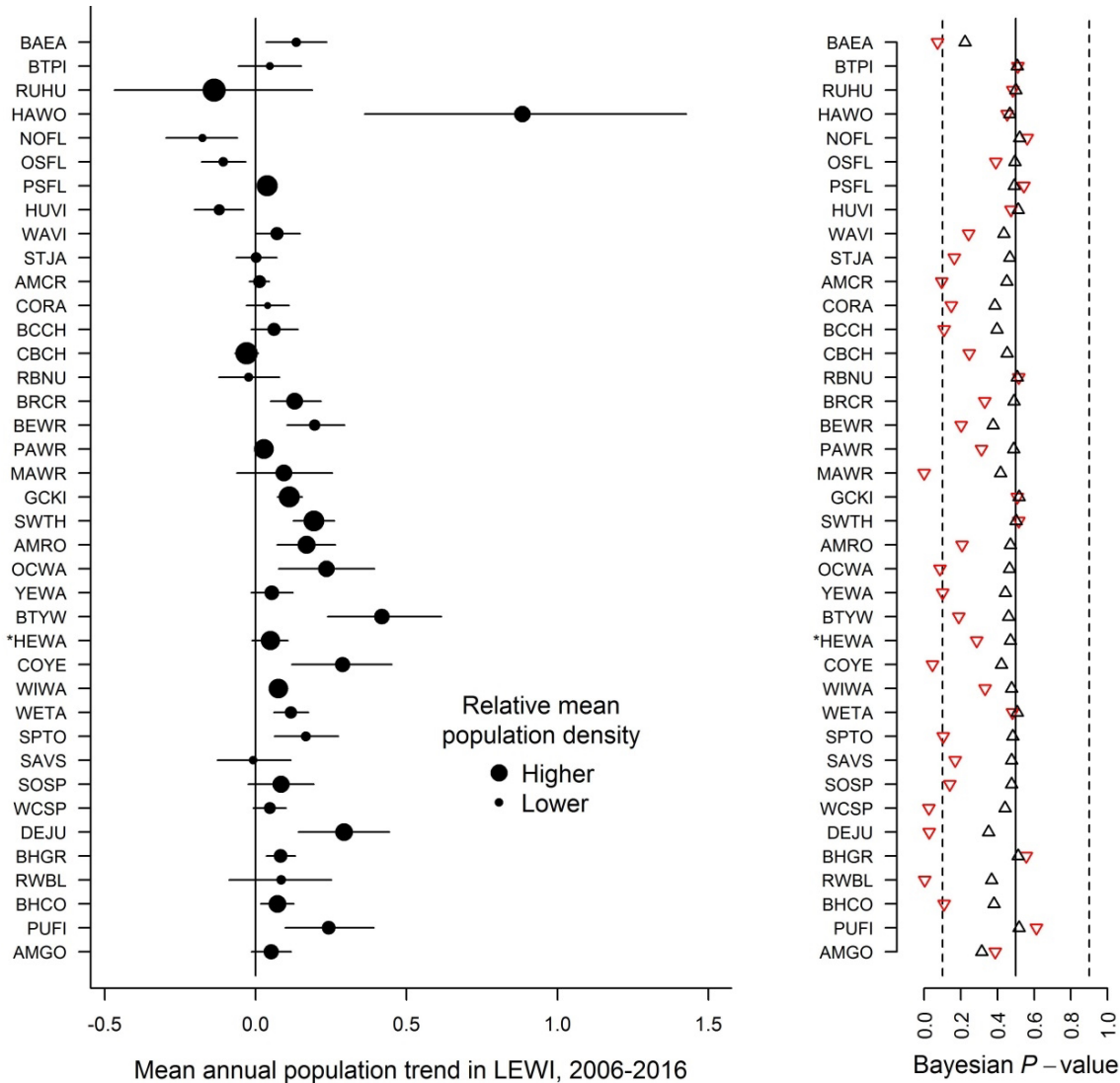


Figure 9. Population trends for species in Lewis and Clark National Historical Park (LEWI). Mean annual trends in population density (left-hand panel) were estimated to be stable or increasing during the survey period (2006–2016) for all but three of 39 landbird species detected commonly in this park. Species are listed top to bottom in taxonomic order (species codes are identified in Table 6). Mean trends (dots) and 95% credible intervals indicate strong support for increasing density in at least 20 species, with declines in only three species: Northern Flicker (NOFL), Olive-sided Flycatcher (OSFL) and Hutton’s Vireo (HUVI). Estimates of mean population density per hectare (relative dot size) ranged from 0.023 for the Common Raven (CORA) to 2.230 for the Chestnut-backed Chickadee (CBCH) and 2.884 for the Rufous Hummingbird (RUHU), although attraction to observers likely leads to overestimation of hummingbird density. Components of model fit were considered adequate if the Bayesian P -value was not extreme (right-hand panel). Fit to the sub-model of species availability (black triangles) was always adequate but fit to the sub-model of perceptibility (inverted red triangles) varied widely. For the Hermit Warbler (HEWA), convergence of parameter estimates was achieved by restricting the scope of inference to the Fort Clatsop portion of LEWI, the only location where they were detected, and to the period 2008–2016, the only years in which they were recorded.

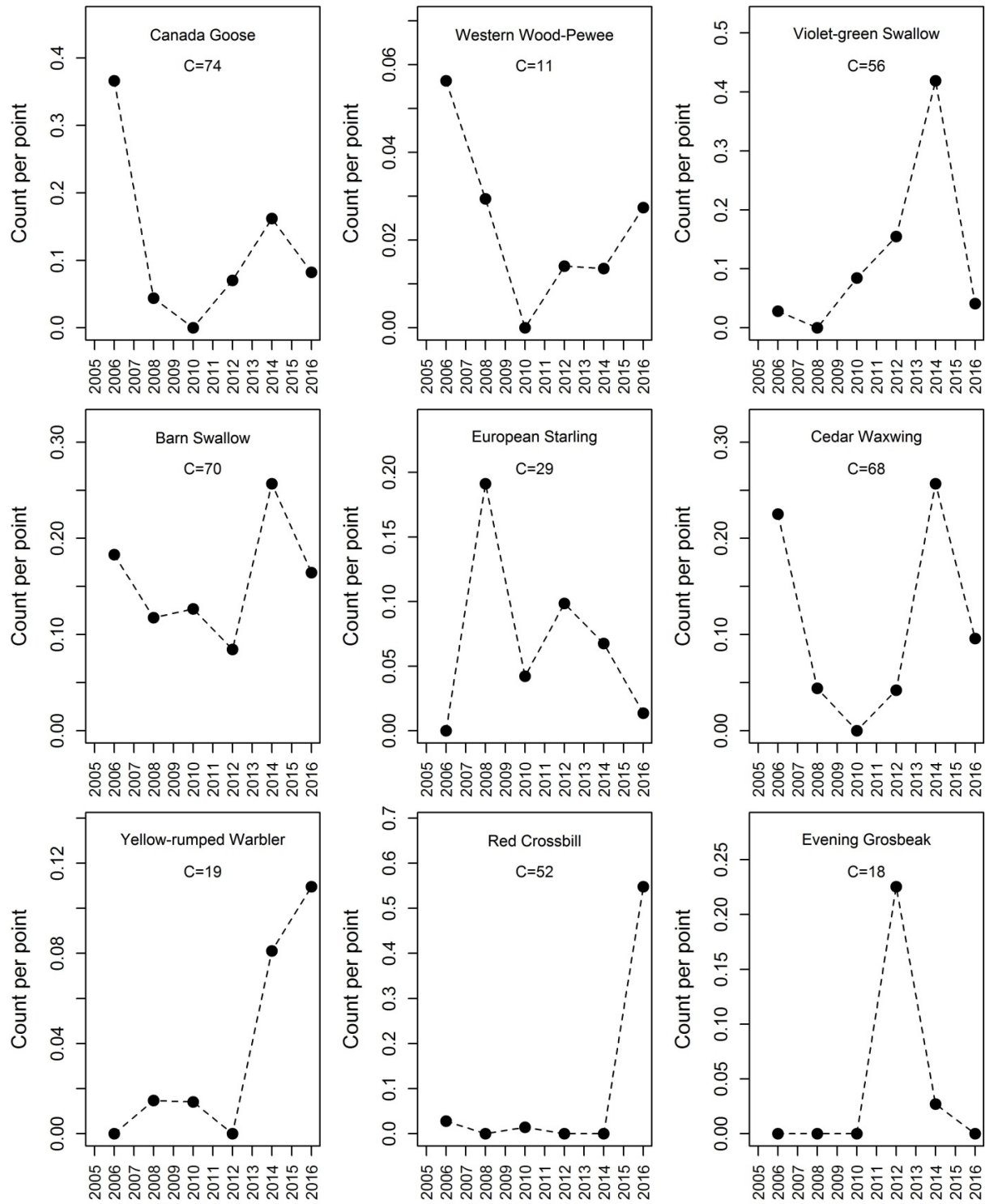


Figure 10. Effort-adjusted counts for several of the less common species at Lewis and Clark National Historical Park. Note variations in the vertical scale and total count across years (C). Population trends were not estimated for these species because flocking behavior and/or low numbers caused poor model performance. Species are displayed in taxonomic order from upper left to lower right.

Mean annual population density estimates (Figure 11) suggest general stability or increase over the monitoring period, with the possible exception of Rufous Hummingbird, Northern Flicker, Olive-sided Flycatcher, Hutton's Vireo and Red-breasted Nuthatch. Regional trends in these species are discussed below. The 95% credible intervals on time series of population density suggest at least the potential for stable dynamics in every species except the Olive-sided Flycatcher. Effort-adjusted counts (Figure 12) show general congruence with modeled estimates of annual population density. However, note that it is possible for the estimated trend in population density to be influenced strongly by one count, as exemplified by counts for the Warbling Vireo, which appeared to decline consistently from 2006 to 2014 followed by a dramatic increase in 2016. Uncertainty in the trend for this species is reflected in the broad 95% CRI for its trajectory of population densities (Figure 11) as well as the zero at one end of its 95% CRI for trend (0.00–0.147; Figure 9). Trends for LEWI and SAJH are estimated from relatively short time series due to the biennial survey protocol in those parks. Each annual count will have less influence when time series are longer and when there are enough data available to estimate random effects of year.

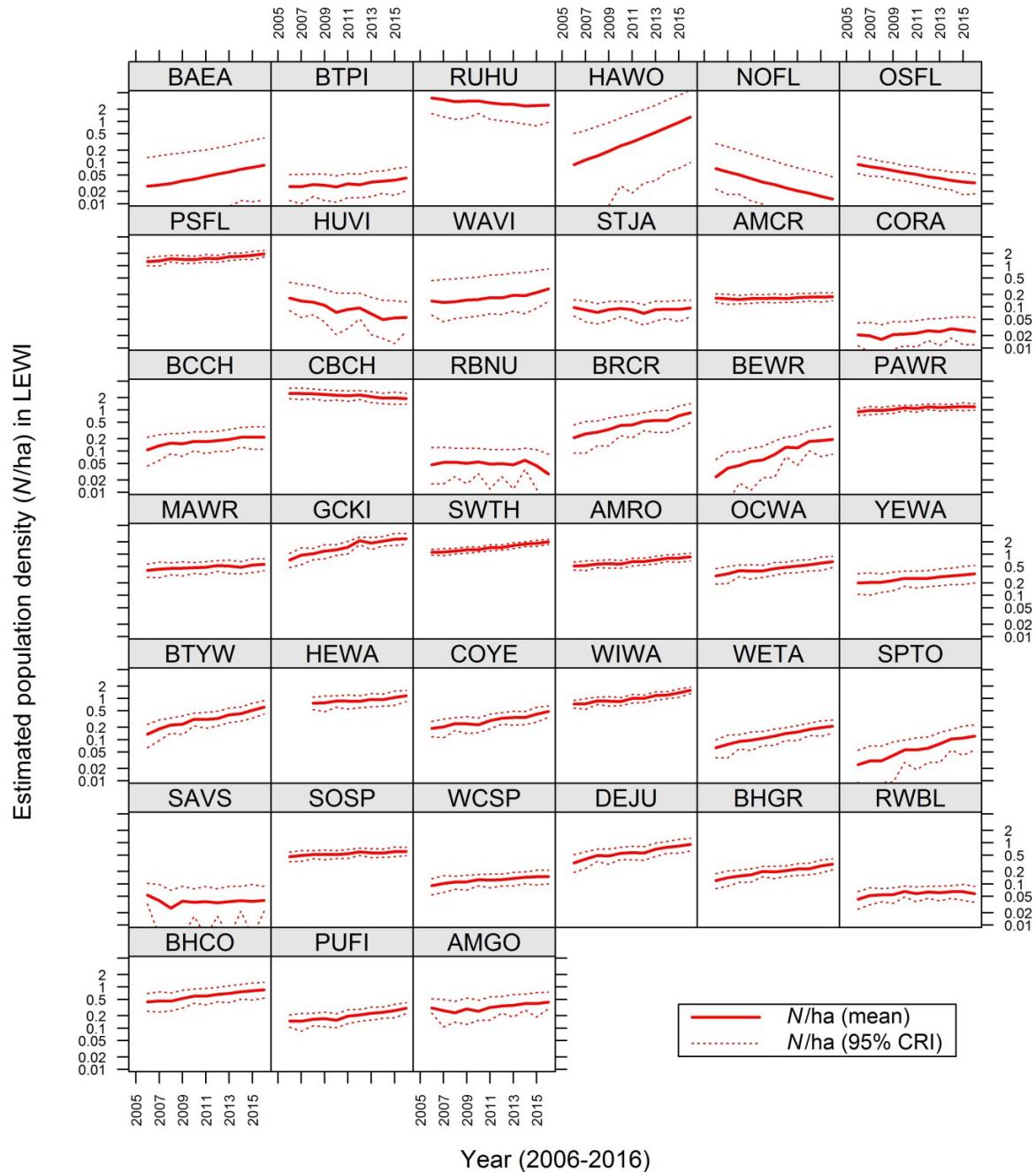


Figure 11. Yearly estimates of population density (N/ha) for 39 species commonly detected in Lewis and Clark National Historical Park (LEWI). Density estimates, summarized here on a \log_{10} scale by means (solid lines) and 95% credible intervals (dotted lines), were based on the basic models of type A listed in Table 2. Species codes are identified in Table 6.

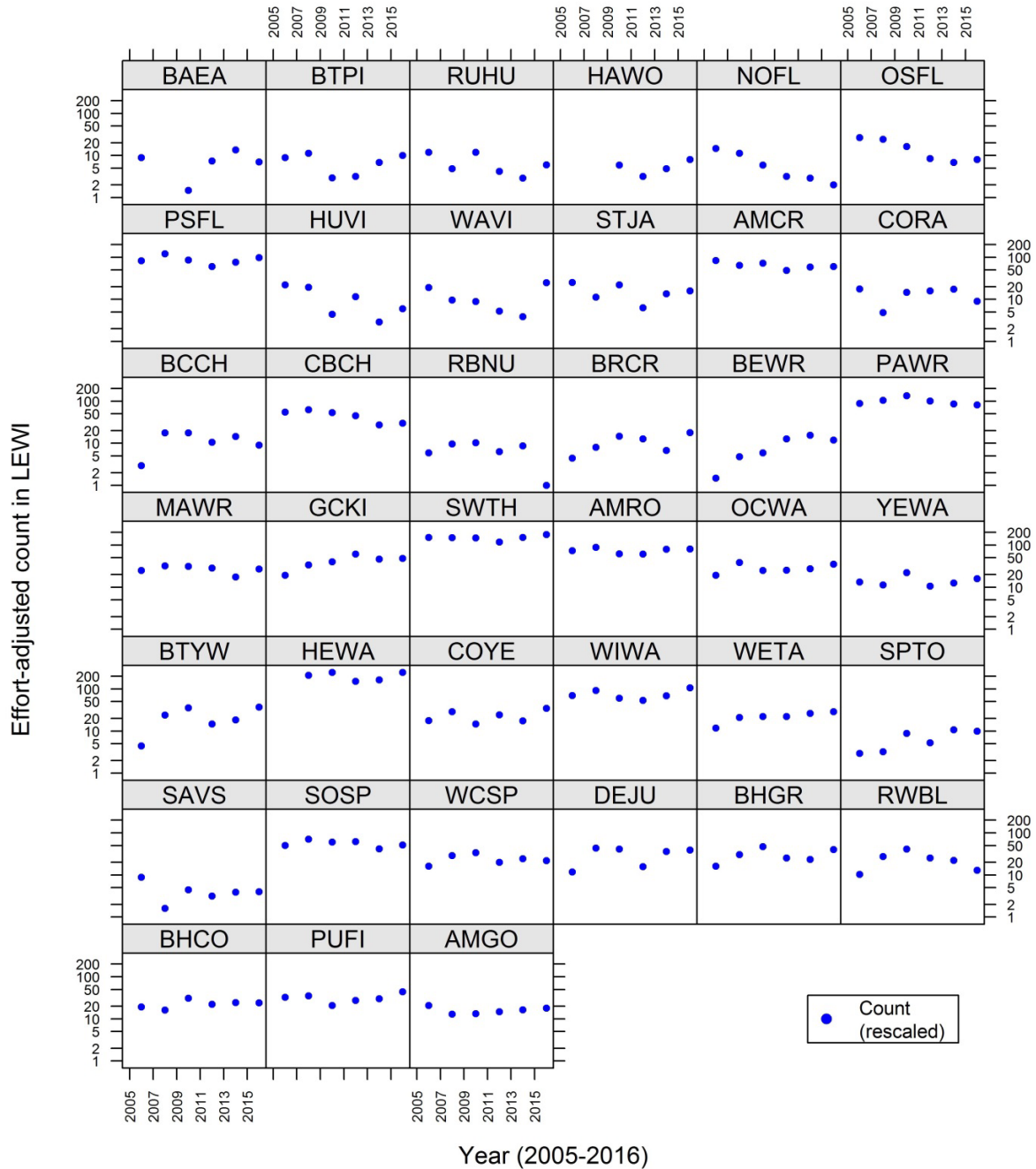


Figure 12. Effort-adjusted counts for 39 species commonly detected in Lewis and Clark National Historical Park (LEWI). Surveys in LEWI were conducted in even-numbered years. Counts per point and minute surveyed were rescaled for comparison on a log₁₀ scale by setting the lowest non-zero count to 1. Counts are missing for odd-numbered years when surveys were not conducted in this park, and counts of zero are not plotted. The number of birds counted (this figure) varies less among species than the estimated population size (Figure 11) due to variation among species in effective survey area. Species codes are identified in Table 6.

Effects of climate in the historical parks

Point-count stations within the historical parks experienced annual anomalies in MST commensurate with the mountain parks (Figure 3), but showed little evidence of anomalous values for PAS. Nevertheless, annual anomalies in PAS explained substantial variation in population density for nine species in SAJH and seven species in LEWI (Figure 13). Effects of PAS varied among parks, however, with unanimously negative effects in SAJH and almost evenly divided (four positive and three negative) effects in LEWI. After accounting for effects of PAS, residual effects of MST also varied among parks. Residual MST (rMST) had predominantly negative effects in SAJH (seven negative and two positive) and predominantly positive effects in LEWI (two negative and five positive). Larger effect sizes also tended to be associated with larger credible intervals (Figure 13). Together, these results suggest longer time-series are needed to clarify effects of climate in these coastal parks.

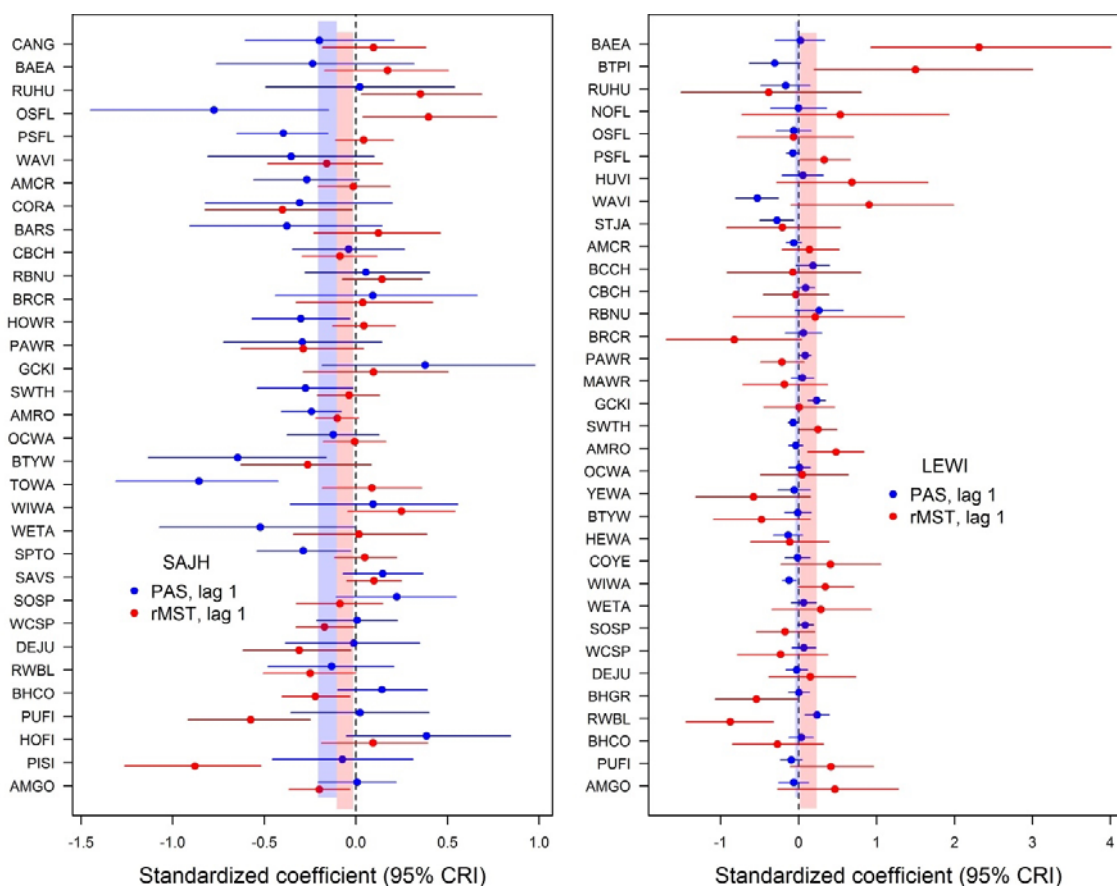


Figure 13. Linear effects of climate in one year on breeding landbird density estimates for the following year in San Juan Island National Historical Park (SAJH) (left-hand panel) and Lewis and Clark National Historical Park (LEWI) (right-hand panel). For each species, effects of local precipitation-as-snow (PAS, blue symbols) and residual mean spring temperature (rMST, red symbols) are displayed as means (dots) and 95% CRIs (horizontal lines). Mean \pm SE for the fitted coefficient of PAS across species (light blue vertical bars) was predominantly negative only in SAJH and was nearly 0 ± 0 (zero) in LEWI. Mean \pm SE for the fitted coefficient of rMST across species (light red vertical bars) was generally negative in SAJH and positive in LEWI. Species codes are identified in Table 6.

Mountain parks overview

For the mountain parks, park-specific trends were derived from multi-park models whenever possible. For 30 of the 42 species analyzed in the mountain parks, it was possible to estimate trends for each of the three parks based on a single, multi-park model (Table 8). Fitting the model to data from three parks simultaneously facilitated the estimation of parameters for parks with lower counts. For example, only 14 Chipping Sparrows (CHSP) were detected during 2005–2016 in OLYM, and CHSP were detected in OLYM in only three of 12 survey years, but we were able to estimate annual population densities in OLYM because 958 CHSP were detected across the mountain parks. However, this approach was not successful when parameters shared among parks in our model appeared to differ among parks in the data. For example, to fit data from parks where a species was rare, we held availability constant among parks; in some cases, our estimates for the constant of availability failed to converge, suggesting heterogeneity among parks that invalidated the assumption of constant availability. In those cases, we attained convergence by fitting the data from each park separately, and we present fits only from those single-park models.

In a previous analysis (Ray et al. 2017 a), trends were estimated for each of 39 landbird species based on data from 10 years of monitoring in the mountain parks. For the current analysis based on 12 years of data, we attempted to model trends in several more species that had been detected too rarely to support models based on the 10-year dataset. Multi-park models were successfully extended to 12-year datasets for Townsend's Solitaire (count = 248 in the mountain parks), Common Raven (count = 229) and Pileated Woodpecker (count = 150). However, key parameter estimates did not converge for multi- or single-park models of data for Cedar Waxwing (count = 266), Band-tailed Pigeon (182), Pine Grosbeak (169), Ruby-crowned Kinglet (167), White-crowned Sparrow (137), Gray-crowned Rosy Finch (129), Dusky Flycatcher (117) or Red-eyed Vireo (110). Several of these species were detected less frequently than the Pileated Woodpecker, which was the most rarely detected species to support our multi-park models. There were also several species with much higher counts that we did not attempt to fit to our models, due to their known flocking behavior: Vaux's Swift, Evening Grosbeak, Red Crossbill and Pine Siskin.

Population trends estimated for the mountain parks over the 12-year monitoring period confirm and extend the generally positive estimates based on the 10-year analysis of Ray et al. (2017 a). Across these mountain parks (Figs. 14–16), there was clear evidence for increase in 42 park populations during 2005–2016, including 13 species increasing in MORA, seven in NOCA and 22 in OLYM. At the same time, there was clear evidence for decline in only five populations, including Clark's Nutcracker in MORA and four species in NOCA: Olive-sided Flycatcher, Mountain Chickadee, Wilson's Warbler and Dark-eyed Junco. Positive trends were evident in species at a wide range of densities, including one of the least common species, Common Raven at 0.005 birds/ha in MORA (Fig. 14), and one of the most common, Chestnut-backed Chickadee at 2.786 birds/ha in OLYM (Fig. 16). As in the historical parks, fits were universally good for the sub-model of species availability, but fits for the sub-model of perceptibility were less acceptable for a larger fraction (up to one third) of the populations in mountain parks.

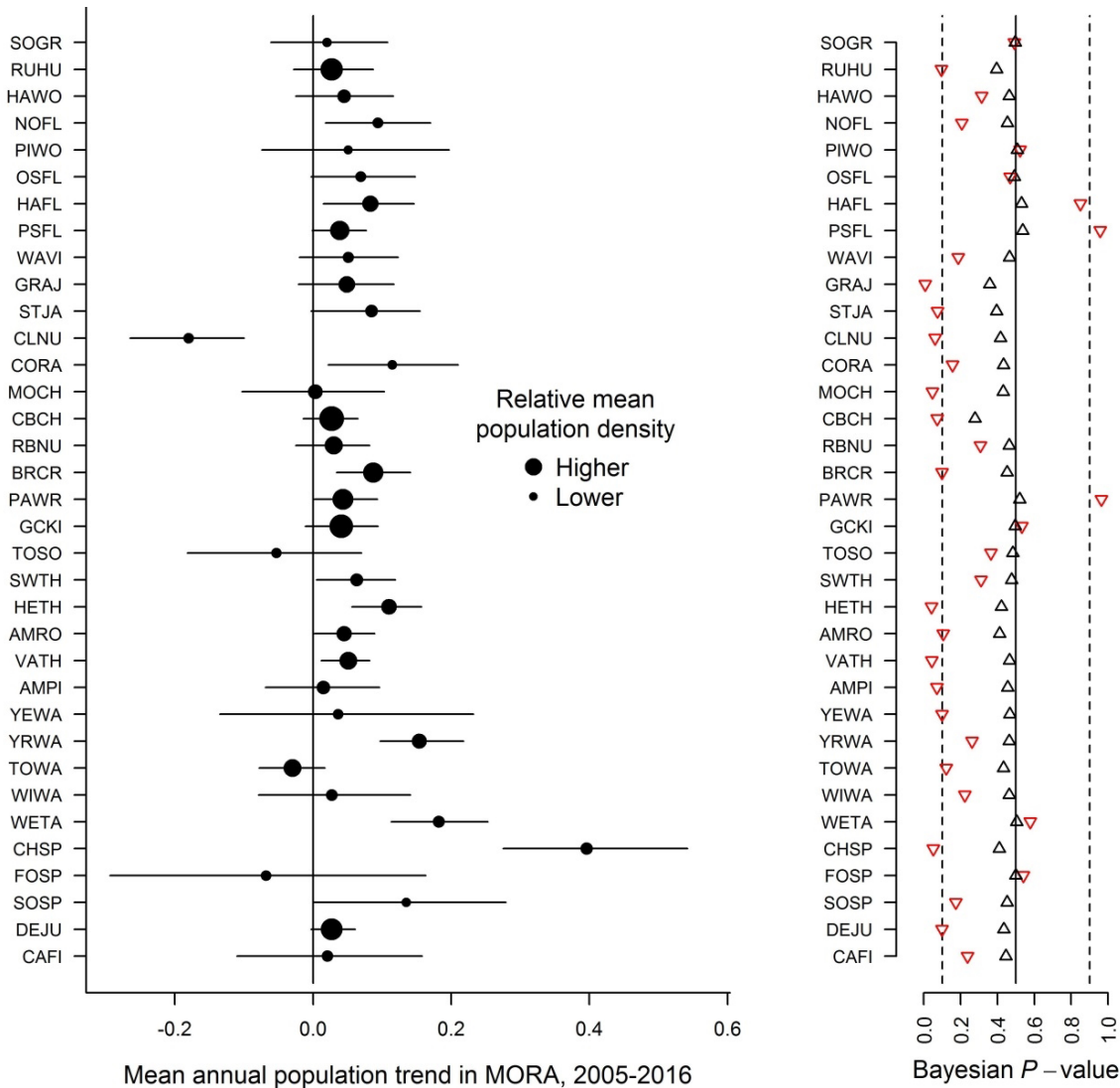


Figure 14. Population trends for species in Mount Rainier National Park (MORA). Mean annual trends in population density (left-hand panel) were estimated to be stable or increasing during the survey period (2005–2016) for most of the 35 landbird species analyzed for this park. Species are listed top to bottom in taxonomic order (species codes are identified in Table 6). Mean trends (dots) and 95% credible intervals (horizontal lines) indicate support for increasing density in 13 of these species. The only supported decline involved Clark’s Nutcracker (CLNU). Estimates of average population density per hectare (relative dot size) ranged from 0.002 for the Pileated Woodpecker (PIWO), to 2.907 for the Chestnut-backed Chickadee (CBCH). Components of model fit were considered adequate if the Bayesian P-value was not extreme (right-hand panel). Fit to the sub-model of species availability (black triangles) was always adequate but fit to the sub-model of perceptibility (inverted red triangles) varied widely. Covariates of detection distance were explored to improve detection models, and effects of noise or forest cover were supported for five species: American Robin (AMRO), Chipping Sparrow (CHSP), Stellar’s Jay (STJA) and Varied Thrush (VATH) detection varied inversely with noise, while Dark-eyed Junco (DEJU) detection varied inversely with forest cover.

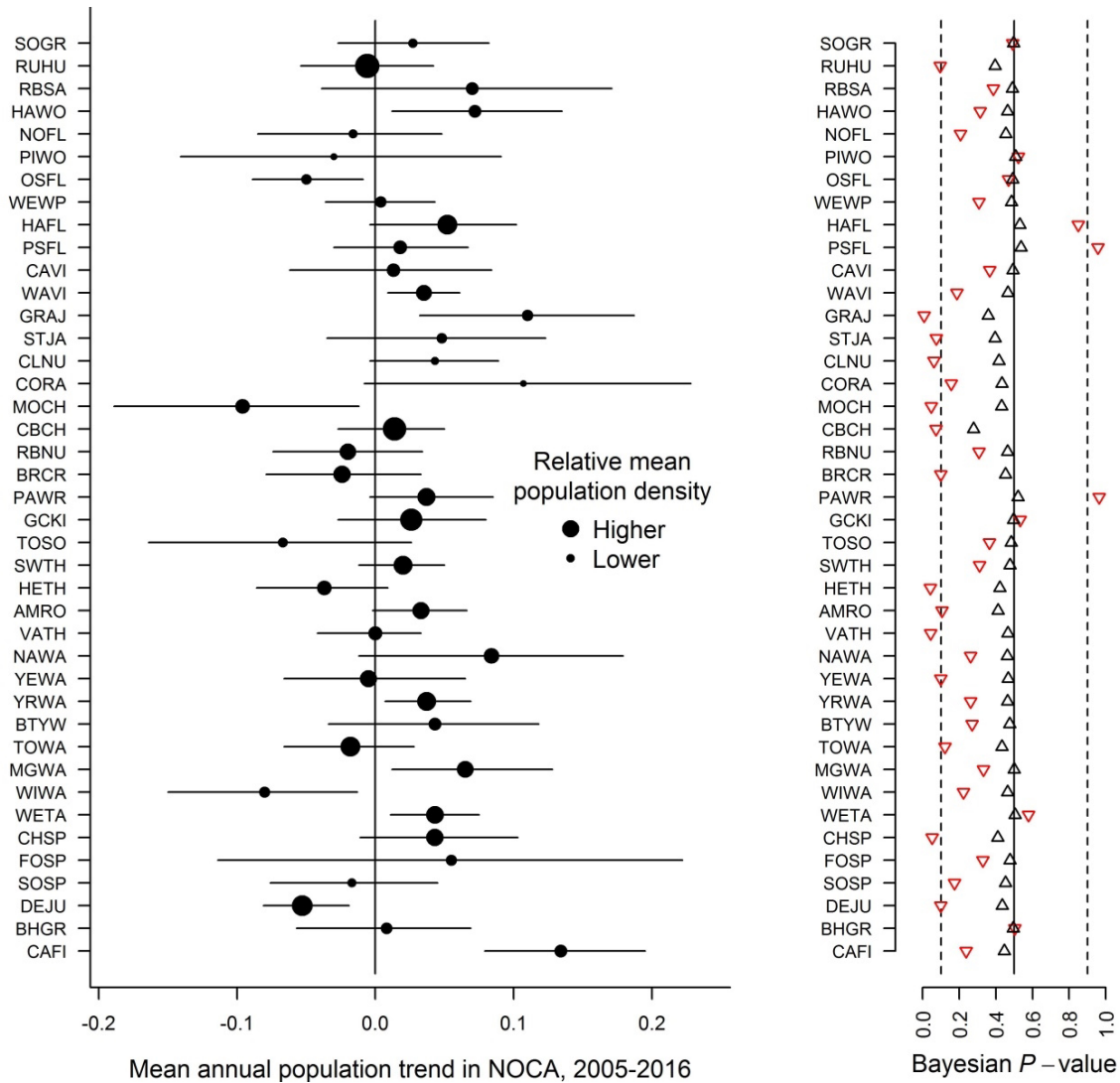


Figure 15. Population trends for species in North Cascades National Park Complex (NOCA). Mean annual trends in population density (left-hand panel) were estimated to be stable or increasing during the survey period (2005–2016) for most of the 41 landbird species analyzed for this park. Species are listed top to bottom in taxonomic order (species codes are identified in Table 6). Mean trends (dots) and 95% credible intervals indicate support for increasing density in seven species, and for decline in four species: Olive-sided Flycatcher (OSFL), Mountain Chickadee (MOCH), Wilson’s Warbler (WIWA) and Dark-eyed Junco (DEJU). Estimates of average population density per hectare (relative dot size) ranged from 0.002 for the Common Raven (CORA), to 2.109 for the Chestnut-backed Chickadee (CBCH) and 2.76 for the Rufous Hummingbird (RUHU), although attraction to observers likely leads to overestimation of hummingbird density. Components of model fit were considered adequate if the Bayesian P -value was not extreme (right-hand panel). Fit to the sub-model of species availability (black triangles) was always adequate but fit to the sub-model of perceptibility (inverted red triangles) varied widely. Covariates of detection distance were explored to improve detection models, and effects of noise or forest cover were supported for the same five species as detailed in results for MORA (Figure 14), because the best models for these species shared detection parameters in common among parks.

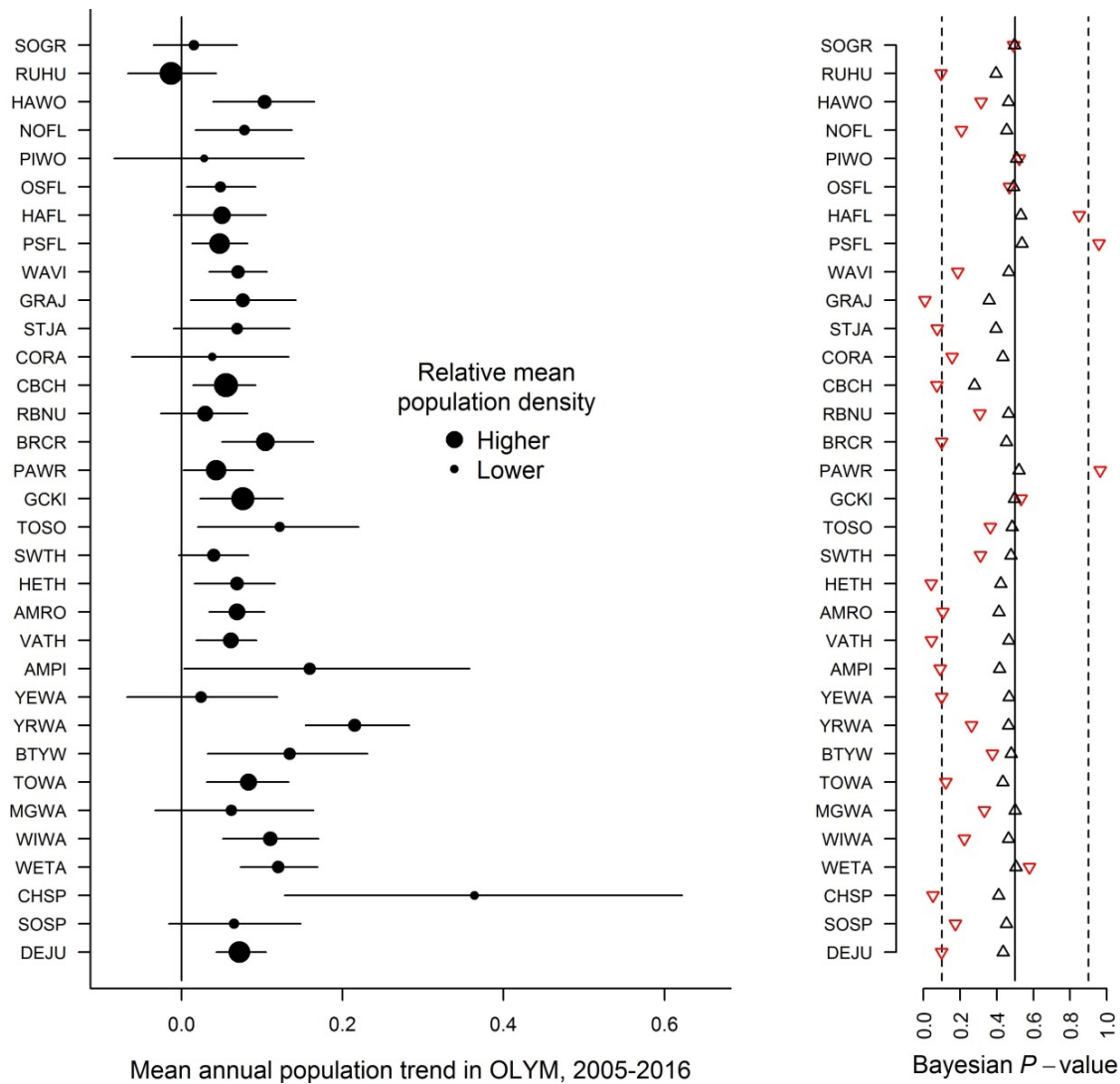


Figure 16. Population trends for species in Olympic National Park Complex (OLYM). Mean annual trends in population density (left-hand panel) were estimated to be stable or increasing during the survey period (2005–2016) for all of the 33 landbird species analyzed for this park. Species are listed top to bottom in taxonomic order (species codes are identified in Table 6). Mean trends (dots) and 95% credible intervals indicate support for increasing density in 22 species, and decline in none. Estimates of average population density per hectare (relative dot size) ranged from 0.003 for the Pileated Woodpecker (PIWO), to 2.786 for the Chestnut-backed Chickadee (CBCH). Components of model fit were considered adequate if the Bayesian P -value was not extreme (right-hand panel). Fit to the sub-model of species availability (black triangles) was always adequate but fit to the sub-model of perceptibility (inverted red triangles) varied widely. Covariates of detection distance were explored to improve detection models, and effects of noise or forest cover were supported for the same five species as detailed in results for MORA (Figure 14), because the best models for these five species shared detection parameters in common among parks.

As discussed above in the section on “Fitted models”, several covariates were explored to improve detection models. Observer, day and hour were not helpful in improving fit statistics or parameter convergence for populations in the mountain parks, but forest presence and noise had predictable

negative effects on detection distance and resulted in small but important improvements to model fit for several species (Table 8). In particular, detection varied inversely with noise for Stellar's Jay, American Robin, Varied Thrush and Chipping Sparrow, while detection varied inversely with forest cover for the Dark-eyed Junco. However, larger improvements to model fit and convergence of parameter estimates resulted from censoring all data from one or more parks where the focal species was rarely detected (Table 8).

There was general correspondence in annual variation between estimated population density and raw counts adjusted for survey effort (Figures 17–22). Both metrics suggested stable or increasing populations for most species, in agreement with estimates of trend over the monitoring period (Figures 14–16). However, annual estimates of density also suggested details not evident in linear trend estimates, such as a decline in 2016 that appears in the time series for several species, including Mountain Chickadee, Yellow Warbler and Townsend's Warbler.

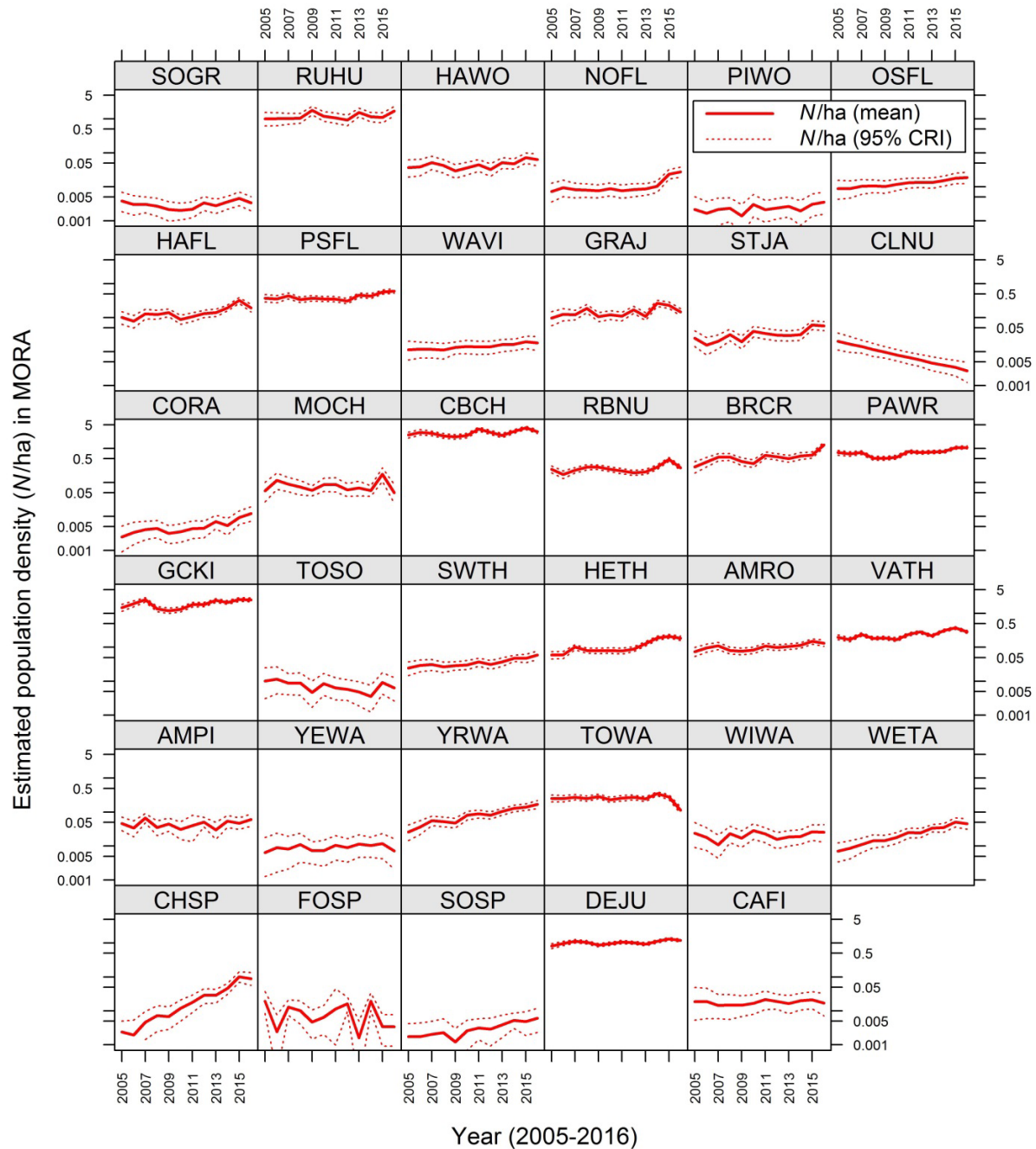


Figure 17. Yearly estimates of population density (N/ha) for 35 species commonly detected in Mount Rainier National Park (MORA). Density estimates, summarized here on a \log_{10} scale by means (solid lines) and 95% credible intervals (dotted lines), were based on the models listed in Table 2 that accounted for linear and nonlinear effects of elevation. Species codes are identified in Table 6.

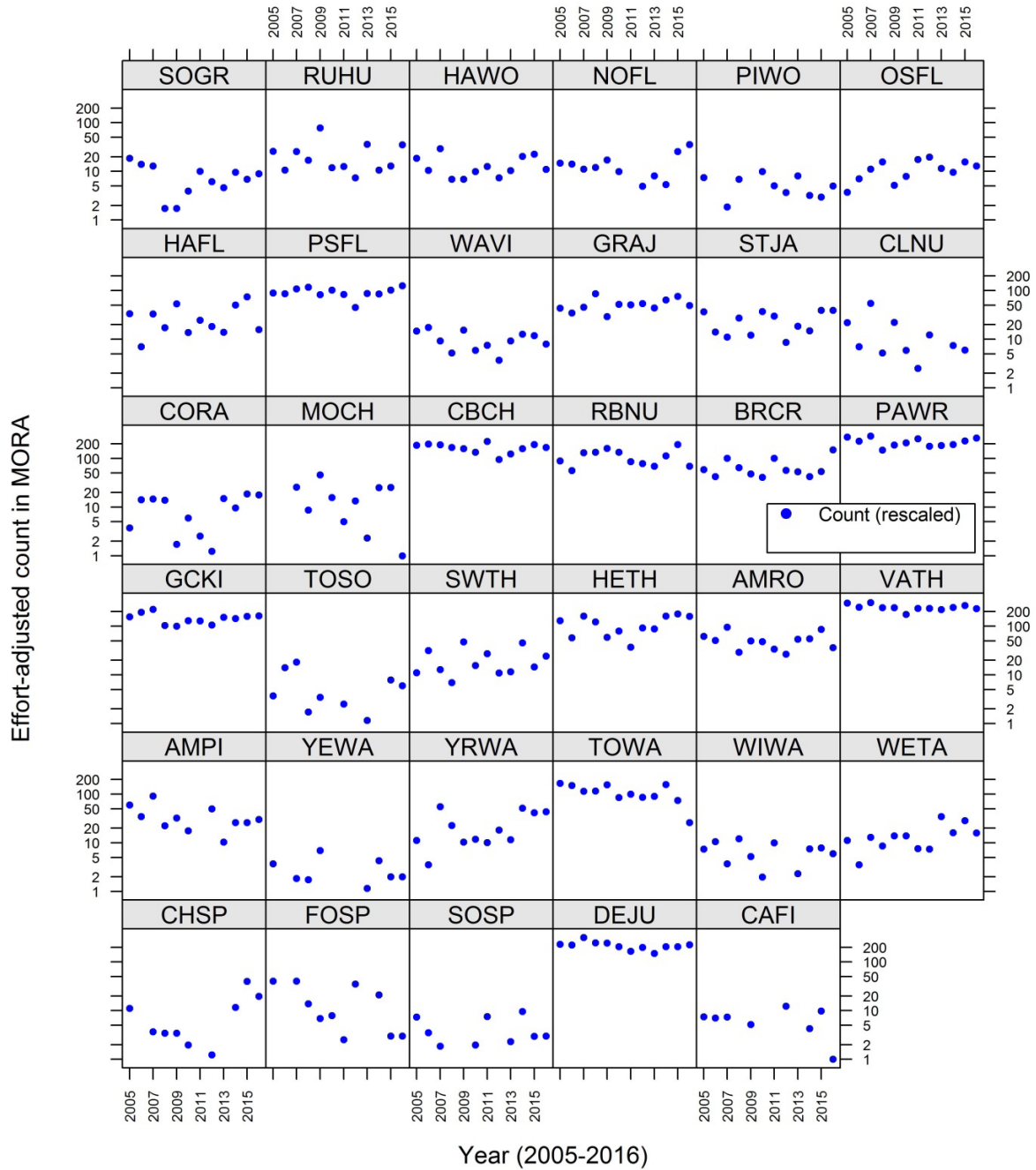


Figure 18. Effort-adjusted counts for 35 species commonly detected in Mount Rainier National Park (MORA). Annual counts per point and minute surveyed were rescaled for comparison on a log₁₀ scale by setting the lowest non-zero count to 1. Counts of zero are not plotted. Species codes are identified in Table 6.

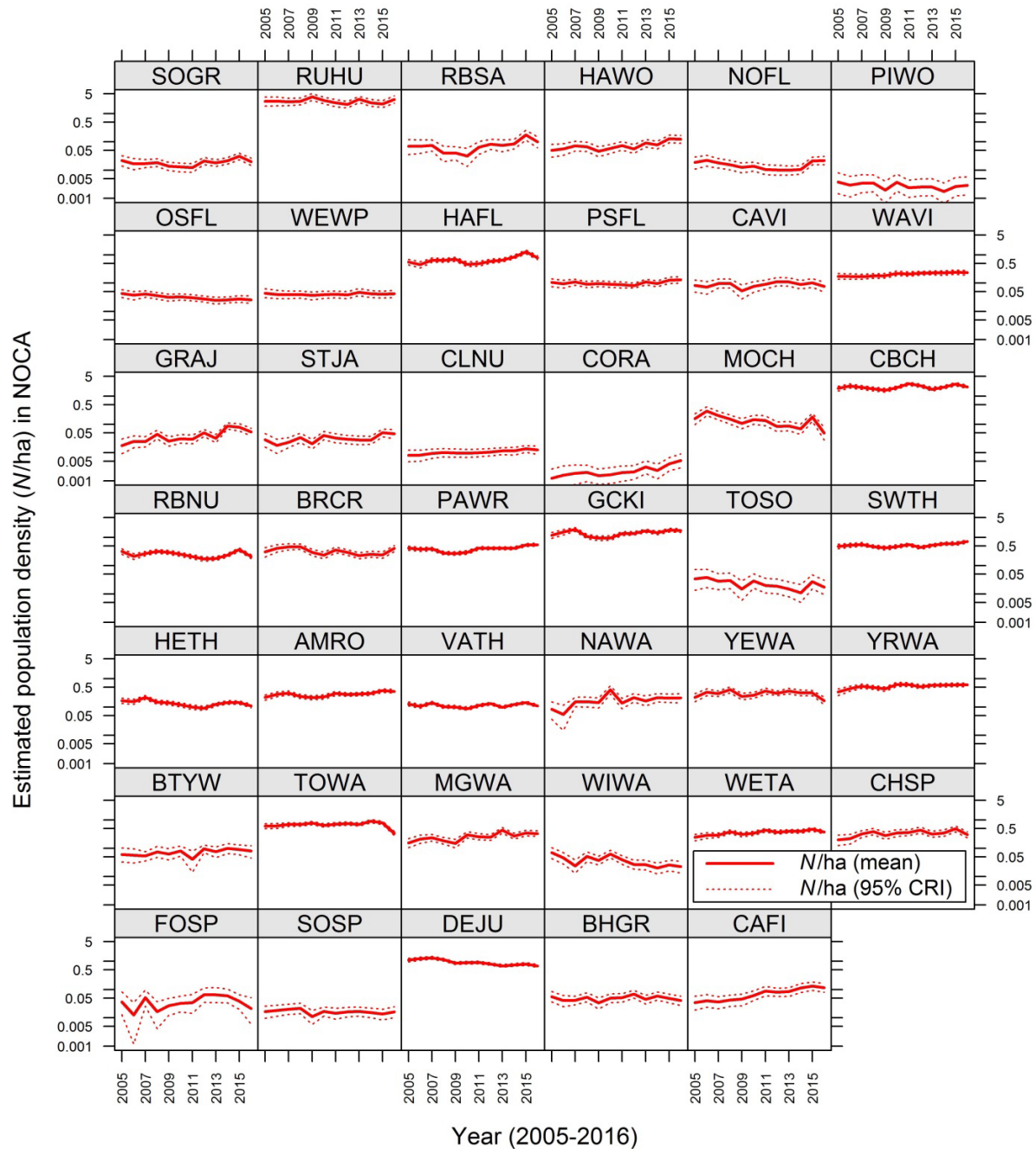


Figure 19. Yearly estimates of population density (N/ha) for 41 species commonly detected in North Cascades National Park Complex (NOCA). Density estimates, summarized here on a \log_{10} scale by means (solid lines) and 95% credible intervals (dotted lines), were based on the models listed in Table 2 that accounted for linear and nonlinear effects of elevation. Species codes are identified in Table 6.

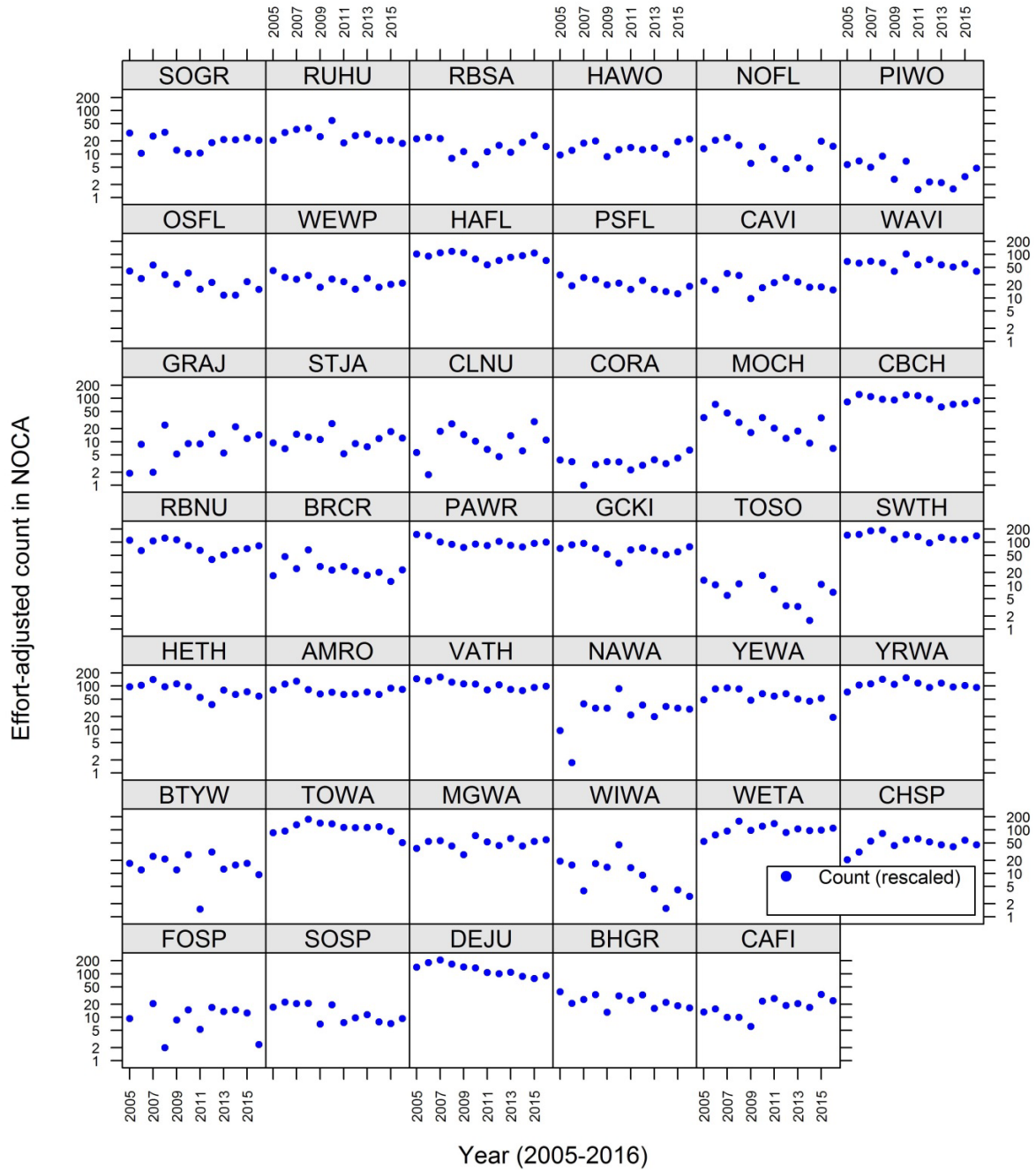


Figure 20. Effort-adjusted counts for 41 species commonly detected in North Cascades National Park Complex (NOCA). Annual counts per point and minute surveyed were rescaled for comparison on a log₁₀ scale by setting the lowest non-zero count to 1. Counts of zero are not plotted. Species codes are identified in Table 6.

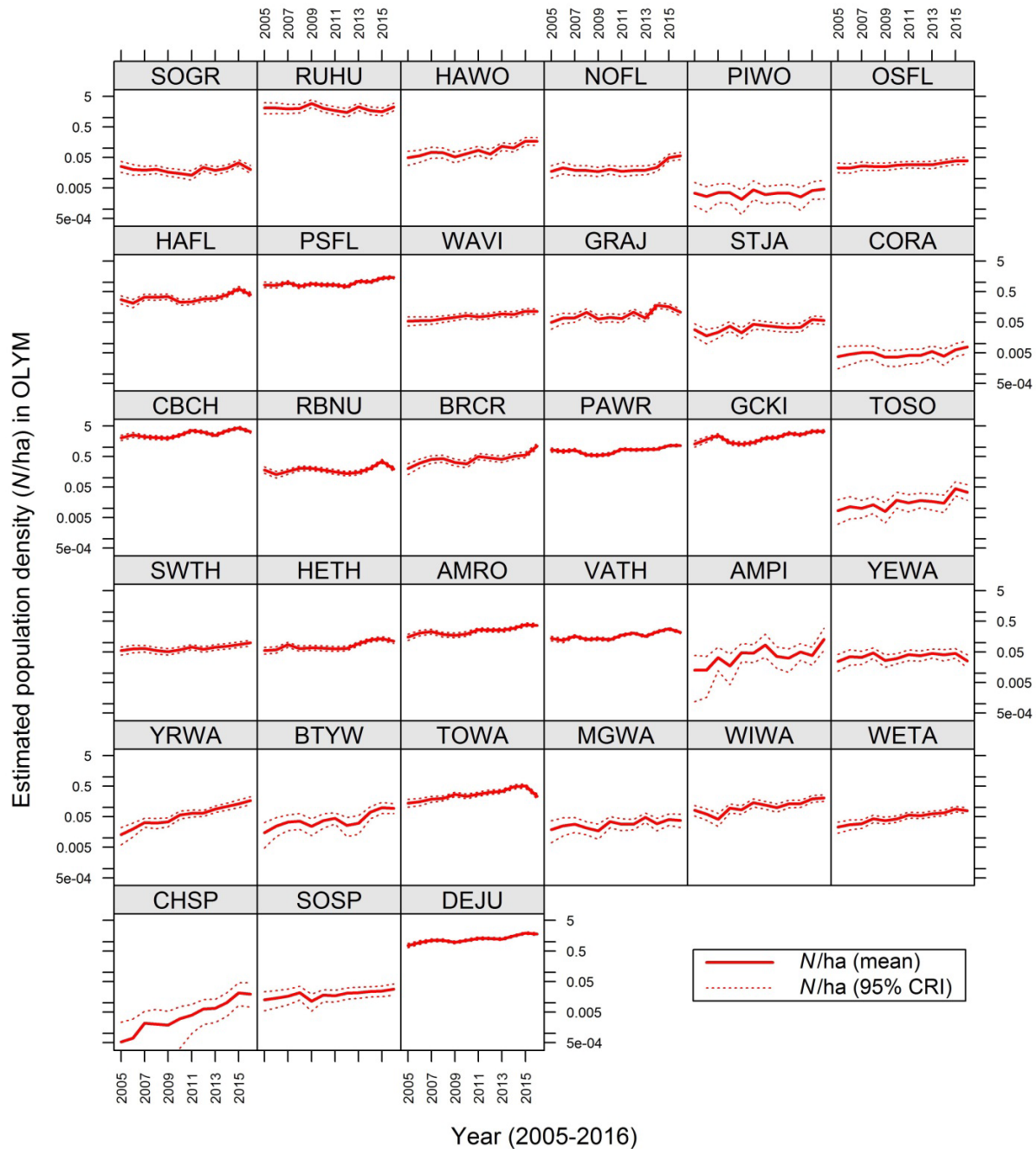


Figure 21. Yearly estimates of population density (N/ha) for 33 species commonly detected in Olympic National Park (OLYM). Density estimates, summarized here on a \log_{10} scale by means (solid lines) and 95% credible intervals (dotted lines), were based on the models listed in Table 2 that accounted for linear and nonlinear effects of elevation. Species codes are identified in Table 6.

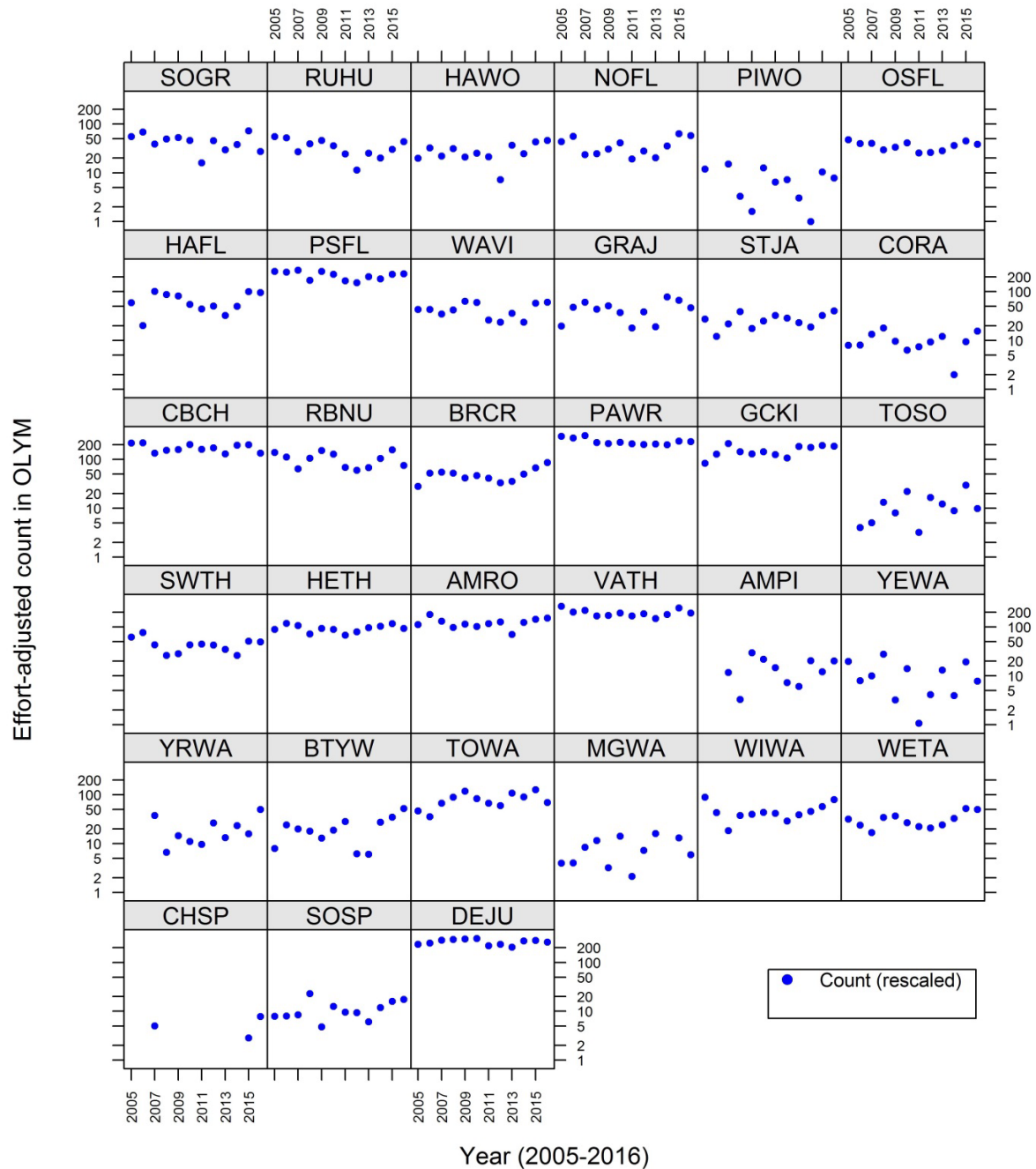


Figure 22. Effort-adjusted counts for 33 species commonly detected in Olympic National Park (OLYM). Annual counts per point and minute surveyed were rescaled for comparison on a log₁₀ scale by setting the lowest non-zero count to 1. Counts of zero are not plotted. Species codes are identified in Table 6.

As with density estimates in historical parks, higher annual variation among counts generally corresponded with higher annual variation and wider credible intervals on density estimates in mountain parks. The credible interval on density, however, also narrowed markedly toward the end of the monitoring period for quite a few species, and this feature was more apparent in mountain parks (Figures 17, 19 and 21) than in historical parks (Figures 7 and 11). Increased precision in

density estimates over time was facilitated by the formal increase in number of minutes surveyed (from 5 to 7 minutes) as well as by an informal increase in the number of point-count stations successfully surveyed by crews during later years (Table 3). Due to differences between the survey protocols for mountain and historical parks, only mountain parks experienced the temporal increase in stations surveyed. In mountain parks, additional stations can be added to the distal ends of transects as time allows, increasing both the number of stations and the reach of the sampling frame into off-trail habitats within the mountain parks. In historical parks, the grid of point-count stations is permanently fixed at a density that provides good coverage of each park. Adding stations in historical parks would result in overlap between stations in the effective area surveyed for species with higher mean detection distances.

For a few populations, there were apparent disparities between time series of density estimates and raw counts during the monitoring period. For example, Warbling Vireo appears to decline in raw counts from MORA (Figure 18), but the same species is estimated to have increased in density within that park (Figure 17). Apparent trends based on raw counts might differ from modeled trends for several reasons. First, there might be random effects of year and/or transect with strong influence on the trend estimate. Half of the transects surveyed in mountain parks are visited only once in every five years, so an anomalous transect might be surveyed infrequently and could appear to disrupt general trends. Year effects alone or in concert with unmodeled effects of directional climate change could cause trend estimates to diverge from raw counts. Fixed covariates of abundance and detection can also vary among years and influence trend estimates. Effects of elevation on population density, combined with an increasing number of surveys conducted in a given elevation class, could alter the proportion of surveys across elevations and affect the density estimate.

Effects of elevation in the mountain parks

For a given species in the mountain parks, we modeled linear and quadratic effects of elevation using coefficients that were constant across parks, while intercepts and trends in density were allowed to vary independently among parks (Table 2). Using this model, effects of elevation on breeding population density were common across the landbird species analyzed (Figure 23). Linear effects of elevation were split among the 42 species common to the mountain parks, with 14 species showing clearly positive effects and 24 showing clearly negative effects (Figure 23). Quadratic effects of elevation were also common and clearly supported for 27 species. Quadratic effects of elevation were also overwhelmingly negative (Figure 23), again suggesting that densities peak somewhere along the elevational gradient for these species. Only four species exhibited breeding densities that were independent of elevation: Sooty Grouse, Rufous Hummingbird, Golden-crowned Kinglet and Varied Thrush.

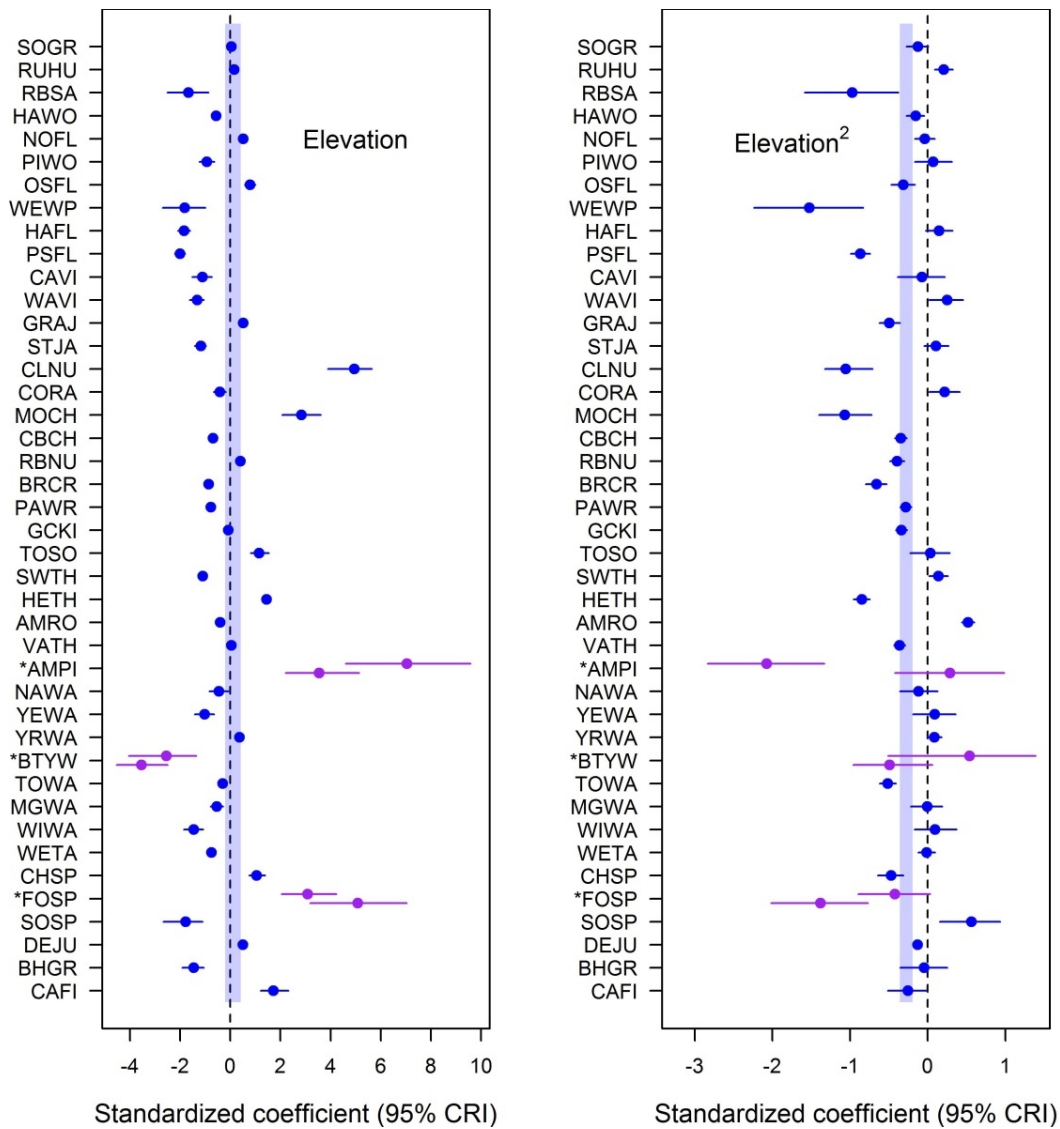


Figure 23. Effects of elevation on breeding landbird densities for 42 species commonly detected in mountain parks of the North Coast and Cascades Network. Each species model included both linear and quadratic effects of standardized elevation, summarized here by the mean (dot) and 95% credible interval (horizontal line) of each fitted coefficient of elevation (left-hand panel) or elevation² (right-hand panel). Species codes are identified in Table 6. Linear effects of elevation were clearly positive ($n = 14$ species) or negative ($n = 24$ species) for all but four species: Golden-crowned Kinglet (GCKI), Rufous Hummingbird (RUHU), Sooty Grouse (SOGR) and Varied Thrush (VATH). Quadratic effects of elevation were supported for fewer species ($n = 27$) and were primarily negative ($n = 21$). Vertical bars (light blue) summarize the overall mean \pm SE for point estimates of the fitted coefficients, demonstrating the generally negative effect of elevation². Three species denoted with asterisks were rare in only one park and were best analyzed using park-specific models applied to each of two parks where they were more common: American Pipit (AMPI), Black-throated Gray Warbler (BTYW) and Fox Sparrow (FOSP). For each of these three species, we obtained two independent estimates of each elevational effect, highlighted as purple point estimates and CRIs. For AMPI, the upper and lower estimates in each pair correspond to effects of elevation in MORA (upper) and OLYM (lower); for BTYW, OLYM (upper) and NOCA (lower); and for FOSP, NOCA (upper) and MORA (lower).

Independent estimates of the effects of elevation were obtained for three species that were analyzed using a pair of single-park models because they were detected too rarely in one or more parks to support a three-park model. For the American Pipit, Black-throated Gray Warbler and Fox Sparrow, pairs of estimates (depicted in purple) and credible intervals for the effects of elevation on population density are shown in Figure 23. These paired estimates were congruent in five of six cases, confirming positive effects of elevation in two cases, negative effects of elevation in one case, negative effects of elevation² in one case, and no effect of elevation² in one case. In the final case, we found negative effects of elevation² for American pipit in MORA but no effect of elevation² in OLYM (Figure 23).

Population densities often differed dramatically between elevational strata (Figures 24–26), and trends were quite congruent among strata within and among parks in the models considered here. This result is in agreement with the stratum-specific models of population trend explored in Ray et al. (2017 a), which found no difference between strata in trends across parks when data were pooled by stratum rather than park. However, aside from a regional compilation of annual population density estimates (see “*Regional stability in locally declining species*”, below), the analyses presented here focus on park-level population dynamics, and do not include a stratum-specific effect on trend because few species were detected with sufficient frequency across all three strata to investigate stratum-level trends within parks. In future years, it will be possible to reveal evidence for elevational range-shifts of breeding populations within parks by fitting stratum-specific trends. Although the number of point-count stations is roughly similar among strata within parks, sampling density varies among strata because the area of each stratum differs. When stratum-specific trends are modeled and population size is appropriately extrapolated to the stratum scale, it is possible for trends in larger populations or larger strata to swamp different trends in smaller populations or smaller strata (Ray et al. 2017 a). This possibility should be explored as sufficient data become available to model stratum-specific trends within parks.

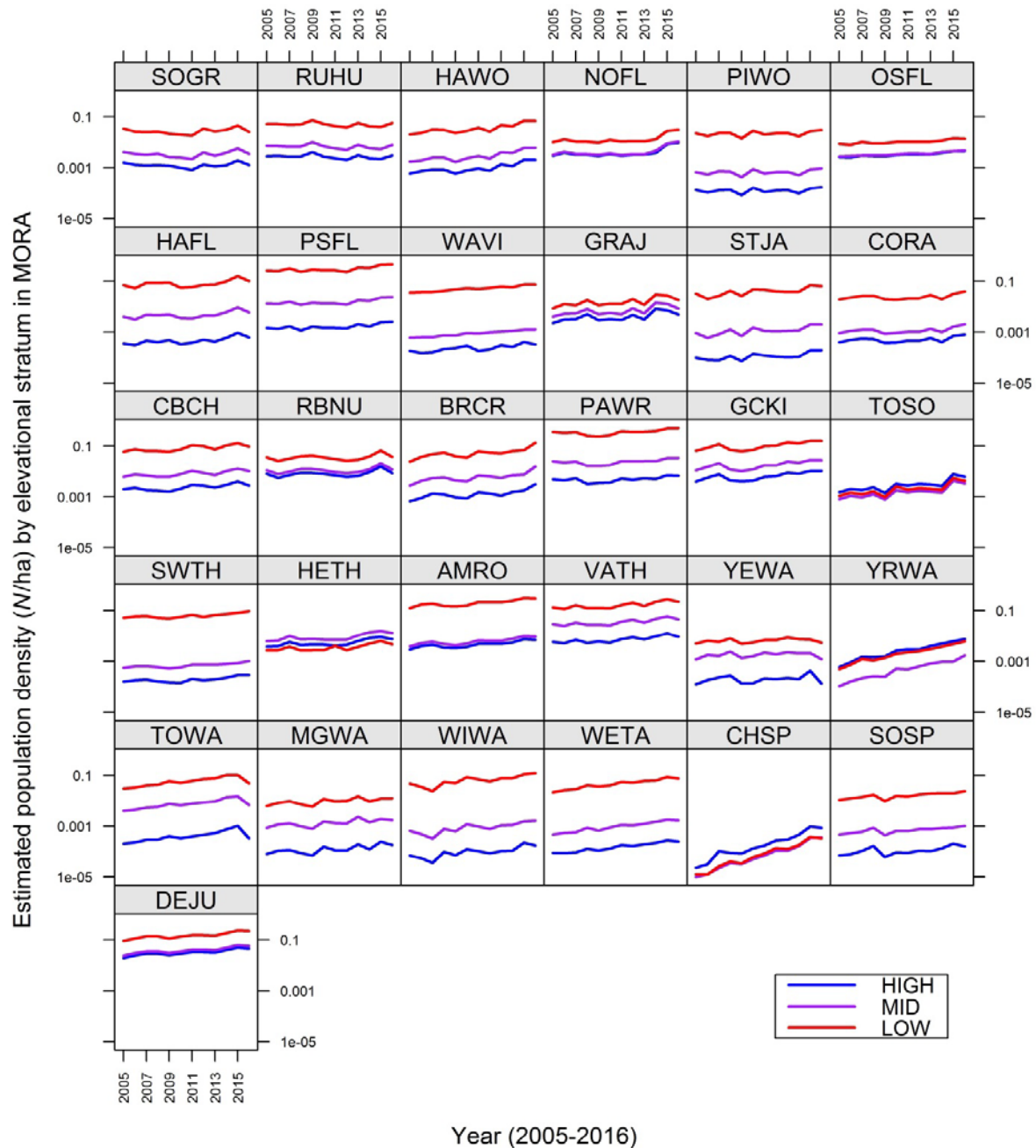


Figure 24. Yearly estimates of mean population density (N/ha), differentiated by elevational stratum, for 33 of 35 landbird species common to Mount Rainier National Park (MORA). Strata in MORA were defined as high elevation (above 1350 m, blue), mid-elevation (800–1350 m, purple) and low elevation (below 800 m, red). Density estimates were based on the multi-park models listed in Table 2 that accounted for linear and nonlinear effects of elevation. Results specific to MORA are shown for each of 33 species that could be analyzed successfully in a multi-park framework. For the other two species, American Pipit (AMPI) and Fox Sparrow (FOSP), MORA-specific models (not shown) also suggest trends that were congruent across elevational strata during 2005–2016. Species codes are identified in Table 6.

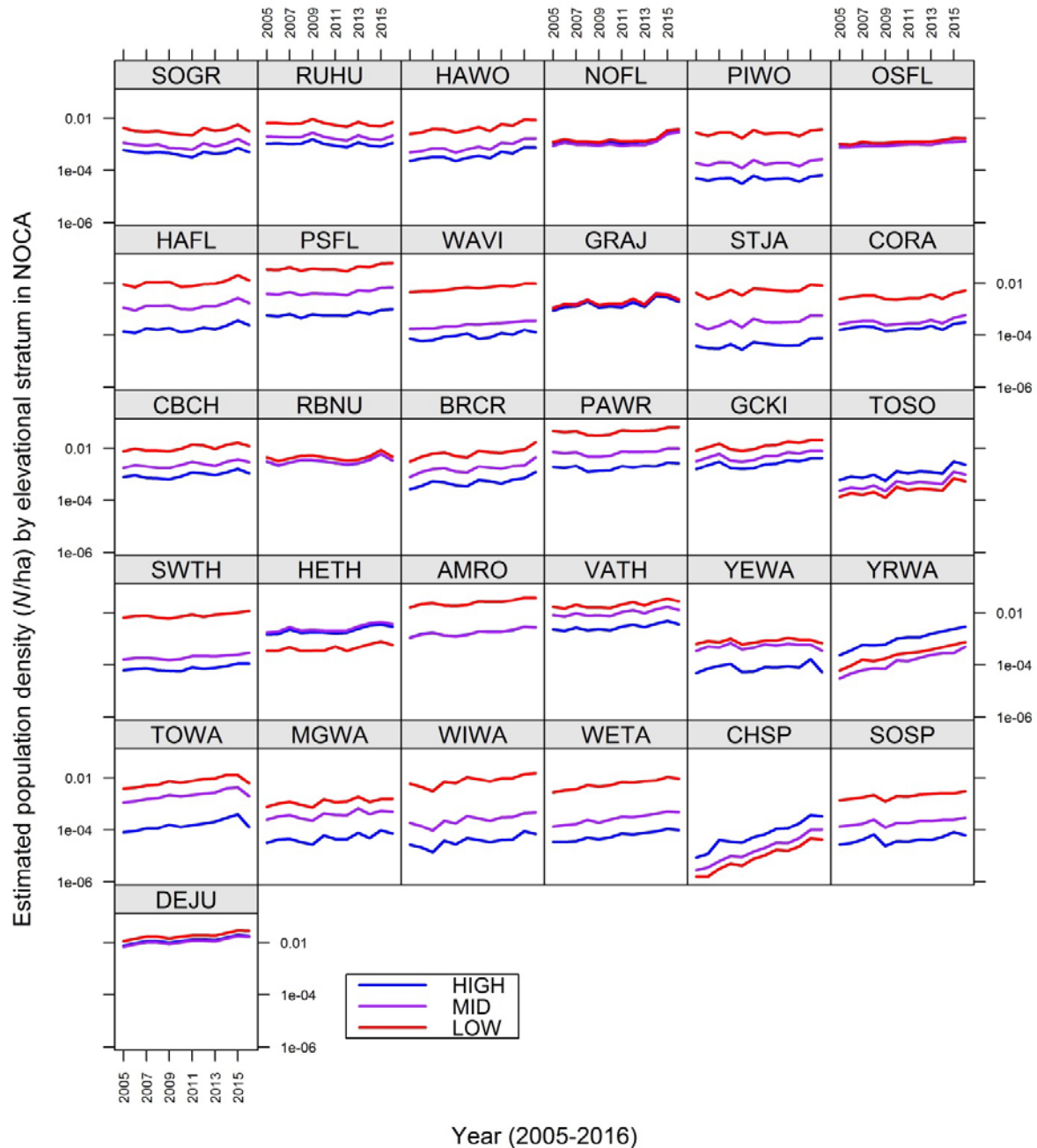


Figure 25. Yearly estimates of mean population density (N/ha), differentiated by elevational stratum, for 36 of 41 landbird species common to North Cascades National Park Complex (NOCA). Strata in NOCA were defined as high elevation (above 1350 m, blue), mid-elevation (650–1350 m, purple) and low elevation (below 650 m, red). Density estimates were based on the multi-park models listed in Table 2 that accounted for linear and nonlinear effects of elevation. Results specific to NOCA are shown for each of the 36 species that could be analyzed successfully in a multi-park framework. For the other five species (Red-breasted Sapsucker [RBSA], Western Wood-Pee-wee [WEWP], Black-throated Gray Warbler [BTYW], Fox Sparrow [FOSP] and Black-headed Grosbeak [BHGR]), NOCA-specific models (not shown) also suggested trends that were congruent across elevational strata during 2005–2016. Species codes are identified in Table 6.

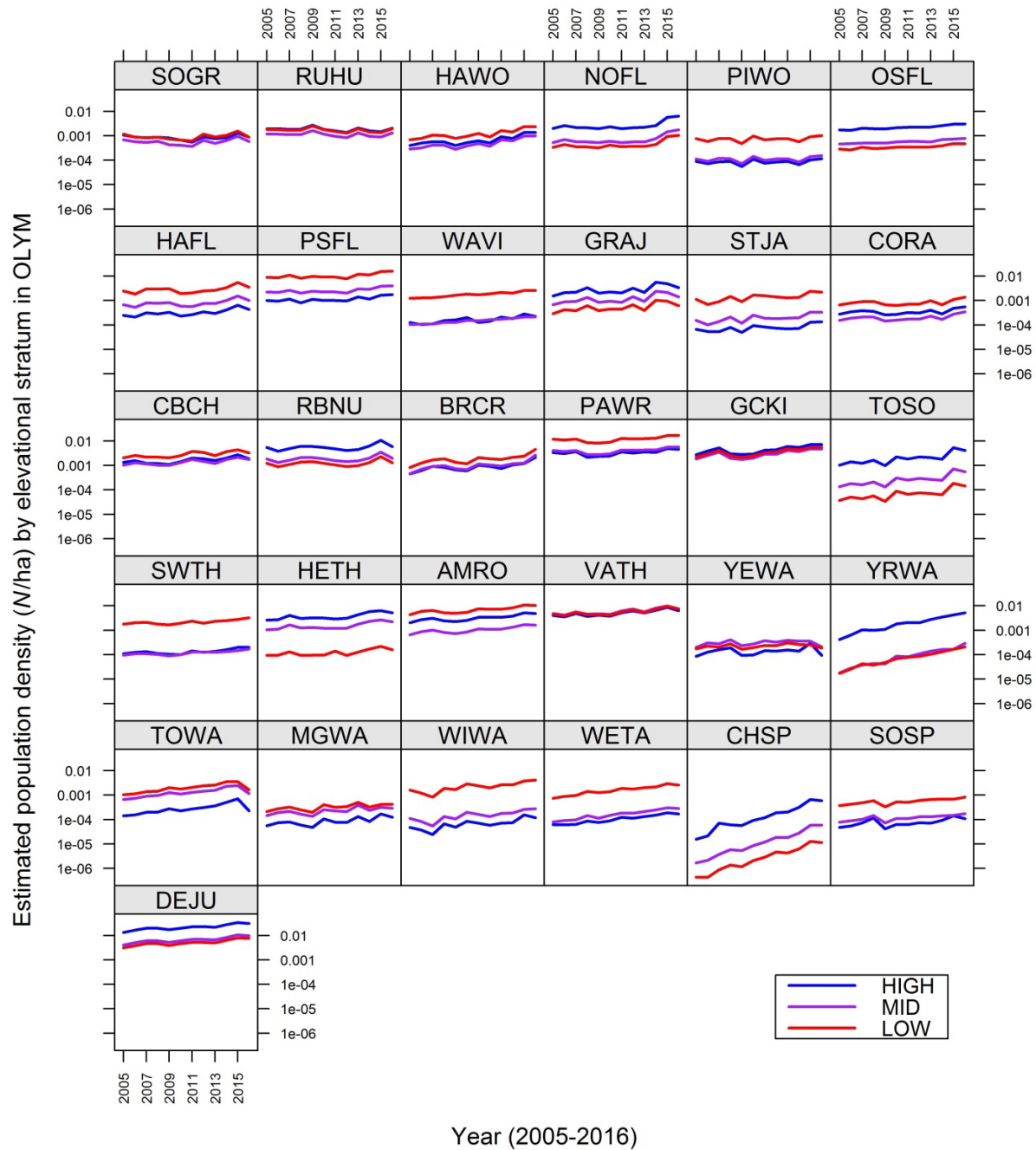


Figure 26. Yearly estimates of mean population density (N/ha), differentiated by elevational stratum, for 31 of 33 landbird species common to Olympic National Park (OLYM). Strata in OLYM were defined as high elevation (above 1350 m, blue), mid-elevation (650–1350 m, purple) and low elevation (below 650 m, red). Density estimates were based on the multi-park models listed in Table 2 that accounted for linear and nonlinear effects of elevation. Results specific to OLYM are shown for each of the 31 species that could be analyzed successfully in a multi-park framework. For the other two species, American Pipit (AMPI) and Black-throated Gray Warbler (BTYW), OLYM-specific models (not shown) also suggested trends that were congruent across elevational strata during 2005–2016. Species codes are identified in Table 6.

Effects of climate in the mountain parks

In the mountain parks, where the period of snow cover can be prolonged, we expected breeding success to be optimal near the long-term mean of PAS, under the assumption that species are adapted to prevailing conditions. Testing this hypothesis required adding a quadratic effect of PAS in year t on breeding bird densities in year $t+1$. We further expected a linear effect of MST in year t on breeding bird densities in year $t+1$. To reduce the number of parameters estimated in the three-park models used here, we assumed that lagged effects of climate were similar among parks, fitting a single coefficient for each of the three hypothesized effects: PAS, PAS² and rMST.

Using this model, effects of climate on breeding population density were common across the landbird species analyzed (Figures 27 and 28). Lagged linear effects of PAS were clearly negative for 14 of the 42 species common to the mountain parks, and were clearly positive for only three species (Figure 27, left-hand panel), in agreement with the hypothesis that deeper snowpacks with prolonged persistence in one year reduce breeding success and recruitment of breeders counted in the next year. The strength of the few positive effects, however, balanced that of the negative effects, such that the mean overall effect of PAS was nearly zero. In contrast, the mean overall pattern of lagged quadratic effects of PAS was quite negative (Figure 27, right-hand panel), with clear negative effects supported for 25 species and clear positive effects supported for only two species, and the magnitude of negative effects overwhelming that of positive effects. This negative effect of lagged PAS² is in agreement with the hypothesis that breeding success is optimized for most species at some intermediate accumulation of snow.

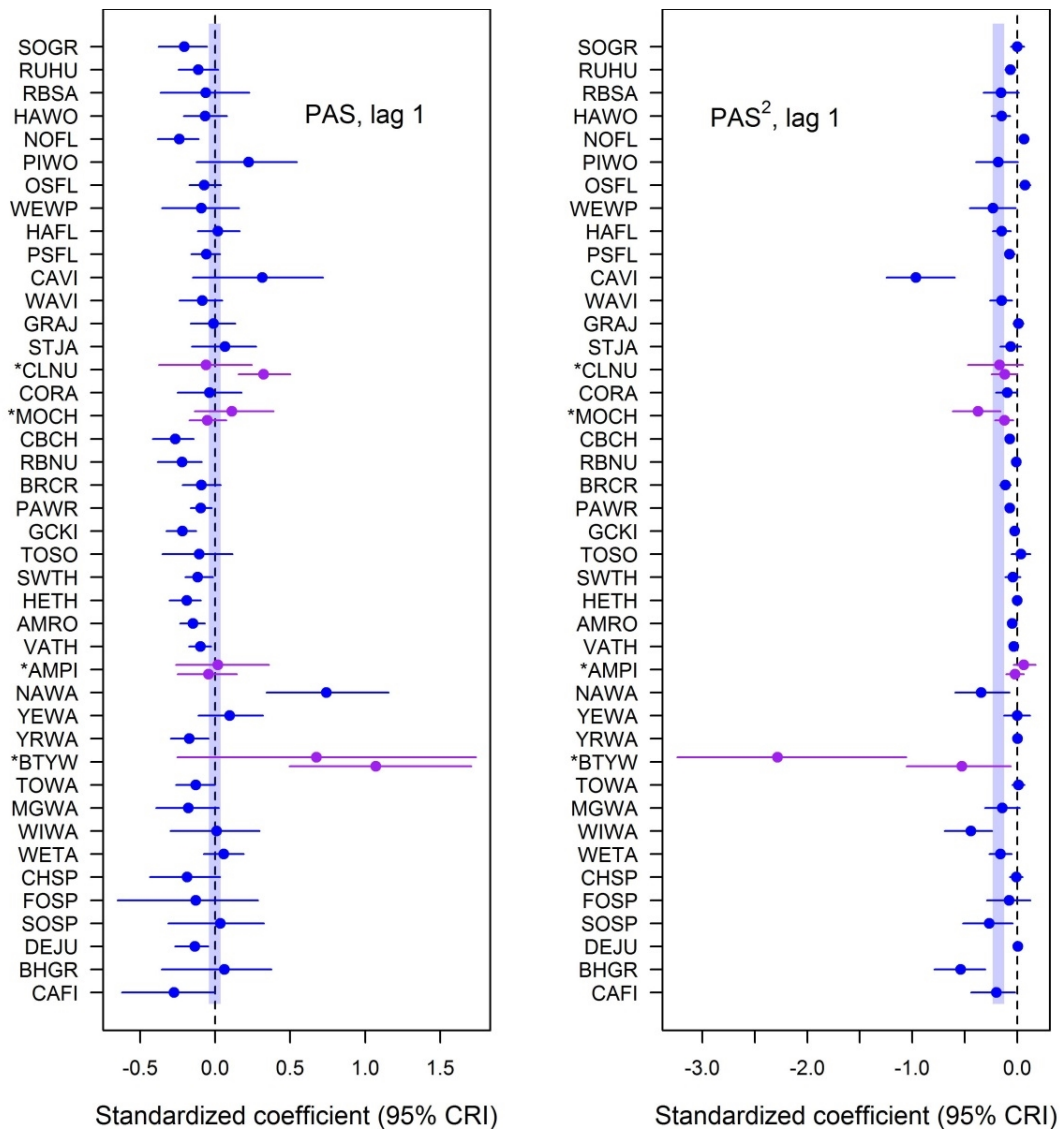


Figure 27. Mean annual effects of local precipitation-as-snow (PAS) in one year on breeding landbird densities in the following year for 42 species commonly detected in mountain parks of the North Coast and Cascades Network. Negative linear effects of PAS (left hand panel) were supported for at least 14 species, compared with only three positive effects, but the 95% credible interval (CRI) overlapped zero for most species. In contrast, negative nonlinear (quadratic) effects of PAS (right-hand panel) were supported for 25 species, compared with only two positive effects, suggesting that breeding success is best at intermediate levels of PAS for most species. Vertical bars (light blue) summarize the overall mean \pm SE for point estimates of the fitted coefficients, demonstrating the mean negative effect of PAS². Four species denoted with asterisks were rare in only one park and were best analyzed using park-specific models applied to each of two parks where they were more common: Clark’s Nutcracker (CLNU), Mountain Chickadee (MOCH), American Pipit (AMPI) and Black-throated Gray Warbler (BTYW). For each of these four species, we obtained two independent estimates of each precipitation effect, highlighted as purple point estimates and CRIs. For CLNU, the upper and lower estimates in each pair correspond to effects of PAS in MORA (upper) and NOCA (lower); for MOCH, MORA (upper) and NOCA (lower); for AMPI, MORA (upper) and OLYM (lower); and for BTYW, OLYM (upper) and NOCA (lower). Species codes are identified in Table 6.

Independent estimates of the effects of PAS were obtained for four species that were analyzed using a pair of single-park models because they were detected too rarely in one or more parks to support a three-park model. For the Clark's Nutcracker, Mountain Chickadee, American Pipit and Black-throated Gray Warbler, pairs of estimates (in purple) and credible intervals for the lagged effects of PAS on population density are shown in Figure 27. These paired estimates are congruent in six out of eight cases, and roughly congruent in a seventh case, confirming lagged effects of PAS² in all four species and lagged effects of PAS in two or three of the four species (Figure 27). The pattern of effects of PAS on Clark's Nutcracker and Mountain Chickadee do not immediately appear to explain the park-specific declines in these species, given that Clark's Nutcracker is declining in MORA and Mountain Chickadee in NOCA.

After accounting for covariance between PAS and MST, residual MST (rMST) was sometimes related to lagged breeding bird densities (Figure 28). However, these relationships were clear for only 12 species and were not overwhelmingly directional, involving nine species with negative effects and three with positive effects. Of the four species providing independent estimates of the effects of rMST, paired estimates were congruent only for the Black-throated Gray Warbler, which was not affected by rMST in either park, so climate effects did not help to explain its increase in OLYM. The positive effect of rMST on Clark's Nutcracker in NOCA relative to MORA might explain the stability of its population in NOCA relative to MORA. However, the lack of effects of rMST on Mountain Chickadee do not help to explain that species decline in NOCA.

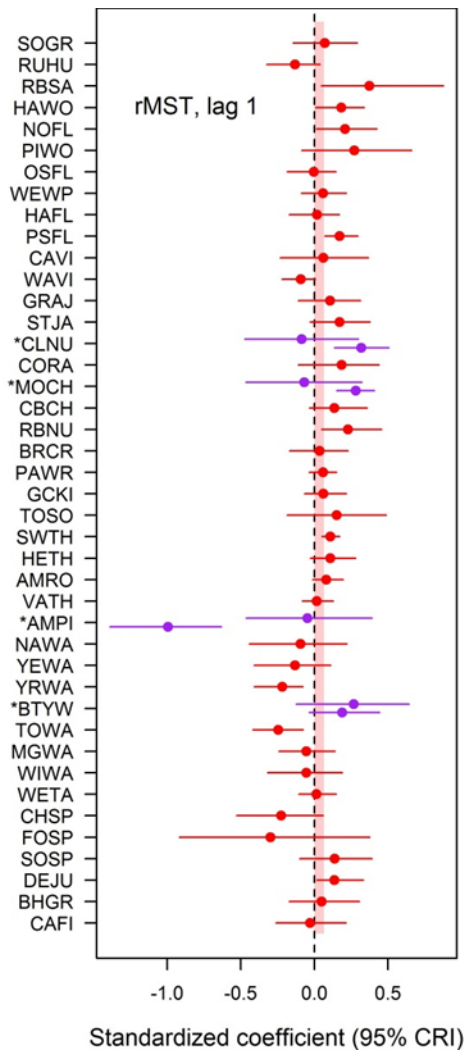


Figure 28. Residual effects of mean spring temperature (MST), after accounting for covariance between MST and PAS. For nine species, breeding landbird densities were positively related to residual MST (rMST) in the previous year; for three species, densities were negatively related to rMST in the previous year; for the remaining 30 species, the 95% credible interval (CRI) for the effect of rMST overlapped zero. The vertical bar (light red) summarizes the overall mean \pm SE for point estimates of the fitted coefficients of rMST, tending slightly positive. Four species denoted with asterisks were rare in only one park and were best analyzed using park-specific models applied to each of two parks where they were more common: Clark’s Nutcracker (CLNU), Mountain Chickadee (MOCH), American Pipit (AMPI) and Black-throated Gray Warbler (BTYW). For each of these four species, we obtained two independent estimates of each temperature effect, highlighted as purple point estimates and CRIs. For CLNU, the upper and lower estimates in each pair correspond to effects of elevation in MORA (upper) and NOCA (lower); for MOCH, MORA (upper) and NOCA (lower); for AMPI, MORA (upper) and OLYM (lower); and for BTYW, OLYM (upper) and NOCA (lower). Species codes are identified in Table 6.

It was rare for estimates of trend to be affected appreciably by the addition of climate covariates. However, for some species in the historical parks, such as the Barn Swallow in the American Camp portion of SAJH, there was strong support for a positive trend only after accounting for effects of climate. To investigate the generality of this effect, we plotted the trend estimate based on climate

models against the trend estimate based on basic or elevation models for every population that we fitted to both models (n = 175), and differentiated results by park (Figure 29). Results from all parks overlap considerably, but it is clear that most points lie along the diagonal of Figure 29, confirming that estimates of trend differ little between the different models of each population. Exceptions occurred only for estimates based on data from the historical parks SAJH (n = 3) and LEWI (n = 12). These exceptions might be due to the relatively sparse data collected from historical parks to date.

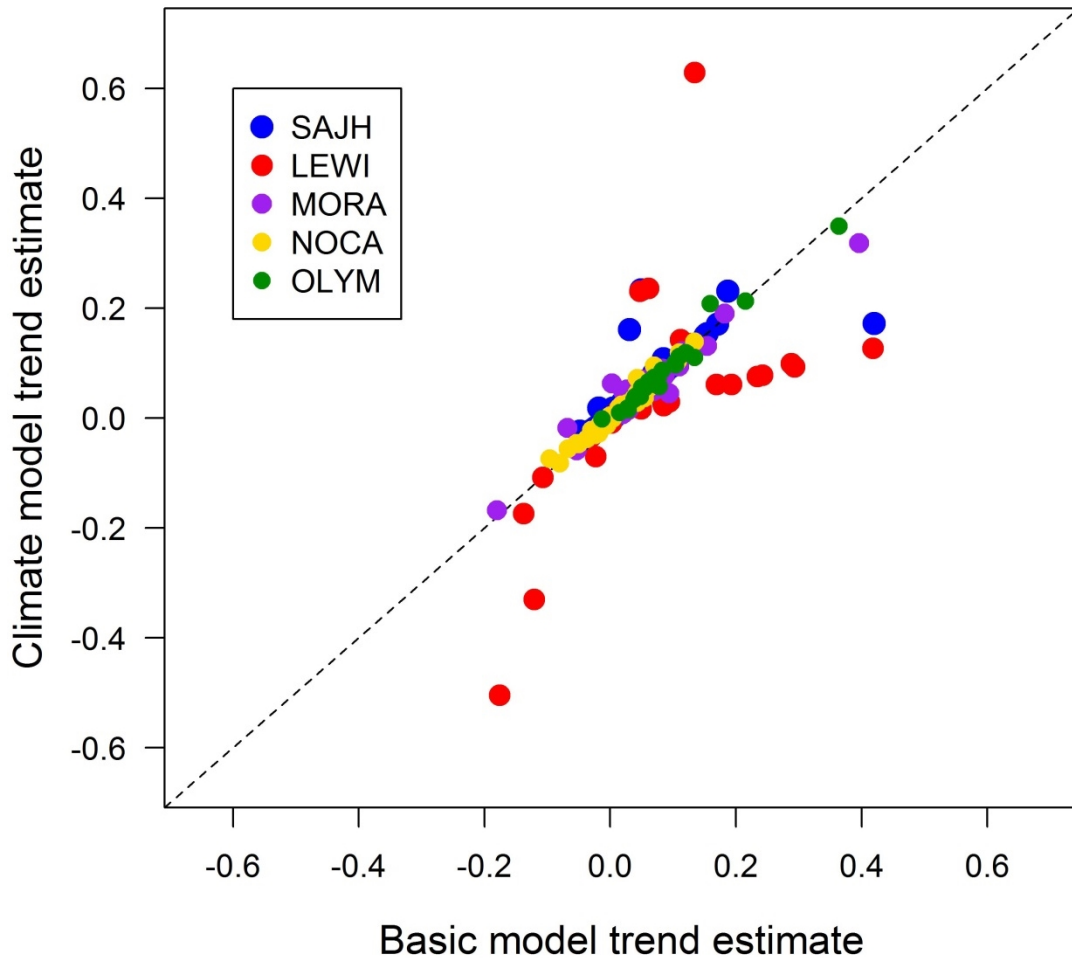


Figure 29. Similarity in trend estimates between basic and climate models for 175 populations differentiated by park. Most points fall near the 1:1 line (dashed), including all points representing populations in the mountain parks. Point sizes are staggered to reveal those plotted over.

Regional stability in locally declining species

Fitted trends for 2005–2016 included a clear decline in at least one park for seven of the species analyzed (Figures 14–16). Given variation in population density among parks, and variation among parks in area and potential population size, it could be possible for a decline in one park to dominate regional dynamics. Alternatively, a species only tending to decline at the park level might be found to exhibit a clearer trend in a regional analysis. For example, the expected trend for Rufous

Hummingbird was negative in four out of five parks, suggesting the potential for a regional decline. Of the seven species exhibiting a clear decline at the park level, only Hutton's Vireo cannot be buoyed by regional dynamics: that species occurred only in one park. Northern Flicker clearly increased in MORA and OLYM, potentially countering a clear decline in LEWI and lack of trend in NOCA. Olive-sided Flycatcher clearly declined in NOCA and LEWI but increased in SAJH and OLYM. Clark's Nutcracker declined in MORA but not NOCA. Mountain Chickadee declined in NOCA but not MORA. Wilson's Warbler declined in NOCA but increased in LEWI and OLYM. Dark-eyed Junco declined in NOCA but clearly increased in LEWI and OLYM. Local declines clearly warrant examination to suggest management actions and to forecast potential trends. Our purpose here, however, is to determine whether local declines appear to have been offset by increasing densities elsewhere during the monitoring period.

Regional trends could be estimated by including data from all five parks in a single model. However, there are sufficient differences in survey structure between mountain and historical parks that a single model might require more parameters than just 12 years of data would support. Alternatively, the regional time series for a species can be constructed using annual estimates of population size at each point across the parks it frequents. Figure 30 shows the regional time series for seven species of potential concern. Most of these time series suggest regional increase or stability, although it would be possible to draw a declining trajectory between the 95% credible intervals for several of these species. Time series for Clark's Nutcracker and Mountain Chickadee appear most compatible with regional decline; for these two species, analyses were limited to MORA and NOCA because they were virtually absent from other parks throughout the study period, and local decline was supported in only one mountain park for each species.

Although a few local declines were revealed by our park-structured analysis, these declines appear to have been largely offset by regional dynamics (Figure 30). Differences in climate among parks might explain some of this variation among park population trajectories. In the analysis of 10-year trends in mountain parks, Ray et al. (2017a) suggested that "the relatively negative snowfall anomaly at NOCA" might counter other processes and confer stability to populations in this region. However, the snowfall anomaly in NOCA stands out less in this 12-year analysis (Figure 3). Stability might also derive from spatiotemporal differences among parks in habitat quality or in the interaction between habitat and climate. For some species, these park populations might form part of a metapopulation with local dynamics that are sufficiently independent to generate regional stability (Hanski and Gilpin 1997). Ray et al. (2017a) suggested that "these parks may function as a network of habitats that vary from year to year in their importance as breeding habitat and potential refugia." This hypothesis might apply in particular to the few species that varied in trend among parks, unless these species exhibit parallel trends across elevational strata within parks (*sensu* Figures 24–26), which would suggest little annual variation in the importance of breeding habitats along an elevational axis. Still, as annual conditions change, the network of protected areas represented by the NCCN might provide dynamic refugia for landbird species.

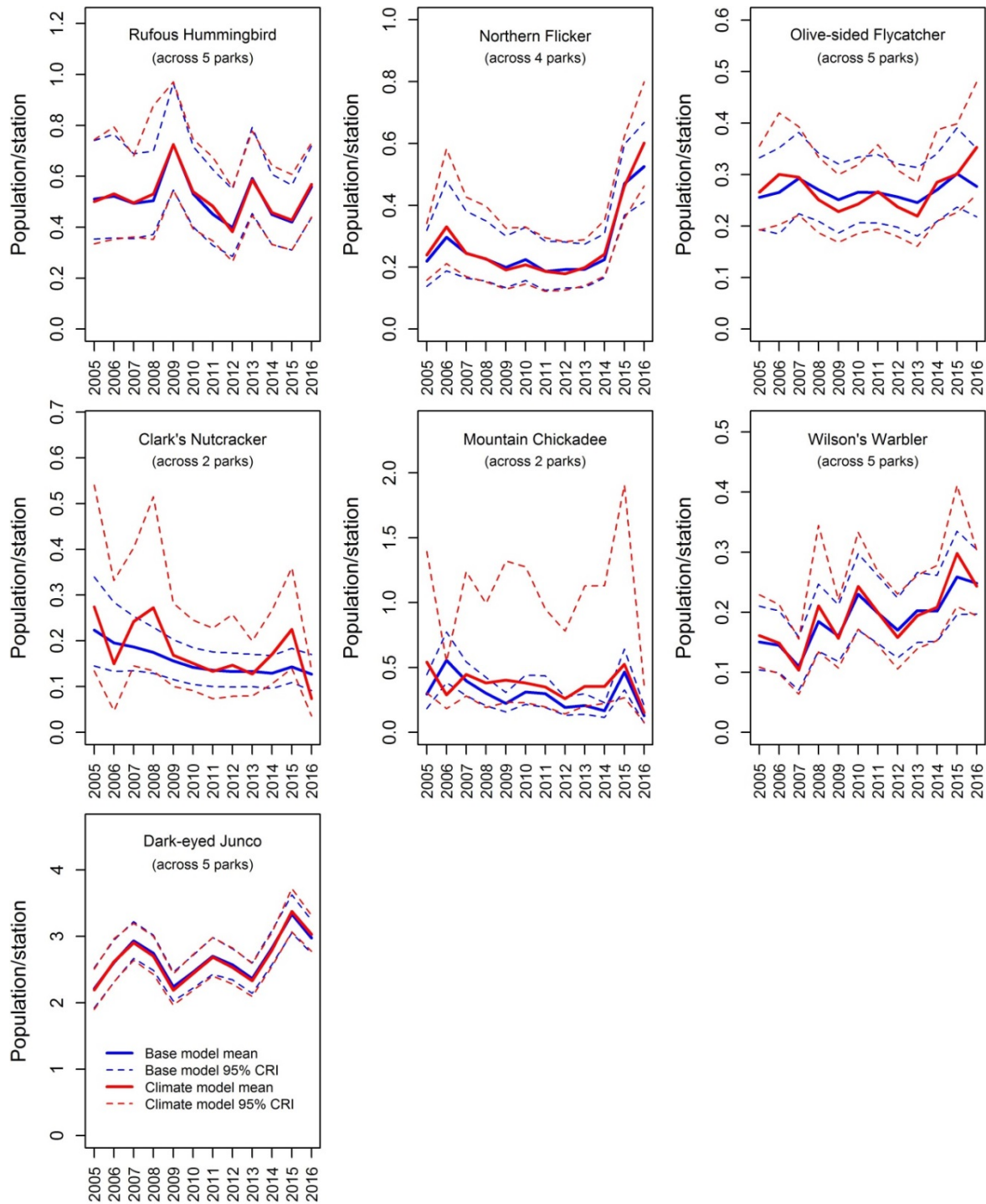


Figure 30. Regional trends in abundance for species exhibiting local decline. Abundance is presented as population size per point-count station (heavy lines = mean, dashed lines = 95% CRI), summed across all stations in all five parks or in all parks where the species was detected frequently enough to support model fits (Northern Flicker in LEWI, MORA, NOCA and OLYM; Clark's Nutcracker and Mountain Chickadee in MORA and NOCA). Estimates from base models (blue lines) are distinguished from climate models (red lines). Hutton's Vireo also declined in one park (LEWI), but was not detected frequently enough in any other park(s) to support a regional analysis.

Conclusions

Using a relatively robust framework for analysis and 12 years of landbird monitoring data from five parks of the North Coast and Cascades Network, we estimate that nearly all of the breeding populations analyzed have been stable or increasing between 2005 and 2016. The populations analyzed represent a large proportion (approximately 80%) of all birds detected in our surveys, suggesting that the trends we found are quite representative of landbirds breeding in these parks. Our results were largely similar among parks and strata at all elevations, even when allowing for stratum-specific trends, which were explored by Ray et al. (2017 a) using 10-year datasets from the mountain parks. Snowfall generally rose during the first half of the study period and fell during the second half, a pattern largely in opposition to mean spring temperatures, and we commonly found evidence that breeders responded to these trends. In general, across the three mountain parks and in one low-elevation park, years of lower breeding densities followed years of higher snowfall. Thus, the slight depression in snowfall in this region over the monitoring period might have contributed to the generally favorable trends we found. There are many possible drivers, however, that might explain our results. Attention should be given to the potential for shifting phenology in breeding behaviors within a season, which could cause apparent trends (or mask real trends) inferred from data like ours that derives from a single visit to each point-count station during a breeding season. Effects of day or elevation might be expected if trends were due to changes in phenology, and we have seen no evidence for such effects in this first synthesis of results from our long-term monitoring plan. However, the data summarized here provide a wealth of opportunities for further analysis and set the stage for targeted studies that could augment the possibilities for inference of trends in this broad study of landbird habitats in the Pacific Northwest.

Literature cited

- Allredge, M. W., K. H. Pollock, T. R. Simons, J. A. Collazo, and S. A. Shriner. 2007. Time-of-detection method for estimating abundance from point-count surveys. *The Auk* 124:653.
- Amundson, C. L., J. A. Royle, and C. M. Handel. 2014. A hierarchical model combining distance sampling and time removal to estimate detection probability during avian point counts. *The Auk* 131:476–494.
- Buckland, S. T., D. R. Anderson, K. P. Burnham, J. L. Laake, D. L. Borchers, and L. Thomas. 2001. *Introduction to distance sampling*. Oxford University Press, Oxford, United Kingdom.
- DeSante, D. F. 1990. The role of recruitment in the dynamics of a Sierran subalpine bird community. *American Naturalist* 136:429–455.
- Fancy, S. G., J. E. Gross and S. L. Carter. 2009. Monitoring the condition of natural resources in US National Parks. *Environmental Monitoring and Assessment* 151:161–174.
- Farnsworth, G. L., K. H. Pollock, J. D. Nichols, T. R. Simons, J. E. Hines, and J. R. Sauer. 2002. A removal model for estimating detection probabilities from point-count surveys. *The Auk* 119:414–425.
- Graham, M. L. 2003. Confronting multicollinearity in ecological multiple regression. *Ecology* 84:2809–2815.
- Hahn, T. P., K. W. Sockman, C. W. Breuner, and M. L. Morton. 2004. Facultative altitudinal movements by mountain white-crowned sparrows (*Zonotrichia leucophrys oriantha*) in the Sierra Nevada. *The Auk* 121:1269–1281.
- Holmgren, M., R. L. Wilkerson, R. B. Siegel, and R. C. Kuntz II. 2011. North Coast and Cascades Network landbird monitoring: Report for the 2010 field season. Natural Resource Technical Report NPS/NCCN/NRTR—2011/473.
- Holmgren, A. L., R. L. Wilkerson, R. B. Siegel, and P. J. Happe. 2014. North Coast and Cascades Network landbird monitoring: Report for the 2013 field season. Natural Resource Data Series NPS/NCCN/NRDS—2014/691. National Park Service, Fort Collins, Colorado.
- Holmgren, A. L., R. L. Wilkerson, R. B. Siegel, and P. J. Happe. 2015. North Coast and Cascades Network landbird monitoring: Report for the 2014 field season. Natural Resource Data Series NPS/NCCN/NRDS—2015/502. National Park Service, Fort Collins, Colorado.
- Holmgren, A. L., R. L. Wilkerson, R. B. Siegel, and R. C. Kuntz II. 2012. North Coast Cascades Network landbird monitoring: Report for the 2011 field season. Natural Resource Technical Report NPS/NCCN/NRTR—2012/605. National Park Service, Fort Collins, Colorado.

- Holmgren, A. L., R. L. Wilkerson, R. B. Siegel, and R. C. Kuntz II. 2013. North Coast Cascades Network landbird monitoring: Report for the 2012 field season. Natural Resource Data Series NPS/NCCN/NRDS—20113/523. National Park Service, Fort Collins, Colorado.
- Holmgren, A. L., R. L. Wilkerson, R. B. Siegel, and J. I. Ransom. 2016. North Coast and Cascades Network landbird monitoring: Report for the 2015 Field Season. Natural Resource Report NPS/NCCN/NRR—2016/1241. National Park Service, Fort Collins, Colorado.
- Holmgren, A. L., R. L. Wilkerson, R. B. Siegel, and J. I. Ransom. 2017. North Coast and Cascades Network landbird monitoring: Report for the 2016 field season. Natural Resource Report NPS/NCCN/NRR—2017/1495. National Park Service, Fort Collins, Colorado.
- IPCC (Intergovernmental Panel on Climate Change). 2013. Summary for policymakers. Pages 3–29 *in*: T. F. Stocker, D. Qin, G.-K. Plattner, M. Tignor, S. K. Allen, J. Boschung, A. Nauels, Y. Xia, V. Bex, and P. M. Midgley, editors. Climate change 2013: The physical science basis. Contribution of Working Group I to the Fifth Assessment Report of the Intergovernmental Panel on Climate Change. Cambridge University Press, Cambridge, UK.
- IPCC (Intergovernmental Panel on Climate Change). 2014. Summary for policymakers. Pages 1–32 *in*: C. B. Field, V. R. Barros, D. J. Dokken, K. J. Mach, M. D. Mastrandrea, T. E. Bilir, M. Chatterjee, K. L. Ebi, Y. O. Estrada, R. C. Genova, B. Girma, E. S. Kissel, A. N. Levy, S. MacCracken, P. R. Mastrandrea, and L. L. White, editors. Climate change 2014: Impacts, adaptation, and vulnerability. Part A: Global and Sectoral Aspects. Contribution of Working Group II to the Fifth Assessment Report of the Intergovernmental Panel on Climate Change. Cambridge University Press, Cambridge, UK.
- Kellner, K. 2015. jagsUI: a wrapper around 'rjags' to streamline 'JAGS' analyses. R package version 1.3.7. Available online: <http://CRAN.R-project.org/package=jagsUI>
- Kéry, M., and J. A. Royle, editors. 2016. Applied hierarchical modeling in ecology: Analysis of distribution, abundance and species richness in R and BUGS. Volume 1, Prelude and static models. Elsevier, Amsterdam and Boston. xxiv, 783 pp.
- Kéry, M., and M. Schaub. 2012. Bayesian population analysis using WinBUGS: A hierarchical perspective. Academic Press, 535 pp.
- Mathewson, H. A., M. L. Morrison, H. L. Loffland, and P. Brussard. 2012. Ecology of willow flycatchers (*Empidonax traillii*) in the Sierra Nevada, California: Effects of meadow characteristics and weather on demographics. Ornithological Monographs 75:1–32.
- Mizel, J. D., J. H. Schmidt, C. L. McIntyre, and M. S. Lindberg. 2017. Subarctic-breeding passerines exhibit phenological resilience to extreme spring conditions. Ecosphere 8(2):e01680. 10.1002/ecs2.1680.
- Pereyra, M. E. 2011. Effects of snow-related environmental variation on breeding schedules and productivity in a high altitude flycatcher (*Empidonax oberholseri*). The Auk 128:746–758.

- Plummer, M. 2003. JAGS: A program for analysis of Bayesian graphical models using Gibbs sampling. Pages 1–10 *in*: K. Hornik, F. Leisch, and A. Zeileis, editors. Proceedings of the 3rd International Workshop on Distributed Statistical Computing (DCS2003), March 20–22, Technische Universität, Vienna, Austria.
- R Core Team. 2017. R: A language and environment for statistical computing. R Foundation for Statistical Computing, Vienna, Austria. URL Available online: <https://www.R-project.org/>.
- Ray, C., J. F. Saracco, M. L. Holmgren, R. L. Wilkerson, R. B. Siegel, K. J. Jenkins, J. I. Ransom, P. J. Happe, J. R. Boetsch, and M.H. Huff. 2017 a. Recent stability of resident and migratory landbird populations in National Parks of the Pacific Northwest. *Ecosphere* 8:e01902.
- Ray, C., J. Saracco, K. Jenkins, M. Huff, P. Happe, and J. Ransom. 2017 b. Development of a robust analytical framework for assessing landbird population trends, dynamics and relationships with environmental covariates in the North Coast and Cascades Network. Natural Resource Report NPS/NCCN/NRR—2017/1483. National Park Service, Fort Collins, Colorado.
- Royle, J. A. 2004. *N*-mixture models for estimating population size from spatially replicated counts. *Biometrics* 60:08–115.
- Royle, J. A., D. K. Dawson, and S. Bates. 2004. Modeling abundance effects in distance sampling. *Ecology* 85:1591–1597.
- Saracco, J. F., A. L. Holmgren, R. L. Wilkerson, R. B. Siegel, R. C. Kuntz II, K. J. Jenkins, P. J. Happe, J. R. Boetsch, and M. H. Huff. 2014. Landbird trends in National Parks of the North Coast and Cascades Network, 2005–2012. U.S. Geological Survey open-file report 2014–1202.
- Schmidt, J. H., C. L. McIntyre, and M. C. MacCluskie. 2013. Accounting for incomplete detection: What are we estimating and how might it affect long-term passerine monitoring programs? *Biological Conservation* 160:130–139.
- Siegel, R. B. 2000. Methods for monitoring landbirds. U.S. Department of Interior National Park Service Technical Report NPS/NRNOCA/NRTR/00–03.
- Siegel, R. B., and R. C. Kuntz II. 2009. Designing a landbird monitoring program at North Cascades National Park Service Complex: Summary recommendations from a September 2000 workshop. Natural Resource Report NPS/NCCN/NRR—2009/075. National Park Service. Fort Collins, Colorado.
- Siegel, R. B., R. C. Kuntz II, R. L. Wilkerson, and K. D. Kuhlman. 2010. Surveying for Spotted Owls in the northeastern portion of North Cascades National Park Service Complex, 2009–2010: Report for the 2009 field season. Natural Resource Technical Report NPS/NCCN/NRTR—2010/334. National Park Service, Fort Collins, Colorado.

- Siegel, R.B., R. L. Wilkerson, and S. Hall. 2009. Landbird inventory for Olympic National Park (2002–2003). Natural Resource Technical Report NPS/NCCN/NRTR–2009/159. National Park Service, Fort Collins, Colorado.
- Siegel, R. B., R. L. Wilkerson, K. J. Jenkins, R. C. Kuntz II, J. R. Boetsch, J. P. Schaberl, and P. J. Happe. 2007. Landbird monitoring protocol for national parks in the North Coast and Cascades Network. U.S. Geological Survey Techniques and Methods 2-A6. 208 pp.
- Siegel, R. B., R. L. Wilkerson, and R. C. Kuntz II. 2008. North Coast and Cascades Network landbird monitoring: Report for the 2007 field season. Natural Resource Technical Report NPS/NCCN/NRTR—2008/114. National Park Service, Fort Collins, Colorado.
- Siegel, R. B., R. L. Wilkerson, and R. C. Kuntz II. 2009. Landbird inventory for Lewis and Clark National Historical Park (2006). Natural Resource Technical Report NPS/NCCN/NRTR—2009/166. National Park Service, Fort Collins, Colorado.
- Siegel, R. B., R. L. Wilkerson, and R. C. Kuntz II. 2009. Landbird Monitoring in the North Coast and Cascades Network: Report for the 2006 Pilot Field Season. Natural Resource Technical Report NPS/NCCN/NRTR—2009/168. National Park Service, Fort Collins, Colorado.
- Siegel, R. B., R. L. Wilkerson, R. C. Kuntz II, and J. McLaughlin. 2009. Landbird inventory for North Cascades National Park Service Complex (2001–2002). Natural Resource Technical Report NPS/NCCN/NRTR–2009/152. National Park Service, Fort Collins, Colorado.
- Siegel, R. B., R. L. Wilkerson, R. C. Kuntz II, J. F. Saracco, and A. L. Holmgren. 2012. Elevation ranges of birds at Mount Rainier National Park, North Cascades National Park Service Complex, and Olympic National Park. *The Northwestern Naturalist* 93:23–39.
- Siegel, R. B., R. L. Wilkerson, H. K. Pedersen, and R. C. Kuntz II. 2009. Landbird inventory of San Juan Island National Historical Park (2002). Natural Resource Technical Report NPS/NCCN/NRTR2009/156. National Park Service, Fort Collins, Colorado.
- Silsbee, G. G., and D. L. Peterson. 1991. Designing and implementing comprehensive long-term inventory and monitoring programs for National Park System lands. Natural Resources Report NPS/NRUW/NRR-91/04, Denver, Colorado.
- Simons, T. R., K. N. Rabenold, D. A. Buehler, J. A. Collazo, and K. E. Fransreb. 1999. The role of indicator species: Neotropical migratory song birds. Pages 187–208 *in*: J. D. Peine, editor. *Ecosystem management for sustainability: Principles and practices illustrated by a regional biosphere reserve cooperative*. Lewis, New York, New York.
- Wang, T., Hamann, A. Spittlehouse, D., and C. Carroll. 2016. Locally downscaled and spatially customizable climate data for historical and future periods for North America. *PLoS ONE* 11(6):e0156720. doi:10.1371/journal.pone.0156720.

- Weber, S., A. Woodward, and J. Freilich. 2009. North Coast and Cascades Network vital signs monitoring report (2005). Natural Resource Report NPS/NCCN/NRR—2009/098. National Park Service, Fort Collins, Colorado.
- Wilkerson, R. L., R. B. Siegel, and R. C. Kuntz II. 2009. Landbird monitoring in the North Coast and Cascades Monitoring Network: Report for the 2008 field season. Natural Resource Technical Report. NPS/NCCN/NRTR—2010/392. National Park Service, Fort Collins, Colorado.
- Wilkerson, R. L., R. B. Siegel, and R. C. Kuntz II. 2010. North Coast Cascades Network landbird monitoring: Report for the 2009 field season. Natural Resource Report Technical NPS/NCCN/NRTR—2010/392. National Park Service, Fort Collins, Colorado.
- Wilkerson, R. L., R. B. Siegel, and J. Schaberl. 2005. Landbird inventory for Mount Rainier National Park (2003–2004). Natural Resource Technical Report NPS/NCCN/NRTR—2009/164. National Park Service, Fort Collins, Colorado.

Appendix 1. Procedures for synthesis of NCCN landbird trends

The synthesis provided in this report can be replicated in future analyses of NCCN landbird monitoring data using a suite of scripts linked directly to the NCCN landbird monitoring database. Procedures for applying these scripts in sequence to reproduce these analyses and graphics are provided here, with some reference to Ray et al. (2017 b), which provides instruction on how to access monitoring and climate data and conduct trend analyses. Each script is fully annotated and can easily accommodate application to data from different periods of time. In every script, we used “****” to flag any lines of code that might require minor revision when altering the focal dataset. All scripts were written in the open-access programming language R (R Core Team 2017), and scripts for estimating trends in population density also include code written in JAGS (Plummer 2003), using the interface package jagsUI (Kellner 2015) to call JAGS from R.

Data preparation

Data recorded during each point-count survey, and data describing each point-count station or site, are accessed using two queries as detailed in Section 3.1 of Ray et al. (2017 b). For the current synthesis, output from these two queries were pre-processed for trend analysis using `script4processingQueryData-synthesis2017.R`, which writes the pre-processed data to two comma-delimited (.csv) files, `nccn.survey.data.2005to2016.csv` and `nccn.site.data.2005to2016.csv`. This data-processing script will require minimal revision to reflect the focal period targeted for analyses, such as altering the range of years designated in the output file names. In this and all other scripts described here, lines of code requiring review and possible revision can be located quickly by searching for comments preceded by “****”.

Two additional scripts can be used to finalize the data included in analyses. To identify and remove or adjust outliers from files like `nccn.survey.data.2005to2016.csv`, use `script4outlierAdjustments.R`. To review point-count station histories and check for bad coordinates, use `script4finalizingNCCNpointCoords.R`. The latter script also creates a .csv file listing the coordinates and elevation of each point-count station or site requiring climate data, `nccn.pts.wna.csv`, which can be used in a query of climate data. Note that the copy of `nccn.pts.wna.csv` used for the current synthesis will suffice for future analyses if the set of point-count stations remains unchanged. Even the retirement of currently active stations should not require alteration of the set of stations included in a synthetic analysis, because annual population density can be estimated for any point within the sampling frame provided appropriate covariate values exist or can be estimated (Kéry and Schaub 2012). The most likely reason for updating `nccn.pts.wna.csv` would be the addition of new stations, which might occur especially at the distal ends of mountain-park transects in years when conditions are good for surveying additional stations along a transect.

Using `nccn.pts.wna.csv` as a query, downscaled climate data can be accessed from ClimateWNA according to the procedure detailed in Appendix 3 of Ray et al. (2017 b). This

procedure involves using `script4climateWNAdata.R` in order to 1) re-format `nccn_pts.wna.csv` as required by ClimateWNA, 2) select the climate variables desired for analysis from the large number of variables downloaded by default from ClimateWNA, 3) explore the focal climate data and 4) format the downloaded data as input for trend analysis. The output from `script4climateWNAdata.R` is an input file for the trend analysis (e.g., `nccn.climate.anoms...csv`, where the ellipsis indicates the focal time period) as well as several graphics summarizing focal climate variables (e.g., Figures 1–3 in the current synthesis).

Trend analysis

For mountain parks, trend analysis procedures are detailed in Ray et al. (2017 a, b). For most species in mountain parks, trends across all three parks are analyzed in a single model, fitted using `script4trendAnalysis-synthesis.R`, which is effectively identical to the script presented in Appendix 4 of Ray et al. (2017 b). Species can also be conveniently analyzed in one park at a time using `script4trendAnalysis-synthesis-1-pk.R`, etc. For historical parks, trend analyses always involve one park at a time, facilitated by several “small-park” adjustments in `script4trendAnalysis-synthesis-sm-pk.R`. Each of these scripts focuses on the “basic” models presented in Table 8 of the current synthesis, but each also includes comments marked “***” to indicate the few lines of code that might require alteration to accommodate other model variants, such as those with other covariates of abundance (e.g., climate) or covariates of detection (e.g., noise). For convenience, a script modified to fit a climate model to data from American Camp only (in SAJH), useful for species occurring only in that sub-park, is included among the files linked to the NCCN landbird database: see `script4trendAnalysis-synthesis-SAJH-clim-AMCAonly.R`. Finally, we have also included a script customized for stratum-level analyses within mountain parks, `script4trendAnalysis-strat-specific-fits.R`. These different versions of the trend analysis script share a common core and further variants can be constructed easily by comparing these basic versions.

Harvesting output from trend analyses

Output from each `script4trendAnalysis...R` consists of several species-specific files (Table A1-1) as well as several files (e.g., `pt-yr-plots1.pdf`) that are not species-specific because they summarize data at the point-count level, such as: the number of point-counts completed by park, year, day-of-year, hour, observer and elevational stratum; the number of point-counts completed in each cover class; the distribution of noise levels during counts; the distribution of counts by elevation, slope and aspect; and (for mountain parks) the association across counts between park and observer or noise. Most of these outputs are also represented in some way within a single text file summarizing model parameters, fitted parameter estimates and statistics related to model fit and convergence. This key text file, hereafter “the output file,” is generally named for the focal species, model type (covariates) and/or park (omitted for three-park models of mountain data): e.g., `FOSPoutElevMORA.txt` is the output file for a basic model of Fox Sparrow trends in Mount Rainier National Park, and `AMROoutClimNoise.txt` is the output file for a model of the American Robin in mountain parks that accounts for effects of climate on abundance and noise on

detection. Table A1-1 describes the .txt output file and each additional output file from an application of `script4trendAnalysis-synthesis-sm-pk.R`.

Table A1-1. Output files generated by `script4trendAnalysis-synthesis-sm-pk.R`, exemplified using an analysis of Bewick’s Wren (BEWR) in San Juan Island National Historical Park (SAJH).

Example output file	Contents
BEWRoutSAJH.txt	Model parameters, parameter estimates, fit and convergence statistics
BEWRoutSAJHMODEL.jagsUI	Model specification including priors and covariates of abundance/detection
BEWRoutSAJHChains.pdf	Diagnostic plots of posterior distributions for estimated model parameters
BEWRoutSAJH.fitStats...pdf	Discrepancy plots and fit statistics for the sub-models of species detection
BEWRoutSAJH.plots1.pdf	Plots and statistics relating raw count to park and elevational stratum*
BEWRoutSAJH.plots2.pdf	Raw count distribution and Poisson regression of count on day/hour/noise
BEWRoutSAJH.plots3.pdf	Plots of unadjusted and effort-adjusted raw counts per station by year
BEWRoutSAJH.plots4.pdf	Poisson regression of effort-adjusted raw count on year
BEWRoutSAJH.plots5.pdf	Plots/statistics relating count or occupancy to cover, elevation and slope
BEWRoutSAJH.plots6.pdf	Plots/Poisson regressions relating count to aspect and climate covariates
BEWRoutSAJH.plots7.pdf	Histograms of detection distance and detection distance-class
BEWRoutSAJH.plots8.pdf	Plots/statistics relating detection interval and distance to select covariates
BEWRoutSAJH.plots9.pdf	Plot of detections by count interval; ANOVAs for interval x distance/hour
BEWR.all.SAJHwClim.csv	Group size (0, 1, ...) and covariates for every focal species (non)detection
BEWR.all.SAJH...wNAs.csv	Same as above but padded with NAs for all station-years not surveyed

*Additional plots and statistics are generated in analyses involving all three mountain parks.

Data can be harvested from a set of output files—specifically the .txt output file for each of a set of modeled species—using a `script4harvestingTXToutFilesToCSV-synthesis...R`. Each script takes as input a comma-separated “species-list” file (`spList...csv`) containing a column of species code names and a column of associated output files, as exemplified in Table A2-2. The `spList...csv` should contain a list of output files that are comparable among species in terms of model type: i.e., it should list the best basic model for each species in a given park, or the best climate model for each species in a park. However, the details of each species model might vary somewhat. For example, covariates of detection were allowed to vary among species in the current synthesis, as would be expected also in future analyses.

For mountain parks, the data-harvesting script further takes its cue from the name of the `spList...csv` file to narrow the harvest to trends specific to the named park. For example, if the output file for a species that breeds in the mountain parks includes a park-specific trend for each of the three parks, only the MORA trend will be harvested if the species-list file is named `spListMORA-bestClimModels.R`.

Table A1-2. Contents of the first few rows of a comma-separated file used as input for the data-harvesting script `script4harvestingTXTOutFilesToCSV-synthesis-mtn.R`. The file in this example was named `spListNOCA-bestClimModels.csv` and contained all the preferred output files from climate-based analyses of species occurring in North Cascades National Park Complex.

Species	Output file
AMRO	AMROoutClimNoise.txt
BHGR	BHGRoutClim.txt
BRCR	BRCRoutClim.txt
BTYW	BTYWoutClimNOCA.txt

The data-harvesting script first harvests all results in the main table of each output file and creates a new set of comma-separated files, each containing the table of results for a given species in the species-list file. For example, the `AMROoutClimNoise.txt` file is stripped of header and footer to generate a new file, `AMROoutClimNoise.table.csv`, which contains only a table of all estimated parameters and fit metrics and their associated means, quantiles and convergence statistics. Some of the subsequent code in the data-harvesting script accesses specific data from this new set of tables to collect the data needed for summary plots and tables in the synthesis: population trends, effects of elevation or climate, and population densities. Additional code in the data-harvesting script returns to the output files to harvest model parameters in the header or footer, such as the maximum detection distance and the percent of detection distances censored to avoid sampling error in the tail of the detection-distance distribution and to meet assumptions of independence between detection interval and distance.

Plotting and tabulating output from trend analyses

The figures contained in the current synthesis can be reproduced using the scripts named in Table A1-3, while tables can be reproduced using those in Table A1-4. Most of these scripts require a “`spList...csv`” file to identify the set of species summarized by each figure or table. Despite the similarity in plots that summarize historical vs. mountain park results, separate scripts were usually developed for each of these two park types, to simplify the code within each script for dealing with the unique features of their results. Finally, two scripts were used to calculate point-count effort per park and year for each species, for use in plots of effort-adjusted counts, etc.:

`script4findingEffortAdjustedCountsPerMinute-mtnPks.R` and
`script4findingEffortAdjustedCountsPerMinute-smPks.R`. These scripts produce the files `effort-adj-cts.by.sp...csv` and `effort-ann-pts.by.sp...csv`, which are required as input to `script4plottingEffort-adjustedCounts.R` and/or `script4fig-sppCt-by-yr...R` (Tables A1-3 and A1-4).

Not all tables in the current report derive from a script. For example, Table 1 summarizes park areas compiled during data QA/QC. Also, several tables and statistics in the text draw certain elements from summaries produced by `script4finalDataSynthesis.R`, although this script writes only one table to file (Table 6) that is actually used in the current report. Scripts used to create tables are listed in Table A1-4.

Table A1-3. Scripts used to generate figures in the current report.

Figure-generating script	Figure(s)	Figure contents
script4climateWNAdata.R	1–3	Annual PAS anomaly; MST anomaly; PAS and MST anomalies by park
script4fig-ha-per-pt-surveyed.R	4	Effective survey area by species and park
script4fig-trendStats-1pk.R	5, 9	Mean population trend by species in SAJH, LEWI
script4plottingEffort-adjustedCounts.R	6, 10	Effort-adjusted count per year for species with counts too low for trend estimation
script4fig-sppN-by-yr-small-pk.R	7, 11	Population size by year and species in SAJH, LEWI
script4fig-sppCt-by-yr-small-pk.R	8, 12	Effort-adjusted counts by year for SAJH, LEWI
script4fig-climateCoefs-synthesis-sm-pks.R	13	Mean effects of climate by species in SAJH, LEWI
script4fig-trendStats-1-mtn-pk.R	14–16	Mean population trend by species in a mountain park
script4fig-sppN-by-yr-mtn-pk.R	17, 19, 21	Population size by year and species in a mountain park
script4fig-sppCt-by-yr-mtn-pk.R	18, 20, 22	Effort-adjusted counts for a mountain park
script4fig-elevCoefs-synthesis-mtn-pks.R	23	Mean effects of elevation by species across mountain parks
script4fig-N.haXstratumXyear.R	24–26	Estimated population size by year, stratum and species in a mountain park
script4fig-climateCoefs-synthesis-mtn-pks.R	27–28	Mean effects of climate by species across the mountain parks
script4fig-trendsBaseVsClim-5pks.R	29	Similarity in climate vs. basic model trends
script4fig-declining-sppN-by-yr.R	30	Regional population trends in species declining locally

Table A1-4. Scripts used to generate tables in the current report.

Table-generating script	Table(s)	Table contents
script4findingEffortAdjustedCountsPerMinute...R	3	Survey effort by year and park
script4finalDataSynthesis.R	7, 4–61	Total count by species and park
script4table-model-type-by-sp-and-pk.R	8-9	Models fitted to species commonly detected
script4resultTables-synthesisAppendix2.R	A2-1 to A2-5	Results from “basic” models by species and park

¹Tabulates results for screen capture

Appendix 2. Fitted model results

Results from models of breeding landbird population density fitted to point-count data collected during 2005–2016 in each of five parks of the North Coast and Cascades Inventory and Monitoring Network. For each park, results are summarized in a table organized by species code. Featured results were drawn from the “basic” models A and B (see Tables 7 and 8 in the main text) that include a linear effect of year and (in mountain parks only) effects of elevation on population density. For each species, we report the maximum detection distance (d_{\max} , in meters), effective survey area (in hectares), mean population density (N/ha) and associated 95% credible interval (CRI), mean annual trend in population density (N/year) and associated 95% credible interval, and two components of model fit: Bayesian P -values for the sub-models of species availability and perceptibility. Tables begin on the next page.

Table A2-1. Results from “basic” models of type A fitted to breeding landbird point-count data from San Juan Island National Historical Park, 2005–2015.

Species code	d_{\max} (m)	Effective area surveyed (ha)	Density (N/ha)		Annual trend (N/yr)		Bayesian <i>P</i> -values	
			Mean	95% CRI	Mean	95% CRI	Availability	Perceptibility
CANG	521	85.28	0.017	(0.011, 0.032)	-0.048	(-0.229, 0.124)	0.314	0.003
BAEA	375	44.18	0.023	(0.015, 0.032)	0.069	(0.005, 0.133)	0.456	0.201
CAQU	254	20.27	0.012	(0.008, 0.019)	0.220	(-0.03, 0.478)	0.492	0.365
MODO	181	10.29	0.012	(0.008, 0.019)	0.547	(0.195, 0.887)	0.739	0.476
RUHU	30	0.28	3.187	(1.811, 6.788)	-0.048	(-0.115, 0.012)	0.515	0.502
OSFL	199	12.44	0.025	(0.016, 0.037)	0.085	(0.014, 0.156)	0.494	0.454
PSFL	80	2.01	0.954	(0.798, 1.143)	0.050	(0.018, 0.080)	0.489	0.235
CAVI	107	3.60	0.072	(0.038, 0.117)	-0.099	(-0.386, 0.190)	0.522	0.425
WAVI	117	4.30	0.120	(0.078, 0.172)	0.073	(0.015, 0.133)	0.488	0.381
AMCR	228	16.33	0.082	(0.064, 0.103)	-0.030	(-0.07, 0.011)	0.448	0.140
CORA	386	46.81	0.037	(0.017, 0.117)	0.171	(0.093, 0.255)	0.429	0.235
BARS	93	2.72	0.894	(0.215, 3.827)	0.187	(-0.026, 0.400)	0.287	0.166
CBCH	61	1.17	1.439	(1.107, 1.822)	0.065	(0.025, 0.105)	0.461	0.280
RBNU	126	4.99	0.228	(0.173, 0.290)	-0.023	(-0.067, 0.020)	0.506	0.583
BRCR	77	1.86	0.508	(0.246, 1.291)	0.151	(0.083, 0.221)	0.509	0.466
HOWR	68	1.45	0.769	(0.562, 0.993)	0.092	(0.058, 0.126)	0.468	0.300
PAWR	95	2.84	0.150	(0.098, 0.217)	0.036	(-0.034, 0.105)	0.490	0.256
GCKI	48	0.72	0.605	(0.328, 1.023)	0.154	(0.088, 0.226)	0.466	0.334
SWTH	126	4.99	0.439	(0.357, 0.535)	0.072	(0.040, 0.106)	0.500	0.392
AMRO	152	7.26	0.812	(0.710, 0.920)	0.028	(0.005, 0.050)	0.498	0.636
EUST	142	6.33	0.264	(0.169, 0.544)	-0.002	(-0.206, 0.197)	0.400	0.001
CEDW	84	2.22	0.669	(0.346, 1.548)	-0.037	(-0.281, 0.208)	0.410	0.011
OCWA	109	3.73	0.540	(0.437, 0.651)	0.049	(0.015, 0.082)	0.496	0.536
YEWA	151	7.16	0.035	(0.012, 0.090)	0.081	(-0.289, 0.471)	0.501	0.353
YRWA	129	5.23	0.066	(0.037, 0.105)	0.209	(-0.049, 0.459)	0.511	0.560
BTYW	82	2.11	0.115	(0.081, 0.171)	0.049	(-0.016, 0.113)	0.472	0.419
TOWA	82	2.11	0.233	(0.154, 0.320)	-0.018	(-0.072, 0.036)	0.461	0.118
COYE	195	11.95	0.070	(0.039, 0.134)	0.303	(0.035, 0.574)	0.485	0.434
WIWA	95	2.84	0.196	(0.136, 0.273)	0.018	(-0.035, 0.072)	0.502	0.453
WETA	110	3.80	0.084	(0.052, 0.139)	0.031	(-0.038, 0.100)	0.520	0.536
SPTO	112	3.94	0.449	(0.366, 0.545)	0.005	(-0.027, 0.039)	0.494	0.441
SAVS	105	3.46	0.816	(0.687, 0.958)	0.027	(-0.001, 0.055)	0.442	0.001
SOSP	163	8.35	0.202	(0.156, 0.256)	0.067	(0.025, 0.110)	0.484	0.365
WCSP	104	3.40	0.314	(0.271, 0.381)	0.055	(0.025, 0.085)	0.450	0.381
DEJU	85	2.27	0.465	(0.324, 0.646)	0.049	(-0.003, 0.102)	0.464	0.277
RWBL	216	14.66	0.081	(0.061, 0.105)	0.007	(-0.040, 0.054)	0.429	0.016

Species code	d_{max} (m)	Effective area surveyed (ha)	Density (N/ha)		Annual trend (N/yr)		Bayesian P-values	
			Mean	95% CRI	Mean	95% CRI	Availability	Perceptibility
BHCO	103	3.33	0.789	(0.639, 0.955)	0.088	(0.054, 0.121)	0.467	0.260
PUFI	146	6.70	0.124	(0.087, 0.165)	0.045	(-0.010, 0.099)	0.510	0.385
HOFI	124	4.83	0.223	(0.165, 0.299)	0.098	(0.047, 0.151)	0.466	0.187
PISI	94	2.78	0.920	(0.260, 4.137)	0.420	(0.258, 0.599)	0.206	0.058
AMGO	97	2.96	0.945	(0.785, 1.130)	0.021	(-0.009, 0.052)	0.439	0.085

Table A2-2. Results from “basic” models of type A fitted to breeding landbird point-count data from Lewis and Clark National Historical Park, 2006–2016.

Species code	d_{max} (m)	Effective area surveyed (ha)	Density (N/ha)		Annual trend (N/yr)		Bayesian P-values	
			Mean	95% CRI	Mean	95% CRI	Availability	Perceptibility
BAEA	361	40.94	0.050	(0.008, 0.217)	0.134	(0.035, 0.235)	0.222	0.073
BTPI	205	13.20	0.031	(0.018, 0.053)	0.047	(-0.057, 0.151)	0.507	0.511
RUHU	22	0.15	2.884	(1.416, 6.216)	-0.138	(-0.468, 0.188)	0.499	0.483
HAWO	96	2.90	0.455	(0.038, 2.080)	0.883	(0.361, 1.426)	0.467	0.452
NOFL	206	13.33	0.034	(0.013, 0.133)	-0.176	(-0.297, -0.060)	0.521	0.561
OSFL	224	15.76	0.055	(0.038, 0.079)	-0.107	(-0.179, -0.033)	0.494	0.390
PSFL	73	1.67	1.539	(1.315, 1.791)	0.039	(0.009, 0.067)	0.492	0.543
HUVI	99	3.08	0.093	(0.047, 0.229)	-0.121	(-0.203, -0.04)	0.513	0.473
WAVI	124	4.83	0.174	(0.080, 0.595)	0.071	(0.000, 0.147)	0.435	0.242
STJA	132	5.47	0.085	(0.056, 0.121)	0.002	(-0.064, 0.070)	0.467	0.164
AMCR	206	13.33	0.163	(0.136, 0.196)	0.013	(-0.021, 0.045)	0.451	0.095
CORA	250	19.63	0.023	(0.013, 0.045)	0.040	(-0.031, 0.111)	0.385	0.147
BCCH	103	3.33	0.174	(0.104, 0.283)	0.061	(-0.015, 0.14)	0.397	0.108
CBCH	49	0.75	2.230	(1.765, 2.783)	-0.030	(-0.068, 0.009)	0.452	0.245
RBNU	102	3.27	0.049	(0.026, 0.105)	-0.023	(-0.122, 0.079)	0.507	0.515
BRCR	53	0.88	0.469	(0.283, 0.763)	0.130	(0.049, 0.217)	0.489	0.330
BEWR	86	2.32	0.100	(0.054, 0.187)	0.196	(0.104, 0.295)	0.375	0.201
PAWR	91	2.60	1.091	(0.947, 1.241)	0.028	(0.002, 0.053)	0.488	0.312
MAWR	78	1.91	0.485	(0.365, 0.614)	0.094	(-0.062, 0.254)	0.416	0.001
GCKI	44	0.61	1.581	(1.219, 1.99)	0.112	(0.072, 0.154)	0.518	0.507
SWTH	102	3.27	1.466	(1.300, 1.644)	0.193	(0.125, 0.261)	0.501	0.515
AMRO	113	4.01	0.664	(0.560, 0.778)	0.169	(0.071, 0.264)	0.470	0.206
OCWA	83	2.16	0.461	(0.352, 0.591)	0.234	(0.076, 0.394)	0.466	0.086
YEWA	103	3.33	0.258	(0.173, 0.380)	0.053	(-0.015, 0.124)	0.443	0.101
BTYW	96	2.90	0.335	(0.238, 0.465)	0.418	(0.238, 0.615)	0.461	0.188
HEWA	91	2.60	0.917	(0.683, 1.187)	0.049	(-0.012, 0.107)	0.471	0.286
COYE	91	2.60	0.302	(0.223, 0.395)	0.288	(0.120, 0.451)	0.421	0.045

Species code	d_{max} (m)	Effective area surveyed (ha)	Density (N/ha)		Annual trend (N/yr)		Bayesian P-values	
			Mean	95% CRI	Mean	95% CRI	Availability	Perceptibility
WIWA	80	2.01	1.036	(0.870, 1.215)	0.075	(0.046, 0.106)	0.476	0.332
WETA	118	4.37	0.131	(0.094, 0.174)	0.117	(0.060, 0.175)	0.508	0.481
SPTO	95	2.84	0.065	(0.033, 0.110)	0.166	(0.062, 0.274)	0.483	0.104
SAVS	88	2.43	0.038	(0.021, 0.075)	-0.008	(-0.127, 0.117)	0.476	0.169
SOSP	110	3.80	0.545	(0.450, 0.649)	0.084	(-0.025, 0.193)	0.476	0.139
WCSP	152	7.26	0.125	(0.092, 0.161)	0.047	(-0.008, 0.101)	0.441	0.025
DEJU	84	2.22	0.600	(0.436, 0.822)	0.293	(0.141, 0.443)	0.352	0.027
BHGR	140	6.16	0.202	(0.155, 0.258)	0.083	(0.036, 0.132)	0.512	0.557
RWBL	211	13.99	0.058	(0.043, 0.078)	0.085	(-0.088, 0.251)	0.367	0.002
BHCO	70	1.54	0.623	(0.429, 0.916)	0.072	(0.017, 0.127)	0.381	0.109
PUFI	120	4.52	0.204	(0.154, 0.268)	0.242	(0.098, 0.392)	0.518	0.612
AMGO	52	0.85	0.328	(0.231, 0.539)	0.051	(-0.014, 0.118)	0.314	0.387

Table A2-3. Results from “basic” models of type B fitted to breeding landbird point-count data from Mount Rainier National Park, 2005–2016.

Species code	d_{max} (m)	Effective area surveyed (ha)	Density (N/ha)		Annual trend (N/yr)		Bayesian P-values	
			Mean	95% CRI	Mean	95% CRI	Availability	Perceptibility
SOGR	197	12.19	0.003	(0.002, 0.004)	0.020	(-0.061, 0.108)	0.496	0.492
RUHU	28	0.25	1.216	(0.970, 1.488)	0.027	(-0.028, 0.087)	0.396	0.096
HAWO	97	2.96	0.045	(0.035, 0.059)	0.045	(-0.025, 0.116)	0.464	0.313
NOFL	220	15.21	0.011	(0.009, 0.014)	0.094	(0.018, 0.170)	0.454	0.207
PIWO	308	29.80	0.002	(0.001, 0.004)	0.051	(-0.074, 0.197)	0.508	0.522
OSFL	180	10.18	0.013	(0.010, 0.016)	0.069	(-0.003, 0.148)	0.492	0.468
HAFL	66	1.37	0.146	(0.124, 0.170)	0.083	(0.015, 0.146)	0.530	0.850
PSFL	72	1.63	0.414	(0.377, 0.456)	0.039	(-0.001, 0.077)	0.537	0.958
WAVI	94	2.78	0.014	(0.011, 0.019)	0.051	(-0.020, 0.123)	0.465	0.187
GRAJ	127	5.07	0.149	(0.128, 0.174)	0.049	(-0.021, 0.117)	0.358	0.007
STJA	127	5.07	0.033	(0.026, 0.040)	0.085	(-0.003, 0.155)	0.396	0.074
CLNU	225	15.90	0.009	(0.006, 0.013)	-0.180	(-0.265, -0.100)	0.417	0.062
CORA	311	30.39	0.005	(0.004, 0.007)	0.115	(0.022, 0.210)	0.432	0.155
MOCH	91	2.60	0.082	(0.061, 0.107)	0.003	(-0.103, 0.103)	0.431	0.046
CBCH	27	0.23	2.907	(2.652, 3.167)	0.027	(-0.014, 0.065)	0.278	0.072
RBNU	120	4.52	0.259	(0.237, 0.283)	0.030	(-0.025, 0.082)	0.464	0.307
BRCR	55	0.95	0.569	(0.500, 0.640)	0.087	(0.034, 0.141)	0.453	0.099
PAWR	91	2.60	0.760	(0.712, 0.808)	0.043	(0.002, 0.093)	0.521	0.963
GCKI	42	0.55	1.915	(1.757, 2.074)	0.041	(-0.011, 0.094)	0.496	0.532
TOSO	196	12.07	0.007	(0.004, 0.013)	-0.053	(-0.182, 0.070)	0.483	0.364

Species code	d_{max} (m)	Effective area surveyed (ha)	Density (N/ha)		Annual trend (N/yr)		Bayesian P-values	
			Mean	95% CRI	Mean	95% CRI	Availability	Perceptibility
SWTH	109	3.73	0.036	(0.029, 0.043)	0.063	(0.005, 0.119)	0.477	0.310
HETH	146	6.70	0.112	(0.102, 0.122)	0.110	(0.056, 0.157)	0.422	0.042
AMRO	120	4.52	0.103	(0.089, 0.116)	0.045	(0.002, 0.089)	0.412	0.106
VATH	189	11.22	0.238	(0.224, 0.251)	0.051	(0.012, 0.082)	0.466	0.043
AMPI	139	6.07	0.045	(0.035, 0.058)	0.015	(-0.069, 0.096)	0.455	0.071
YEWA	86	2.32	0.009	(0.005, 0.015)	0.036	(-0.135, 0.232)	0.467	0.099
YRWA	93	2.72	0.084	(0.072, 0.098)	0.154	(0.097, 0.218)	0.464	0.262
TOWA	71	1.58	0.255	(0.231, 0.282)	-0.030	(-0.078, 0.017)	0.432	0.122
WIWA	85	2.27	0.021	(0.014, 0.029)	0.027	(-0.079, 0.141)	0.463	0.222
WETA	113	4.01	0.024	(0.019, 0.029)	0.182	(0.113, 0.253)	0.504	0.578
CHSP	94	2.78	0.029	(0.021, 0.038)	0.396	(0.275, 0.542)	0.410	0.052
FOSP	211	13.99	0.009	(0.006, 0.014)	-0.068	(-0.294, 0.163)	0.499	0.540
SOSP	116	4.23	0.003	(0.002, 0.005)	0.135	(0.001, 0.279)	0.453	0.174
DEJU	91	2.60	1.034	(0.972, 1.099)	0.027	(-0.003, 0.061)	0.435	0.098
CAFI	103	3.33	0.018	(0.011, 0.028)	0.021	(-0.110, 0.158)	0.445	0.237

Table A2-4. Results from “basic” models of type B fitted to breeding landbird point-count data from North Cascades National Park Complex, 2005–2016.

Species code	d_{max} (m)	Effective area surveyed (ha)	Density (N/ha)		Annual trend (N/yr)		Bayesian P-values	
			Mean	95% CRI	Mean	95% CRI	Availability	Perceptibility
SOGR	197	12.19	0.019	(0.016, 0.022)	0.027	(-0.027, 0.082)	0.496	0.492
RUHU	28	0.25	2.760	(2.318, 3.264)	-0.006	(-0.054, 0.042)	0.396	0.096
RBSA	91	2.60	0.076	(0.058, 0.100)	0.070	(-0.039, 0.171)	0.490	0.385
HAWO	97	2.96	0.075	(0.060, 0.094)	0.072	(0.012, 0.135)	0.464	0.313
NOFL	220	15.21	0.015	(0.012, 0.019)	-0.016	(-0.085, 0.048)	0.454	0.207
PIWO	308	29.80	0.003	(0.002, 0.005)	-0.030	(-0.141, 0.091)	0.508	0.522
OSFL	180	10.18	0.032	(0.027, 0.038)	-0.050	(-0.089, -0.009)	0.492	0.468
WEWP	126	4.99	0.041	(0.034, 0.049)	0.004	(-0.036, 0.043)	0.485	0.307
HAFL	66	1.37	0.678	(0.624, 0.736)	0.052	(-0.004, 0.102)	0.530	0.850
PSFL	72	1.63	0.102	(0.087, 0.118)	0.018	(-0.030, 0.067)	0.537	0.958
CAVI	94	2.78	0.089	(0.072, 0.107)	0.013	(-0.062, 0.084)	0.493	0.366
WAVI	94	2.78	0.206	(0.183, 0.231)	0.035	(0.009, 0.061)	0.465	0.187
GRAJ	127	5.07	0.042	(0.035, 0.051)	0.110	(0.032, 0.187)	0.358	0.007
STJA	127	5.07	0.032	(0.026, 0.039)	0.048	(-0.035, 0.123)	0.396	0.074
CLNU	225	15.90	0.010	(0.008, 0.014)	0.043	(-0.004, 0.089)	0.417	0.062
CORA	311	30.39	0.002	(0.002, 0.004)	0.107	(-0.008, 0.228)	0.432	0.155
MOCH	91	2.60	0.141	(0.114, 0.172)	-0.096	(-0.189, -0.012)	0.431	0.046

Species code	d_{max} (m)	Effective area surveyed (ha)	Density (N/ha)		Annual trend (N/yr)		Bayesian P-values	
			Mean	95% CRI	Mean	95% CRI	Availability	Perceptibility
CBCH	27	0.23	2.109	(1.927, 2.294)	0.014	(-0.027, 0.050)	0.278	0.072
RBNU	120	4.52	0.255	(0.232, 0.278)	-0.020	(-0.074, 0.034)	0.464	0.307
BRCR	55	0.95	0.332	(0.286, 0.383)	-0.024	(-0.079, 0.033)	0.453	0.099
PAWR	91	2.60	0.399	(0.371, 0.428)	0.037	(-0.004, 0.085)	0.521	0.963
GCKI	42	0.55	1.425	(1.303, 1.560)	0.026	(-0.027, 0.080)	0.496	0.532
TOSO	196	12.07	0.024	(0.015, 0.039)	-0.067	(-0.164, 0.026)	0.483	0.364
SWTH	109	3.73	0.531	(0.495, 0.568)	0.020	(-0.012, 0.050)	0.477	0.310
HETH	146	6.70	0.138	(0.126, 0.150)	-0.037	(-0.086, 0.009)	0.422	0.042
AMRO	120	4.52	0.283	(0.259, 0.308)	0.033	(-0.002, 0.066)	0.412	0.106
VATH	189	11.22	0.115	(0.107, 0.123)	0.000	(-0.042, 0.033)	0.466	0.043
NAWA	97	2.96	0.178	(0.149, 0.211)	0.084	(-0.012, 0.179)	0.462	0.262
YEWA	86	2.32	0.299	(0.264, 0.338)	-0.005	(-0.066, 0.065)	0.467	0.099
YRWA	93	2.72	0.534	(0.495, 0.576)	0.037	(0.007, 0.069)	0.464	0.262
BTYW	88	2.43	0.073	(0.057, 0.091)	0.043	(-0.034, 0.118)	0.475	0.270
TOWA	71	1.58	0.686	(0.637, 0.738)	-0.018	(-0.066, 0.028)	0.432	0.122
MGWA	91	2.60	0.260	(0.230, 0.296)	0.065	(0.012, 0.128)	0.500	0.331
WIWA	85	2.27	0.038	(0.029, 0.048)	-0.080	(-0.15, -0.013)	0.463	0.222
WETA	113	4.01	0.358	(0.332, 0.387)	0.043	(0.011, 0.075)	0.504	0.578
CHSP	94	2.78	0.335	(0.292, 0.380)	0.043	(-0.011, 0.103)	0.410	0.052
FOSP	135	5.73	0.038	(0.028, 0.054)	0.055	(-0.114, 0.222)	0.476	0.328
SOSP	116	4.23	0.016	(0.012, 0.021)	-0.017	(-0.076, 0.045)	0.453	0.174
DEJU	91	2.60	0.929	(0.870, 0.992)	-0.053	(-0.081, -0.019)	0.435	0.098
BHGR	121	4.60	0.049	(0.040, 0.060)	0.008	(-0.057, 0.069)	0.494	0.503
CAFI	103	3.33	0.073	(0.057, 0.094)	0.134	(0.079, 0.195)	0.445	0.237

Table A2-5. Results from “basic” models of type B fitted to breeding landbird point-count data from Olympic National Park Complex, 2005–2016.

Species Code	d_{max} (m)	Effective area surveyed (ha)	Density (N/ha)		Annual trend (N/yr)		Bayesian P-values	
			Mean	95% CRI	Mean	95% CRI	Availability	Perceptibility
SOGR	197	12.19	0.024	(0.017, 0.024)	0.015	(-0.035, 0.069)	0.496	0.492
RUHU	28	0.25	2.443	(1.635, 2.443)	-0.013	(-0.067, 0.043)	0.396	0.096
HAWO	97	2.96	0.111	(0.072, 0.111)	0.103	(0.039, 0.165)	0.464	0.313
NOFL	220	15.21	0.030	(0.021, 0.030)	0.078	(0.017, 0.137)	0.454	0.207
PIWO	308	29.80	0.006	(0.002, 0.006)	0.028	(-0.084, 0.152)	0.508	0.522
OSFL	180	10.18	0.034	(0.024, 0.034)	0.048	(0.006, 0.092)	0.492	0.468
HAFL	66	1.37	0.367	(0.295, 0.367)	0.050	(-0.01, 0.105)	0.530	0.850
PSFL	72	1.63	1.040	(0.913, 1.040)	0.047	(0.013, 0.082)	0.537	0.958

Species Code	d_{max} (m)	Effective area surveyed (ha)	Density (N/ha)		Annual trend (N/yr)		Bayesian P-values	
			Mean	95% CRI	Mean	95% CRI	Availability	Perceptibility
WAVI	94	2.78	0.092	(0.069, 0.092)	0.070	(0.034, 0.106)	0.465	0.187
GRAJ	127	5.07	0.108	(0.080, 0.108)	0.076	(0.011, 0.142)	0.358	0.007
STJA	127	5.07	0.044	(0.029, 0.044)	0.069	(-0.010, 0.134)	0.396	0.074
CORA	311	30.39	0.007	(0.003, 0.007)	0.038	(-0.062, 0.133)	0.432	0.155
CBCH	27	0.23	3.016	(2.568, 3.016)	0.055	(0.014, 0.092)	0.278	0.072
RBNU	120	4.52	0.205	(0.171, 0.205)	0.029	(-0.026, 0.082)	0.464	0.307
BRCR	55	0.95	0.518	(0.397, 0.518)	0.104	(0.050, 0.164)	0.453	0.099
PAWR	91	2.60	0.863	(0.768, 0.863)	0.043	(0.002, 0.089)	0.521	0.963
GCKI	42	0.55	2.305	(1.993, 2.305)	0.076	(0.023, 0.126)	0.496	0.532
TOSO	196	12.07	0.028	(0.012, 0.028)	0.122	(0.020, 0.220)	0.483	0.364
SWTH	109	3.73	0.077	(0.059, 0.077)	0.040	(-0.004, 0.083)	0.477	0.310
HETH	146	6.70	0.091	(0.075, 0.091)	0.069	(0.016, 0.116)	0.422	0.042
AMRO	120	4.52	0.269	(0.225, 0.269)	0.069	(0.034, 0.103)	0.412	0.106
VATH	189	11.22	0.184	(0.163, 0.184)	0.061	(0.018, 0.093)	0.466	0.043
AMPI	141	6.25	0.077	(0.028, 0.077)	0.159	(0.003, 0.358)	0.415	0.090
YEWA	86	2.32	0.046	(0.027, 0.046)	0.024	(-0.068, 0.119)	0.467	0.099
YRWA	93	2.72	0.081	(0.057, 0.081)	0.215	(0.154, 0.283)	0.464	0.262
BTYW	79	1.96	0.058	(0.033, 0.058)	0.134	(0.032, 0.231)	0.478	0.375
TOWA	71	1.58	0.304	(0.252, 0.304)	0.083	(0.031, 0.133)	0.432	0.122
MGWA	91	2.60	0.039	(0.022, 0.039)	0.062	(-0.033, 0.164)	0.500	0.331
WIWA	85	2.27	0.135	(0.098, 0.135)	0.110	(0.051, 0.170)	0.463	0.222
WETA	113	4.01	0.058	(0.044, 0.058)	0.120	(0.073, 0.169)	0.504	0.578
CHSP	94	2.78	0.012	(0.003, 0.012)	0.364	(0.128, 0.622)	0.410	0.052
SOSP	116	4.23	0.025	(0.014, 0.025)	0.065	(-0.016, 0.148)	0.453	0.174
DEJU	91	2.60	1.319	(1.186, 1.319)	0.072	(0.043, 0.105)	0.435	0.098

The Department of the Interior protects and manages the nation's natural resources and cultural heritage; provides scientific and other information about those resources; and honors its special responsibilities to American Indians, Alaska Natives, and affiliated Island Communities.

NPS 963/146521, July 2018

National Park Service
U.S. Department of the Interior



[Natural Resource Stewardship and Science](#)

1201 Oakridge Drive, Suite 150
Fort Collins, CO 80525